ADVANCED MASTERS IN STRUCTURAL ANALYSIS
OF MONUMENTS AND HISTORICAL CONSTRUCTIONS

Master's Thesis

Maria Francisca Nobre Meneses

Sensitivity analysis of the seismic behavior of ancient masonry buildings

This Masters Course has been funded with support from the European Commission. This publication reflects the views only of the author, and the Commission cannot be held responsible for any use which may be made of the information contained therein.

Portugal | 2013

DECLARATION

Name:	Maria Francisca Nobre Meneses
Email:	kikanmeneses@gmail.com

Title of the Msc Dissertation:	Sensitivity analysis of the seismic behavior of ancient masonry buildings
Supervisor(s):	Nuno Leite Mendes, Paulo Barbosa Lourenço
Year:	2013

I hereby declare that all information in this document has been obtained and presented in accordance with academic rules and ethical conduct. I also declare that, as required by these rules and conduct, I have fully cited and referenced all material and results that are not original to this work.

I hereby declare that the MSc Consortium responsible for the Advanced Masters in Structural Analysis of Monuments and Historical Constructions is allowed to store and make available electronically the present MSc Dissertation.

University:	Universidade do Minho, Portugal
Date:	16th July 2013
Signature:	_____

This page is left blank on purpose.

ACKNOWLEDGEMENTS

The present thesis was developed within the framework of SAHC Erasmus Mundus Masters Course (www.msc-sahc.org). I would like to thank the European Union for providing me with the opportunity to be a part of the Advanced Masters in Structural Analysis of Monuments and Historical Construction (SAHC) program and for their financial support through the SAHC Consortium Scholarship. I would like to thank Prof. Paulo Lourenço and Prof. Nuno Mendes for the total availability and help during these past months and also to our colleague Leonardo Avila for the perfect help in a key moment.

I would like to express my gratitude particularly to Prof. Pere Roca and Prof. Luca Pelà of Universitat Politècnica de Catalunya for their help, guidance and dedication during my course work in Barcelona.

I would like to thank my colleagues in Barcelona for the friendship we created together and for all the wonderful moments we lived and that I will never forget.

Last, but for sure not the least, I would like to thank my family for the total support and to let me live and follow this dream. Thank you very much for your unconditional love.

This page is left blank on purpose.

ABSTRACT

The study of the vulnerability of ancient buildings is receiving much attention in the recent decades due to the increasing interest in the conservation of the built heritage and the awareness that life and property must be preserved. The different types of masonry present common features that provide high seismic vulnerability to these buildings, such as the high specific mass, the low tensile strength, the low to moderate shear strength and the low ductility. In addition to the influence of the material properties, the seismic behavior of ancient masonry buildings depends on factors such as the geometry of the structure, connections between orthogonal walls, connections between structural walls and floors, connections between walls and roof, the foundation behavior, the stiffness of the floors and the behavior of the non-structural elements.

The present study aims at evaluating the variation on response of the structure varying the material and geometrical properties of the ancient masonry buildings. The response is obtained through the non linear dynamic and static analysis with time integration and is focused on the dynamic behavior of the masonry walls and timber floors. First, a reference numerical model is prepared according to the experimental tests carried out at shaking table. Then, a sensitivity analysis is carried out and the global behavior, the in plane and out-of-plane displacements of the masonry walls and the damage are compared with respect to the reference numerical model. Several parameters can be considered in the sensitivity analysis, namely: the number of floors, the aspect ratio of the spandrels, the aspect ratio of the lintels, the Young's modulus of the masonry walls, the Young's modulus of the floors. The expected major results coming from this work are the definition of the seismic response range of ancient masonry buildings taking into account the deviations on its properties, and the identification and quantification of the parameters that most influence its seismic performance.

Keywords: *Gaioleiro* building, seismic performance of ancient masonry buildings, dynamic non linear analysis

This page is left blank on purpose.

RESUMO

O estudo da vulnerabilidade dos edifícios antigos está a obter atenção crescente durantes as últimas décadas devido ao crescente interesse na conservação do património construído e a consciência de que este deve ser preservado. Os diferentes tipos de alvenaria apresentam características comuns que propiciam a alta vulnerabilidade sísmica destes edifícios como a massa específica elevada, a baixa resistência à tração, a baixa a moderada resistência ao corte e a baixa ductilidade. Além da influência das propriedades do material, o comportamento sísmico de edifícios em alvenaria antiga depende de fatores tais como a geometria da estrutura, as ligações entre as paredes ortogonais, ligações entre as paredes e pavimentos, ligações entre paredes e telhado, a rigidez dos pisos e o comportamento dos elementos não-estruturais.

O presente estudo tem como objetivo avaliar a variação na resposta da estrutura quando se modifica as propriedades do material e propriedades geométricas dos edifícios de alvenaria antiga. A resposta é obtida através da análise dinâmica e estática não-linear com integração no tempo e é focado no comportamento dinâmico das paredes de alvenaria e pisos de madeira. Em primeiro lugar, um modelo numérico de referência é preparado de acordo com testes experimentais efetuados em mesa sísmica. Em seguida, uma análise de sensibilidade é efetuada e o comportamento global, o comportamento no plano e para fora do plano das paredes de alvenaria e os danos são comparados em relação ao modelo de referência. Vários parâmetros podem ser considerados na análise de sensibilidade: o número de andares, o rácio dos nembos, o rácio dos pilares, o módulo de deformabilidade das paredes de alvenaria, o módulo de deformabilidade dos pisos. Os principais resultados esperados provenientes deste trabalho são a definição da gama de resposta sísmica de edifícios antigos de alvenaria, tendo em conta os desvios em suas propriedades, bem como a identificação e quantificação dos parâmetros que mais influenciam o seu desempenho sísmico.

Palavras chave: Edifícios gaioleiros, comportamento sísmicos de edifícios de alvenaria antigos, análise dinâmica não linear

This page is left blank on purpose.

INDEX

LIST OF FIGURES

1. INTRODUCTION

1.1 FRAMEWORK AND MOTIVATION

Tourism is continually becoming more important to the society in general and to the economy of cities and countries in particular. As a consequence, the importance of preserving and keeping the old city centers and other building heritage is obvious. It is estimated that the existing building stock in Lisbon is half composed by ancient masonry buildings, and more than 60% of them need structural intervention and should be evaluated according to their seismic vulnerability. (Simões & Bento, 2012)

In 1755 Lisbon suffered from a catastrophic earthquake, destroying a significant part of the city. Despite the present reduced activity, the seismic events are recurrent and so a strong earthquake can take place again in Lisbon. The seismic risk is related with the possible economical losses and causalities, and it is determined taking into account the seismic hazard, the seismic vulnerability of buildings and the assets exposure. The seismic hazard is associated directly with the tendency of the region for the occurrence of earthquakes. In Portugal the trend of the seismic hazard is generally higher in the South that in the North. The seismic vulnerability of buildings is related to the structural damage caused by a given earthquake. The assets exposure is associated with the presence of more or less vulnerable constructions depending, consequently, on the population density and on the economic development of the region. Since the seismic risk is always present, because it is not possible to have null seismic danger, safety cannot be understood as the absence of risk but shall be referred to as “acceptable risk”. As pointed in Simões & Bento (2012), the correct determination of the seismic vulnerability is more important or severe than the uncertainties related to the seismic hazard (this last one is not possible to control). The seismic vulnerability is depending on the properties of the constructions, which can be analyzed, for example, depending on the period which they were built.

The earthquake of 1755 had an important role on the transformation of the Lisbon’ building stock as it leads the way to the appearance of a new masonry type of building – The *Pombalino*. Presently there are three types of masonry buildings: *Pré-Pombalino* (built before 1755), *Pombalino* (built between 1755 and 1840) and *Gaioleiro* buildings (from 1870 to 1940). In Figure 1 an example of *Pré-Pombalino* and *Pombalino* buildings in Lisbon is presented. Later, the appearance of the concrete and the codes for anti-seismic constructions was another crucial event and changed completely the seismic vulnerability of the new buildings: *Placa* (“slab”) buildings appeared around 1930 with the inclusion of concrete floors (stiff diaphragms) and after frame reinforced concrete buildings. For determine quantitatively the seismic vulnerability of ancient masonry buildings it is necessary to do the qualitative analysis of it by establishing: the date of construction, typology, materials, construction methods, the structural system of that period and the current state of conservation. In

the case of historical constructions, all the uncertainties and variability regarding the material characteristics, influence of unknown previous phenomena (e.g. soil settlements) and the possible incomplete data on alterations and repairs carried out in the past, make the seismic vulnerability difficult to predict.

Figure 1 – a) Pré-Pombalino buildings in Lisbon; b) Example of Pombalino building in Lisbon.

The scope of the thesis is to assess the influence of some of the ancient masonry buildings' properties on their seismic vulnerability. The objective is to change some parameters and evaluate its influence on the seismic performance of this type of buildings, namely on the in plane and out-of-plane response of the masonry walls and damage. The present study will be specially focused on the sensitivity analysis of the masonry *gaioleiro* buildings, which exist in a high number in a "noble" part of the Portuguese capital (Figure 2). This building typology presents some aspects of the *Pombalino* buildings, but they do not have a good construction quality and so the city grew fast based, generally, on poor masonry buildings that are still now in use. Furthermore, this thesis aims to evaluate the application of modern techniques of structural analysis (pushover analyses), currently used for reinforced concrete and steel structures, to ancient masonry buildings with flexible floors.

Figure 2 – High quality *gaioleiro* building located in *Avenida da Liberdade*, Lisbon.

1.2 THE *GAIOLEIRO* BUILDING

The *gaioleiro* buildings are currently not fitting the present housing requirements of the Lisbon inhabitants and many of them are in a state of severe degradation. As a consequence, a lot of them suffered in the last 90 years some transformations and were already strengthened in a way that sometimes where not the most suitable and some others present major security problems for its residents.

1.2.1 Historical context

On November 1st (all Saint's day) 1755, Lisbon woke up with an earthquake of magnitude of about 9 (Richter magnitude scale), which would prove to be one of the deadliest earthquakes to ever strike Europe. This incident destroyed almost all the city, including its building stock, and other dozens of other Portuguese villages along the coast. Around 11am the first of three tsunami waves struck Lisbon which, despite only of approximately 5m high, funneled into the city via the Tagus river estuary causing great damage and loss of life. The Tsunami waves arrived to the UK, Northern Africa, and the Caribbean. Most of the city's residents were gathered in churches and cathedrals on that Sunday morning, when a little after 9:30 am a terrible rumbling noise was followed moments later by intense shaking that lasted several minutes, collapsing most of the city's buildings. However, the worst was yet to come. Fires spread quickly among the ruins, engulfing the city of Lisbon, turning the city into a hell that would burn for days. Following this incident and taking into account the necessity to rebuild the city in an orderly way, Marquês de Pombal, secretary of state on that time, commissioned Eugénio dos Santos and Carlos Mardrel to design a new urban plan for the city, based on a regular and complex block grid, with wide streets, connecting the two main squares – Rossio and Terreiro do Paço (Figure 3). The new urban plan included also rigid directions related with architect project design of the buildings such as the number of floors, area, façade design, etc.

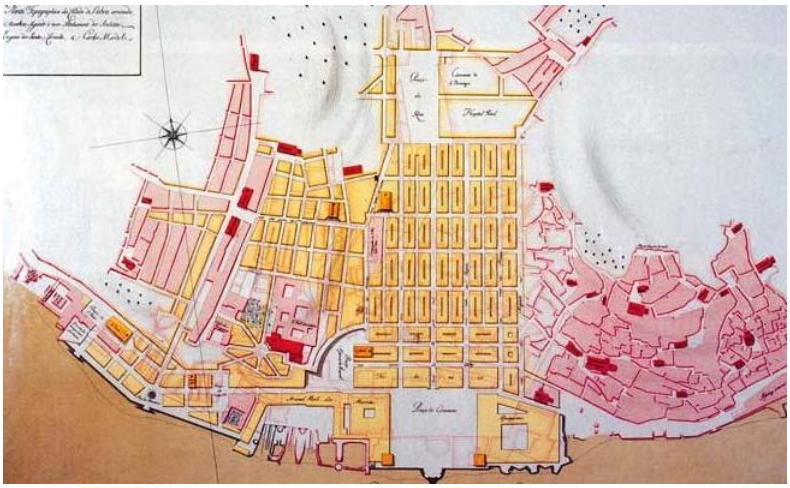

Figure 3 – Eugénio dos Santos' Urban plan of the new part of Lisbon after the Earthquake (Ordem dos Engenheiros, 2013)

The typical *Pombalino* building have four floors: the first with windows and balconies, the second and third with simple windows, the last floor is an attic and the ground floor is occupied with shops, as shown in Figure 4. The most innovative and important aspect of this new building typology was the insertion of a resisting wooden structure inside the walls giving seismic resistance to the building (Figure 5). This "wooden cage", whose structure is based on the "frontal" walls creating an orthogonal grid that receives the joist's floor. This kind of wood cage (*gaiola*) is essential to the locking of the structure and improves the seismic behavior of the building. The vertical, horizontal (beams) and diagonal (struts) joists, form a kind of wooden crosses called *Santo André*. All these elements are interconnected by assemblies and nailing fixation and are filled after with solid brick masonry, ceramic or irregular stone fragments and lime mortar. These walls have thicknesses between 15 and 22 cm and the woods commonly used in its manufacture are oak and pine.

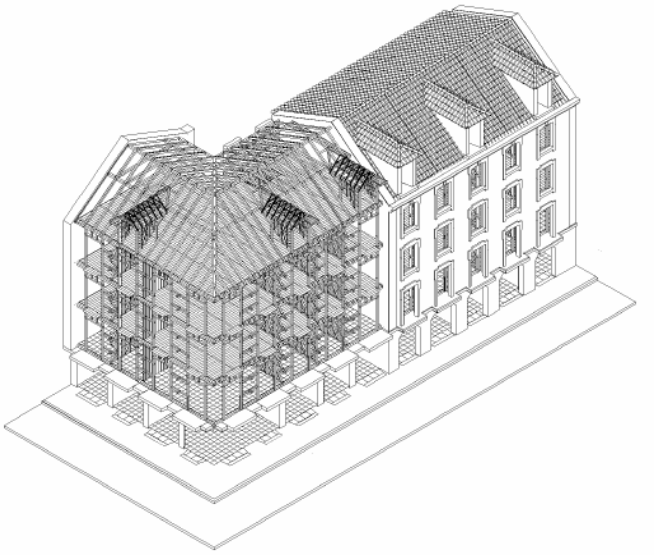

Figure 4 – *Pombalino* building with and without the masonry enclosure walls to observe the wooden structure. (Paula & Cóias, 2006)

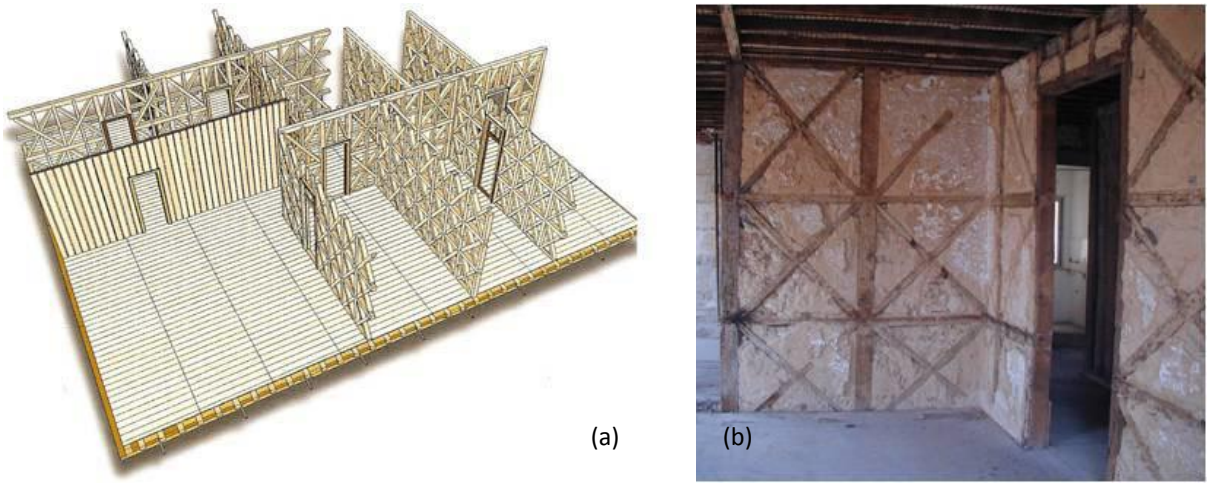

Figure 5 – a) Details of the floors and walls (*gaiola).* b) Santo André's Cross (Appleton J. , 2003)

Starting from the end of the 19th century, Lisbon experienced a great urban expansion, especially to the North part of the city, contradicting the city tendency of growth parallel to the river. This expansion followed a plan developed by Ressano Garcia, which was inspired in a way by the new Parisian boulevards, with avenues with central lanes divisions with floors and trees and wide streets. The expansion plan was very pragmatic; Ressano Garcia adapted the plan to fit in the terrain, included existing streets in its grid and changed the scale of blocks according to the topography of the land.

After more or less one century, the memory of the earthquake started to fade. The significant increase of population in the mid of 18th century and the rapid growth of the city made possible the appearance of a new building typology called *gaioleiros*. The *gaioleiro* buildings are associated with the construction of Bairro de Camões occupying the hill on the east side of Santa Marta Street and Avenidas Novas adjacent to Fontes Avenida Pereira de Melo and Avenida da República (Figure 6). The buildings were aggregated in blocks with interior yards and surrounded by a grid of secondary streets, wider than the streets of the *Pombalino* downtown. (Simões & Bento, 2012)

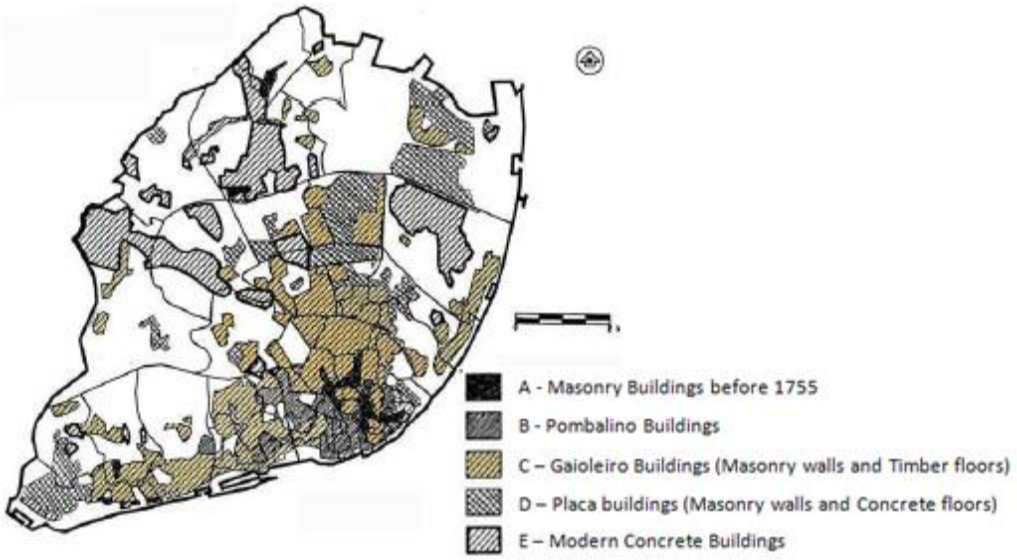

Figure 6 – Distribution of the Lisbon' Building stock typologies. (Cardoso, Lopes & Bento, 2003)

The *gaioleiro buildings* were built between 1870 and 1930 in a quicker way, inexpensively and with guaranteed money return, and are clearly labeled as low quality buildings. This denomination has the objective to expose the considerable structural alterations done in the design of the buildings comparing with those from the previous period; the g*aiola Pombalina* was completely changed (the timber structure started to be simplified and the rubble masonry infill replaced by industrial masonry bricks) and has no longer the necessary quality to proper resist to an earthquake. The quality of the materials used and the construction techniques adopted were also inferior to the ones used in the Pombalino buildings.

Figure 7 – Examples of *Gaioleiro* building in Lisbon.

These buildings have physic and constructive characteristics that distinguish them from others Lisbon's building typologies, some of them are presented in (Appleton J. , 2003). There is a greater freedom than in the *Pombalino* in respect to the windows' dimension and stonework, as example the dimensions of the windows increased and the spandrels got smaller. It is possible to use on the same floor simultaneous windows and balcony doors. The decorations of the façades appear to have some French influence. The balconies and *marquises* are made with a very slender steel structure with decorative and functional properties. These elements present a mix floor solution constituted by steel I or T inverted beams and masonry brick vault connected by a layer of lime mortar or cement. In the rear façade is common to find metallic stairs and there are large shafts for light and ventilation of the interior divisions. The stairs are located, approximately, at the central position of the plan, resulting in some structural symmetry. Another characteristic is common lack of structural continuity, in which connections between the orthogonal load-bearing walls and between the load-bearing walls and the floors are not adequate. According to Appleton (2005), the area of implantation varies from around 127.8 m^2 to 529.0 m^2, with widths ranging between 6.5 m and 15.2 m, and depths between 16.5 m and 28.0 m. The *gaioleiro* buildings are usually semi-detached and the pounding should be considered when the adjacent buildings present different heights or if the separation distance is not large enough to accommodate the displacements. It is noted the "block" effect is usually beneficial and provides higher strength to the building, as shown in Ramos & Lourenço (2004). A detailed description of the structural elements of these buildings will be presented next.

The *gaioleiro* building characterize a transition period from the anti-seismic practices and the modern reinforced concrete frame buildings, passing through the *Placa* buildings which include both bearing masonry walls and concrete floors. A summary of the evolution of the Lisbon's building stock is presented schematically in Figure 8.

Before 1755	Old masonry buildings		Bearing masonry walls and timber floors
After 1755	'Pombalino' buildings		Reconstruction after 1755 Earthquake Bearing masonry walls and timber floors Interior wood structure with locking properties
1880-1940	'Gaioleiro' buildings		Higher buildings with bearing masonry walls and timber floors Back balconies made of steel beams and ceramic bricks Interior wood structure with weaker structural conception
1940-1960	'Placa' buildings		Bearing masonry walls and reinforced concrete slabs Reinforced framing elements start to appear on the ground floor
Before 1960	First Period of Reinforced Concrete buildings		Before the seismic codes ('Regulamento de Segurança das Construções contra os Sismos[1] (RSCCS)' published in 1958 and 'Regulamento de Solicitações em Edifícios e Pontes[2] (RSEP)' published in 1961)
Before 1985	Second Period of Reinforced Concrete buildings		Before the modern seismic codes ('Regulamento de Segurança e Acções para Estruturas de Edifícios e Pontes[3] (RSA)' published in 1983)

Figure 8 – Summary of Lisbon's building stock. (Simões & Bento, 2012)

1.2.2 Description of the properties

Some distinguishable architectonic properties are the decoration of the front façade including some *Art Nouveau* details or with a stripe of tiles, windows with labored stone frames. The general configuration of a *gaioleiro* apartment is narrow and long. If the façade's width was at least 15m one building would have two apartments for floor and between four and seven floors. There are four distinguishable types of *gaioleiro* buildings (Figure 9):

1. Small to medium size buildings with narrow façades, one apartment per floor, lateral shaft and lateral stairs;
2. Large buildings size with wide front façades and one big apartment per floor;
3. Large buildings with wide front façades, a central stair, two lateral shaft (eventually another one central) and two apartments per floor.
4. Large buildings located in corners with two or more shafts, central stairs and two or more apartments per floor.

a) b)

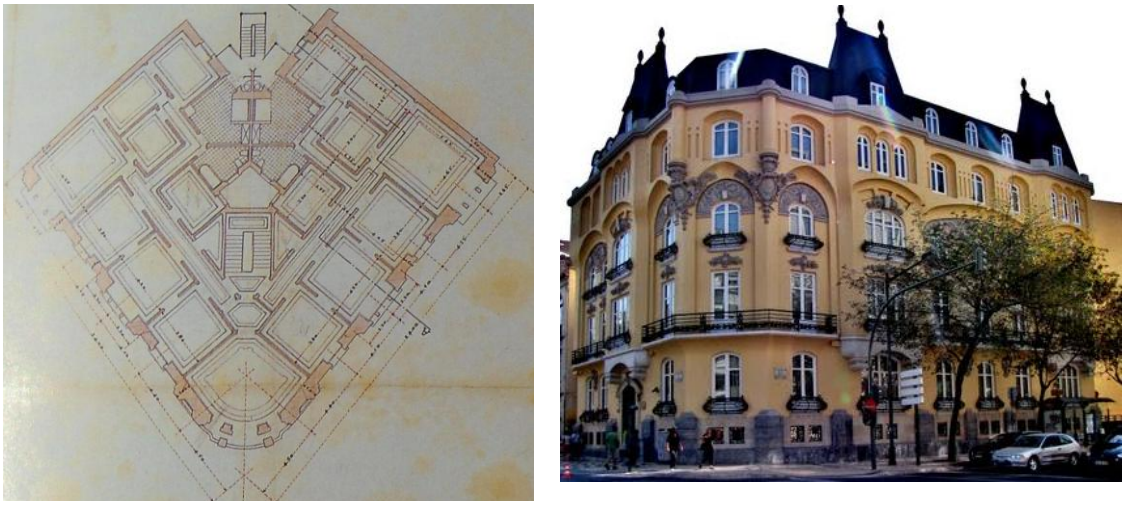

(c)

Figure 9 – Plan of different types of *gaioleiro building*. a) Narrow front façade (one apartment per floor); b) Wide front façade (example with two apartments per floor); c) Corner building. (Adapted from Andrade (2011)).

1.2.2.1 Foundations

The soil where there is a significant presence of *gaioleiro buildings* is mostly composed by sandy-clay soils with low resistance rocks. The *gaioleiro* buildings were commonly supported on caissons or on arches structure (Figure 10b). When the adequate foundation soil was more than three meters deep, they could be supported on direct foundation made with continuous walls in limestone masonry solid grounded (Figure 10a). If it was possible to use direct foundations, the dimensions would depend on the characteristics of the soil and dimensions of the wall - on the façades usually between 1.10 to 1.50m and below the gable and light-shaft walls around 0.60 to 0.70 m thick (Appleton, 2003).

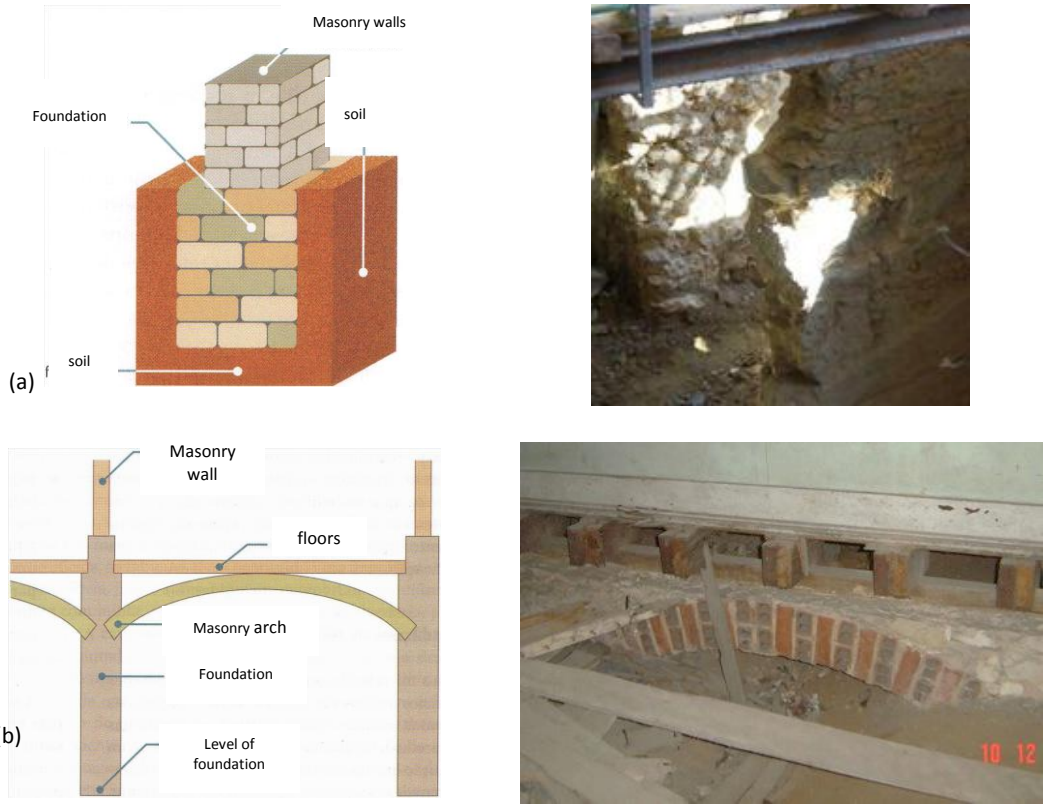

Figure 10 – Types of foundations. a) Direct foundations; b) Semi-direct foundations using arches.

1.2.2.2 Walls

The load-bearing walls, as the exterior walls, were built in rubble stone masonry with lime mortar and sand (Figure 11a) and can present a reduction of thickness in elevation of the building (Figure 11c). It is common to find variation of the main walls' thickness in height for economic reasons and reduction of the self-weight of the walls. A weaker out-of-plane performance of the masonry walls is prone to happen in *gaioleiro* buildings, due to the poor connection between the walls and floors, and between orthogonal masonry walls.

The front façade walls are typically 0.60 to 1.0 m thick on the ground floor, with a decreasing thickness with the elevation of the building, resulting in rooftop walls with 0.30 to 0.40 m of thickness. The back façade walls were

usually 0.50 to 0.60 m thick. Vertical and horizontal timber struts were used to reinforce the masonry walls around door and window openings. However, the experience has demonstrated that often these elements do not exist.

a) b) (c)

Figure 11 – Wall composition. a) Exterior rubble stone masonry wall; b) Back façade made with solid brick masonry. c) Reduction of the thickness along the height (dimensions in meters). (Andrade, 2011)

A new wall configuration was adopted and resulted from the simplification of the *Pombalino* cage. The truss elements of the *frontal* walls were removed and the rubble infill was by brick masonry, solid on the lower floors and hollow on the upper, or by lath and plaster for the partition walls. The partition walls, which show almost no load-bearing capacity, were made by vertical timber strips with approximately 0.15 m large and horizontal timber square strips filled on the breaks by rubble masonry, resulting in walls with 0.10 to 0.15 m thickness (Figure 12 a) (Simões & Bento, 2012).

a) b)

Figure 12 – Interior walls. a) Interior wall made with brick masonry; b) *Lath and plaster* walls (Appleton J. , 2003)

The side walls, or gable walls, are frequently shared by adjacent buildings and are interrupted by shafts, in order to provide natural light and ventilation to the interior rooms. Ventilated masonry boxes on the ground floor prevented the rising moisture from the soil and the rotten of the interior wooden structures (Simões &

Bento, 2012). The shaft and gable walls were originally built in rubble stone masonry with 0.40 to 0.50 m thickness, but later evolved to bricks masonry walls, with 0.30 to 0.15 m thickness.

1.2.2.3 Floors

The *gaioleiro buildings* can have floors with metallic frame, applied in compartments with high moisture like the kitchen and bathrooms, or timber frame in the other zones. The most common are the wooden ones used in the entire floor.

The steel floors (Figure 13) were gradually adopted on the kitchen, bathrooms and balconies and were built with iron beams in shape of I or T profile and brick masonry disposed in vaults, interconnected by air lime mortar or cement. The use of steel flooring became popular, due to the supposed superior durability of iron in relation to wood, especially in areas in contact with water. However, due to the insufficient protection of these elements against corrosion, this solution turned out to be equally vulnerable (Simões & Bento, 2012).

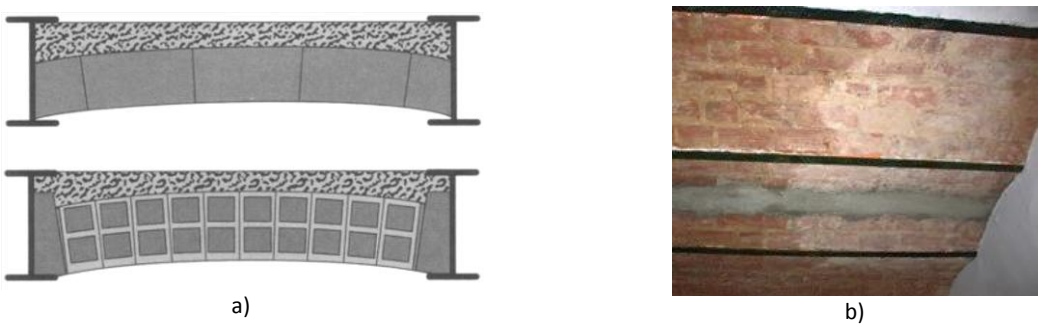

a) b)

Figure 13 – Steel frame flooring. a) Steel I profiles; b) Brick masonry disposed in vaults (Appleton J. , 2005).

The floors with timber frame are more common and are composed of a grid (usually pine wood) of timber joists, floorboards and ring joists, over which board flooring is laid. The width and height of the timber joist ranges, from 0.07 m to 0.08 m and from 0.16 m to 0.22 m, respectively, and the spacing varies from 0.20 m to 0.40 m. The final floorboards, with more or less 0.02 m of thickness, are placed over the joists. Three types of connections between floors and walls can be found (Appleton J. , 2005):

a) Insertion of the timber joist into a pocket of the wall with only a few centimeters of support (Figure 14 a);
b) incorporation of steel anchors, nailed to the timber joists and embedded into the walls (Figure 14 b);
c) In case of pavements with joists the connection includes the joist and an anchorage (Figure 14 c);

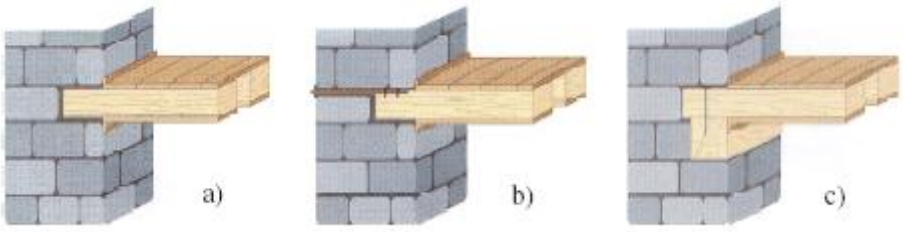

Figure 14 – Types of pavement-wall connections. a) Insertion of timber joist at the pocket of the wall; b) Steel anchor; c) Connection with rim joist. (Appleton J. , 2005)

1.2.2.4 Roof

In the major part of this kind of ancient masonry buildings, the roof structure is inclined and made of timber, allowing the use of the attics – mansard roof. In order to take the most advantage of this space the slope of the roof increased in comparison to the typical *Pombalino* roof. The use of these spaces is made independently of the rest of the building' structure, since the interior space was divided by a timber truss structure independent from the rest of the building, as the compartment walls were not connected with the interior building structure. The loads transmission from the roof structure to the resistant walls could be done in two ways: through direct support of the trusses on the walls, for the support of trusses on stone cantilevers, or using a transition beam to promoted a better distribution of the loads on the wall.

1.2.2.5 Stairs

The staircases were made in pine wood and supported in the structural walls. They could be located in the center of the building, usually around a central hall, lighted and ventilated by skylights, or located along the side of the gable wall, depending on the size of the building.

The exterior steel frame stairs appear at a later stage by imposition of the municipality that, in 1892, forced the implementation of stairs overlapping the rear façade to be used in fire situations.

1.3 DEVELOPMENT AND PRESENTATION OF THE DISSERTATION

The present study is divided in 6 chapters. The first chapter aims to make the introduction to the gaioleiro typology and its main properties and characteristics. A brief historical overview of the 1755 Lisbon's earthquake is presented. Through the second chapter a general overview of the seismic behavior of masonry structures is provided. Furthermore, a brief presentation of the types of seismic analysis performed on the current thesis is made. In the third chapter the preparation of the numerical model in the program Diana is discussed and the chapter is ending with the presentation of the reference model. The fourth chapter is dedicated to the reference model's results: it starts with the analysis of the dynamic properties and it is followed by the discussion of the results obtained with the non linear dynamic analysis and non linear static analysis. Furthermore, a discussion about the application of the pushover method and comparison between these two non linear analyses is carried out. The results and conclusions about variations imposed to the reference model is accessible in chapter five. The objective is to determine the properties that most influence the seismic behavior of this type of buildings. As done in the previous chapter, the comparison between the models was made applying the non linear dynamic analysis and non linear static analysis.

The main conclusions of the case study as well as recommendations are presented in the final Chapter (sixth chapter). The chapter also includes a short survey of opportunities for further research.

2. SEISMIC PERFORMANCE OF ANCIENT MASONRY BUILDINGS

2.1 INTRODUCTION

Ancient buildings where mostly made of masonry, which is a composite material of units (brick, block, stone) and mortar (clay, cement, chalk, lime). The properties and resisting characteristics of the masonry are depending on the properties of the constituents (units, mortar and their interfaces) and the construction techniques which depend also on the builder. Despite the dispersion of masonry buildings' characteristics, it is possible to point out the common features of the masonry mechanical behavior: high specific mass, low tensile strength, low to moderate shear strength and low ductility (quasi-brittle behavior), anisotropic structural material, non-homogeneous and non-elastic (Mendes, 2012). From the previous characteristics it is possible to conclude that masonry performs well when working in compression, but has a lower capacity to bear shear and tensile stresses. These stresses have to be sustained by the walls, taking advantage of the self-weight of the structure and the friction between stones and mortar. Masonry walls have a good performance in its plane, supporting the vertical axial loads, which only introduce compressive stresses on them. However, when the walls are subjected to horizontal excitations the vertical loads will tend to bend the walls, increasing the tensile and shear stresses, which this material is practically unable to resist (Simões & Bento, 2012). The seismic vulnerability of masonry buildings is extremely dependent on the load-bearing walls, which are normally arranged in orthogonal planes, and connections between the floors and the walls. Furthermore, the stiffness of the floors have a high influence on the seismic vulnerability of the buildings. In general, the ancient masonry buildings present flexible floors.

The mechanical properties, which determine the load-bearing capacity and deformability of masonry walls are: the compressive strength of masonry f_c, the tensile strength of masonry f_t, the Young's modulus E, the shear modulus G, and initial shear strength under zero compressive stress f_{vk0}. These parameters can be determined by means of experimental tests or by equations as a function of the mechanical properties of the masonry components. The compressive strength of the units is ranging between 5 MPa and 130 MPa, and the mortar strength normally between 1.5 to 3.5 MPa. Table 1 presents the typical masonry mechanical properties.

Table 1 – Mechanical properties s of masonry. (Tomazevic, 1999)

	Stone Masonry	Brick Masonry
Compressive strength [MPa]	0.3-0.9	1.5-10.0
Tensile strength [MPa]	0.08-0.21	0.10-0.70
Young's modulus [MPa]	200-1000	1500-3800
Shear modulus [MPa]	70-90	60-165

The elements that most influence the seismic performance of the structural walls are shown in Figure 15. The walls, both interior and external, are cut by openings like windows, doors and arches that will define the spandrels, piers, pillars and lintels. The effect of the presence of openings on the diagonal shear failure will be studied in the present thesis; wall openings weaken the in plane resistance of walls by decreasing the size of its cross-section. These openings also cause stress concentrations on the corners, which promote the formation of diagonal cracks. These cracks start at the opening corners and progress in a zig-zag trend through the mortar joints or diagonally through the masonry units in the wall. This cracking can further reduce wall capacity. Shariq et al. (2007) analyzed the influence of wall openings in the seismic response of a single storey and with only one room masonry building by changing the dimensions of the building in plan. The following conclusions were drawn: a) the increase of the aspect ratio of a room with openings, by keeping one side fixed, results in the increasing of the maximum principal tensile stress and maximum shear stress; b) increasing the openings in a wall results in high stresses around openings, the maximum principal tensile stress occurs along the short wall and the maximum shear stress occurs in the long wall.

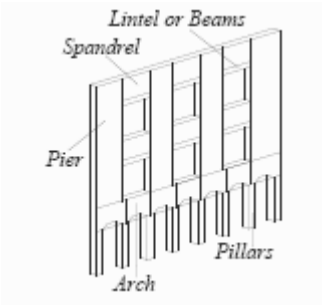

Figure 15 - Identification of macro elements' structural elements. (D'Ayala & Novelli, 2010)

The openings define the geometry of the piers and spandrels, which provide the gravity and lateral load resisting systems. Thus, their properties and dimensions influences highly the in plane failure of the masonry walls. The damage can appear both on spandrels and piers, however, the behavior is different since the axis of the spandrel is horizontal and in the piers is vertical. Furthermore, the normal stress in the piers is much higher due to the vertical loads.

According to (FEMA 306, 1998) piers can have considerable deformability and ductility if certain failure mechanisms prevail. Axial stress, aspect ratio, boundary conditions, and relative strength between mortar joints and units determine the failure mechanisms of masonry piers (Yi, 2004). Depending on the parameters described before there are four typical failure modes of masonry walls in their plan, as shown in Figure 16:

Rocking failure –As refered on *(*FEMA 306, 1998) the wall-pier rocking behavior mode, the wall or pier acts as a rigid body rotating about the toe after flexural cracking develops at the heel. The rocking mode typically occurs when material shear capacity is high, piers are slender, and compressive stress is low. Post cracking deformations can be large and relatively stable for many cycles;

Shear sliding failure – when the shear force in a pier is larger than the bed joints shear strength, sliding cracks develop in the bed joints at one end of the structural element and the failure takes place;

Diagonal cracking (shear failure) – the damage of this type of failure is shown by the development of stepped diagonal tension cracks, propagating along the mortar bed joints and head joints in the case of strong unit-weak mortar masonry, or straight cracks going through the units if the strength of the unit is similar to that of the mortar (Yi, 2004).

Toe crushing - the initial cracking of the masonry in tension (in the bed joints for piers, in both head joints and bricks in spandrels) and the subsequent crushing of the diagonal opposite compressed corners of the element. Since the toe of a pier is the zone with higher concentrated compressive stress, the compressive failure will develop in this area.

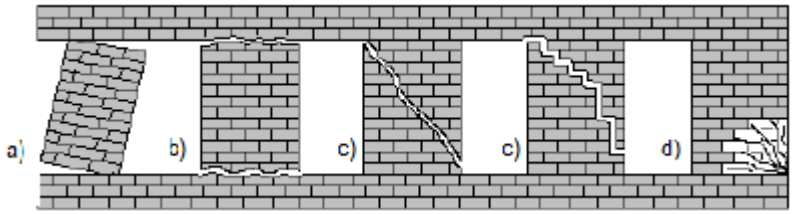

Figure 16 - In plane collapse mechanisms of piers. a) Rocking b) Sliding c) Diagonal tension d) Toe crushing. (Yi, 2004)

Rocking and sliding failure modes present large deformation capacities, since the stepped diagonal tensile cracks also presents large deformation capacity, due to the units slide between each other and dissipate energy. On the other hand, the diagonal cracks going through the units make lead to rapid strength deterioration, which represents a very brittle failure mode. Toe crushing is also a type of brittle failure mode, because the crushing zone rapidly loses its compressive strength (Yi, 2004).

Experimental and numerical analyses have shown that spandrel beams have a significant influence on the seismic behavior of URM (Unreinforced Masonry) structures, since they influence the stiffness and strength of the structure. However these elements normally are often not considered when designing URM structures,

because their force-deformation characteristic is still not completely studied (Beyer & Mangalayhu, 2013). Considering the FEMA 306 (1998) there are two different failure modes of spandrels:

Spandrel joint sliding - Bed-joint sliding located in the ends of the spandrel when the in plane moment capacity of the spandrel is reached, but before the shear capacity of the spandrel is reached. This mode can be relatively ductile and can allow for significant drift, providing a reliable lintel. As the spandrel displaces, the nonlinear mechanism of response may move to other portions of the wall such as the piers.

Spandrel unit cracking - the moment at the end of the spandrel causes brittle vertical cracking though the masonry units. Depending on the lintel construction, this can lead to a local falling hazard or modify the height of the piers. In the cracked portion of the spandrel is assumed to lack both shear and tensile capacity.

Figure 17 presents the behavior of a spandrel subjected to bending and shear. These elements evidence a limited shear capacity. However, they offer a significant dissipative capacity associated to large damage (extensive cracks).

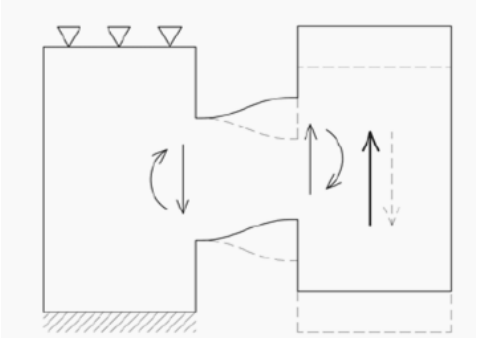

Figure 17 - Schematic spandrel loading. (Gattesco, Clemente, Macorini, & Noè, 2008)

2.1 OUT-OF-PLANE BEHAVIOR

When not properly connected to roof, floor and orthogonal walls, the masonry walls can easily become unstable and collapse under out-of-plane dynamic actions. During an earthquake, the inertial forces (the mass from roof and diaphragms) will be concentrated in this structural element (Figure 18) and will determine its vibration, bending deformation and cracking, which may lead to instability and possible failure. However, if the connections between the walls and diaphragms are adequate, the out-of-plane wall will no longer behave as a cantilever but as one-storey-high panels. After cracking, each portion of this wall behaves as macro elements (portions of the buildings with homogeneous construction characteristics and structural behavior) which can rotate if the gravity forces of the wall are not sufficient to prevent overturning and dynamic stability (Yi, 2004).

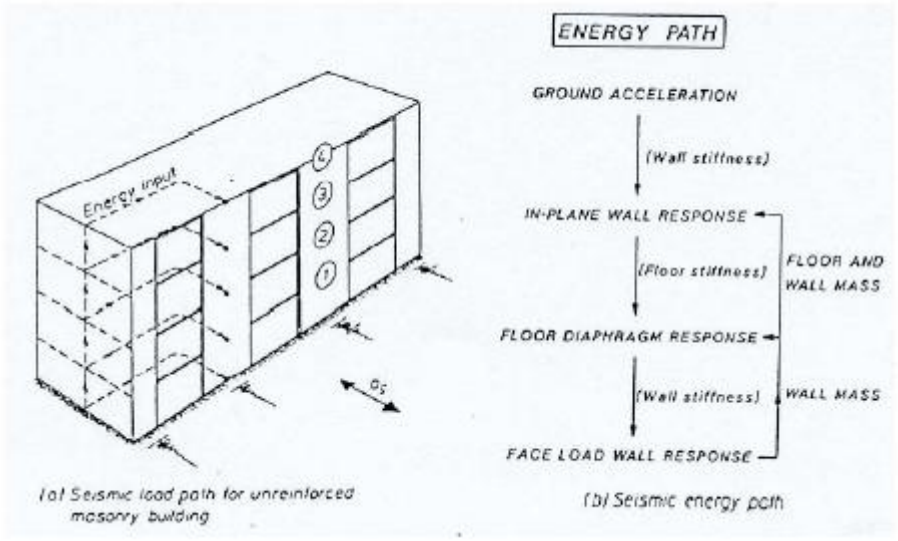

Figure 18 – Seismic response of a typical URM building. (Paulay & Priestley, 1992)

Figure 19 – Example of overturning of the façade. a) Cathedral of San Paolo in Mirabello, Italy after the May 20, 2012 Emilia Romagna earthquake. b) Church of San Martino in Sant'Agostino, Italy (Parisi & Augenti, 2013).

The most important variables involved on out-of-plane Ultimate Limit State are "*the vertical stress on the wall, the height-to-thickness ratio of the wall, and the input velocity provided to the wall by the diaphragms"* (FEMA 306, 1998). There are three basic out-of-plane failure types: one way bending between vertical supports, two way bending – end walls represent either three or four boundary conditions and return wall separation. The wall failure can be generated in the intersection of the orthogonal walls, in the failure localized in the conners,

in the piers of the ground floor and due to bending between floor levels. The most common mechanism occurs mainly with the detach of the façade and it can have several causes (Figure 19). To evaluate the out-of-plane collapse it is useful to individuate the possible collapse mechanisms on the base of abacuses of the typical damage occurring in different constructive typologies that were made based on the real knowledge on the previous collapse of masonry buildings. An example of an abacus for current buildings is presented in Figure 20.

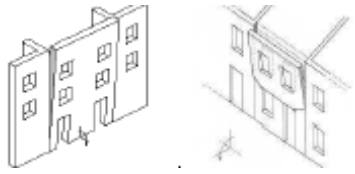	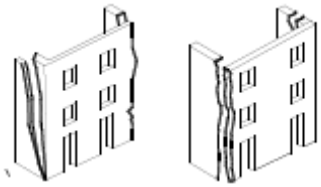	
Overturning of a single vertical macro element structure in case of weak connection with the adjacent vertical macro element structures	Overturning of a single vertical macro element structure in case of good connection with one of the adjacent vertical macro element structures	Overturning of a single vertical macro element structure in case of good connection with both adjacent vertical macro element structures
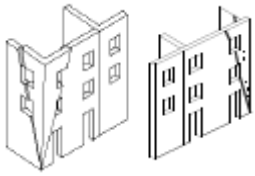	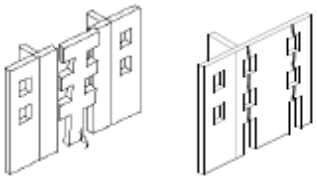	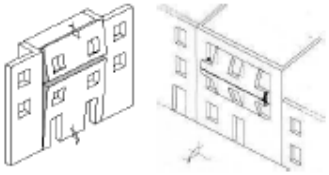
Corner overturning which involves a portion of two vertical macro element structures	Overturning of a single vertical macro element structure in case of weak connection within the vertical macro element structure	Out-of-plane of a single vertical macro element structure in case of presence of restraining elements on vertical macro element structure

Figure 20 - Out-of-plane failure mechanisms for unrestrained walls. (D'Ayala & Novelli, 2010)

2.2 IN PLANE BEHAVIOR AND COLLAPSE

In plane response dictates the upper limit to building strength but usually the building fails before in plane strength is exceeded. Unreinforced masonry buildings may exhibit ductile inelastic behavior under combined vertical and horizontal loads due to the ductility provided by friction. In these buildings, the in plane resisting mechanism is assured by the piers and spandrels that are carrying the self-weight (in piers), and the lateral loads due to the seismic actions imposed at the base. The lateral and vertical loads lead to tension, and shear combined with compression within the masonry wall. Fracture and failure of masonry walls under shear compression is intricate because of the complex interaction of shear failure along the mortar joints and compression failure often at the toe of the wall (Chaimoon & Attard, 2006).

Mechanisms of lateral force resistance depend on the width to height ratio of the structural element, on their boundary conditions and on the magnitude of the normal force, bending moment and shear force, and then on the characteristics of the brick, of the mortar and of the brick/mortar interface (Magenes & Calvi, 1997). As

described in (Paulay & Priestley, 1992) different properties lead to different wall configurations and, based on the inelastic behavior, the walls can be divided generally in the following groups:

i) *Cantilever walls without openings*. Such walls are typically found adjacent to other buildings or on alleys, and act as cantilevers up from the foundation (FEMA 306, 1998). The loads will be distributed through the floors acting as diaphragms. Also, the floors will stabilize the wall against lateral buckling. Walls of this kind with low ratio h_w/l_w will have high flexural strength. Still to activate this flexural resistant, and because of its low high, the wall has to be able to take the shear loads on the top part.

The idealization of openings is dependent on the geometry of the spandrels and piers, creating different types of walls based on the behavior strong pier–weak spandrel or strong spandrel–weak pier, as it is presented here:

ii) *Structural walls with openings.* Walls that include openings which will produce a certain pattern which should not decrease too much the flexural strength. The structural walls can be interconnected between them by beams much weaker than the walls behaving mainly as cantilevers. This configuration is assumed as the best masonry structural model for a ductile response, as the walls act as props and the maximum moments and energy dissipation occurs at the base of the walls.

iii) *Coupled walls with pier hinging.* Walls composed by piers weaker than the spandrels. Thus, the damage will be concentrated at piers (examples in Figure 21). At lower level the piers can fail due to the diagonal compression (shear failure which is not a ductility failure) or due to masonry crushing.

Figure 21 – In plane damage on piers.

iv) *Coupled walls with spandrel hinging.* It occurs when spandrels, connecting the walls, are weaker than the piers. The spandrels will take the bending moments and damage will occur in both elements allowing the energy to dissipate over the entire structure. This is the most desirable wall configuration. In Figure 22 an example of in plane damage on spandrels is presented.

Figure 22 – In plane damage on spandrels. (Beyer & Mangalayhu, 2013)

Figure 24 presents some of the common collapse mechanisms and damage associated to each element.

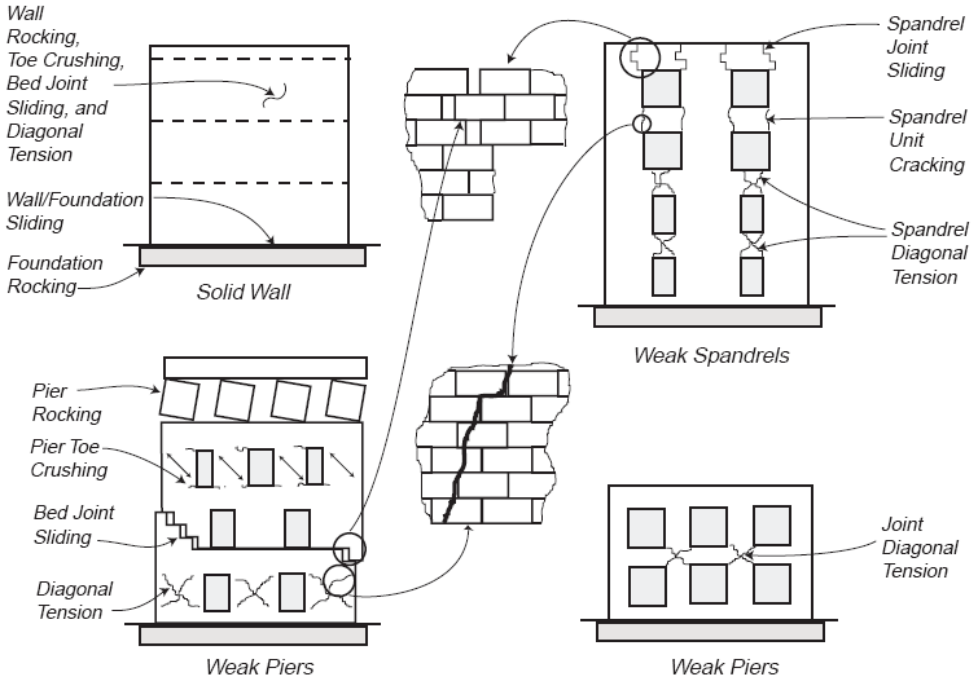

Figure 23 - In plane behavior of masonry walls. (Adapted from FEMA 306 (1998))

2.3 DIAPHRAGMS

The floors and roof structure also play an important part on collecting and transmitting the inertia forces to the vertical structural systems. The capacity to distribute the horizontal seismic loads depends on the in plane stiffness of the diaphragms composing the floors. As said before, in URM the floors are flexible and the connections are not as adequate as they should be and as a consequence is not possible to redistribute the horizontal loads. The main advantage of the stiff diaphragm is to assume compatible horizontal displacements

in every point of each floor and therefore to allow the distribution of the seismic forces proportional to the stiffness of the resistant vertical elements. If the proportional distribution was applicable it would be possible to control the stresses distribution and avoid the failure of the façades. The effect of the floors in the behavior of the buildings when subjected to horizontal loads is presented in Figure 25.

Flexible diaphragms and inadequate tie-in connection between walls and floor can also provoke excessive displacement at the floor level and overturning of the perimeter out-plane walls. Retrofitting of ancient masonry buildings is often including the strengthening of the floors as a way to simultaneously decrease the out-of-plane displacements and increase the distribution of shear forces to the lateral resisting walls.

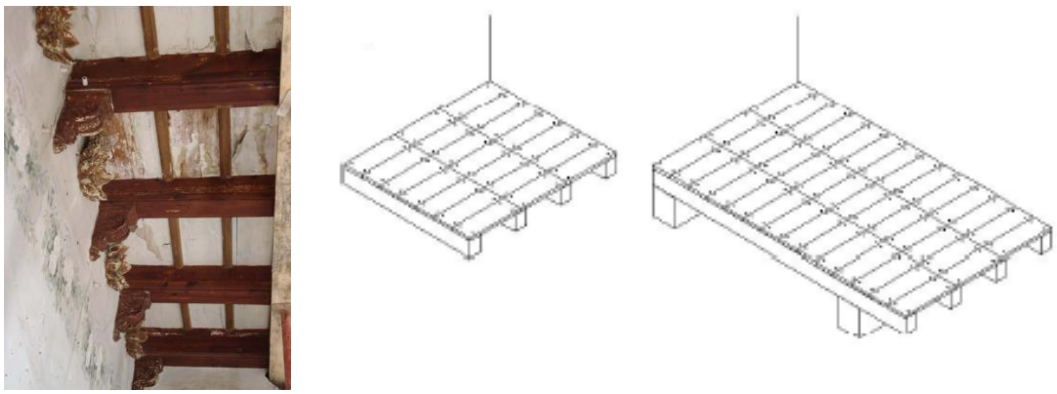

Figure 24 – Examples of wooden layout floors. (Brignola & Podestà, 2008)

To have in plane stiff diaphragms, yet badly connected to the walls, can generate undesirable collapse mechanisms as the expulsion of the corners and torsion mechanisms due to the differences between the position of the centre-of-mass and the centre-of-stiffness. As a consequence if the building has a layout which has the tendency to have torsional effects, probably it is not advised to increase the stiffness of the floors even if it decreases the tendency to out-of-plane failures (Brignola & Podestà, 2008).

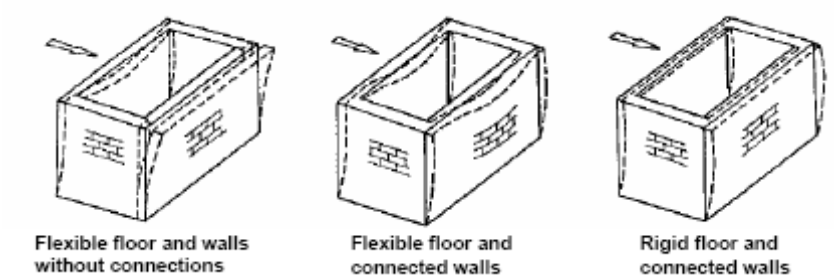

Figure 25 – Behavior in functions of connections links between walls and type of floors.

As suggested by Brignola & Podestà (2008), to consider the flexible floors its overall stiffness can be considered as a combination of the in plane stiffness of the diaphragm ($k_{eq,d}$) and the stiffness of the connections between floors and walls (k_C). The total deformation of the floors is the sum of the deformations of the diaphragm and connections. As a consequence, if the connections are rigid ($k_C = \infty$) the overall deformation is only a function of

the internal stiffness of the diaphragm. However, if the diaphragms are rigid ($k_{eq,d} = \infty$) the stiffness of the connections should be taken into account. The equivalent stiffness of the floors ($k_{eq,d+c}$), which should be used in the assessment, design and strengthening analyses, is given by the combination of both contributions (1/keq,d+c = 1/keq,d + 1/kc).

2.4 PERFORMED SEISMIC ANALYSIS

Analysis on historic structures can be performed mainly in three types: linear analysis, non linear analysis and limit analysis. Linear analysis can be linear static analysis or modal dynamic analysis. Non linear analysis can be connected to the material, geometrical and contact non linearity. It is also possible to carry out non linear analyses with damage models. The limit analysis can be of static analysis and kinematic analysis which will lead to the determination of the collapse loads.

The linear analyses are the simplest and most widely used. The nonlinear analyses are closer to the reality however they are more complex. To perform a nonlinear static analysis it is common to use the pushover analysis, which consists in applying monotonic incremental loads to set up the capacity curve of the model and accounts for the nonlinear behavior of the structure. The non linear dynamic time history analysis is the most complex one and takes into account the variation of the properties of the model during the time and so it is necessary to define the nonlinear hysteretic behavior of materials and structure.

In the case of masonry structures and for strong accelerations, it is mandatory to perform a kinematic analysis, which can be a simplified one with the verification of the accelerations or non linear analysis considering the blocks rigid (the bodies will only rotate or displace). After analyzing the typology of the building, and based on the available abacus, it is necessary to select the possible mechanisms by means of kinematics models and based on equilibrium conditions which provide a collapse, calculate the coefficient C = a/g for the elementary mechanism, i.e. the seismic mass multiplier that leads the element to failure.

2.4.1 Static Linear Analysis

Before doing the non linear analysis a static linear analysis was performed. This type of analysis is the most easy and less complex analysis described in the codes. It is commonly used to model static loads that are permanently applied to the structure (e.g. self-weight, foundation settlement), normally leading to a pre-yield elastic response.

2.4.2 Dynamic Properties

The dynamic characterization of the structure is essential to know the response of the building and to obtain the vibration modes and natural frequencies of the model studied. The structure has a number of modes equal to the number of degrees of freedom and each degree of freedom correspond to one vibration mode and one

frequency value. Generally, in the case of reinforced concrete buildings, the first modes are more representative of the dynamic behavior, since they illustrate the mode shapes with high deformation and modal participation factor. Nevertheless, since ancient masonry buildings have deformable floors, some local modes can appear within the first mode shapes, so it is necessary to analyze carefully the deformed shape and their modal participation factor. The modal participation factor is obtained as the ratio between the modal excitation factor Eq.(1) and the modal mass Eq. (2), and it gives a measure of how strongly a given mode is participating in the dynamic response of the structure.

$$L_i = \phi_i^T . M . r \tag{1}$$

$$M_i = \phi_i^T . M . \phi_i \tag{2}$$

However, since mode shapes ϕ_i can be normalised in different ways, the absolute magnitude of the modal participation factor has in effect no meaning, and only its relative magnitude with respect to the other participating modes is of significance. The analysis of the effective modal mass as a measure of the importance of each of the structure's modes is even more useful, since it is possible to know the amount of mass, $m_i$that is being excited by each mode i. Modes with high values of effective modal mass are likely to contribute significantly to the response (Chopra, 1995). A number of modes should be presented until reaching a contribution of around 90% of the total mass in each direction.

In the case of masonry unreinforced buildings with flexible floors the torsional mode shape is not present like it happens in the case of reinforced concrete buildings. On the other hand the structure with flexible floors will present some modes shapes where the structure is not maintaining the original angles between the gable walls and the façades.

2.4.3 Non linear static analysis - *Pushover*

Analytical computations based on conventional force-based methods have indicate sometimes the total collapse of masonry structures, due to considerable seismic actions in situations where the actual behavior of the structures was only the partial collapse or even only some cracks. These relevant differences are being overcome by using more refined displacement-based approaches such as the pushover analysis. The application of pushover methods for the assessment of existing masonry buildings has been introduced into seismic codes and some of the most used methods are: N2 method presented in Eurocode 8, the method of ATC40 and the method presented on Fema 273/356.

In general, the pushover analysis presented on the codes is based on a simplified mechanical approach which considers the non linear behavior of structures by means of their capacity curve; the plot relating the increasing horizontal force distribution and the horizontal displacement can be obtained reducing the pushover analysis result through the definition of an equivalent SDOF system. The seismic demand is estimated in terms of

spectral displacement (performance point), intersecting the so called Capacity Spectrum (the Capacity Curve plotted in terms of spectral acceleration and displacement) with the earthquake response spectrum, plotted in AD format (acceleration vs. displacement) and properly reduced to take into account the effects of energy dissipation related to non linear structural response (Galasco, Lagomarsino, & Penna, 2006). The limit states are then defined with reference to the displacement capacity.

Normally, to perform static non linear analysis, two different distributions can be adopted (Galasco, Lagomarsino, & Penna, 2006):

- Modal distribution – it is able to represent the structural dynamic amplification, which increases the action on higher storeys;
- Uniform distribution – it is able to describe the behavior of a building under extensive damage, preventing force redistributions among levels.

These two distributions may be assumed as boundary conditions for seismic analyses since the actual result, coming from the non linear dynamic analyses, is assumed to be within these two solutions and the real failure mode is predicted by one of the two distributions (Galasco, Lagomarsino, & Penna, 2006).

The displacement control point, normally located on the top floor, is also highly influencing the results of the method; this difficulty is more evident in masonry buildings since there it is not possible to assume the master node as the story's center of mass. In Galasco et al. (2006) it is studied the influence of the master nodes; for example, the results were more accurate when the master node was actually located on the weaker wall but the failure was achieve for the same maximum displacement for all the different nodes.

The N2 method proposed by Fajfar (2000) is a static non linear analysis with modal distribution of the loads and is one of the most used methods for seismic analysis of reinforced concrete buildings in Europe; if the N2 method is used, then the lateral loads applied are proportional to the first mode shape of the structure and the value of the horizontal forces in the *i*-the level, P_i, is defined through the Eq. (3). Even the pattern of lateral loads to use is not clear, in a practical way; for example, in case of doubt, use both distributions and consider the envelope of the results.

$$P_i = p \times m_i \times \Phi_i \tag{3}$$

Where,

p – is the magnitude;

m_i – Story mass;

Φ_i – Displacement shape of the *i*-the mode.

The limitations of this method lies on the supposition that the N2 method is accurate for structures that oscillate predominantly in the first mode, which means that is not as accurate for structures where higher

mode effects are significant; Traditional masonry buildings have flexible diaphragms and this prevents from assumption of rigid floors and the exclusion of the contribution of the higher modes. In addition, a different architectural disposition of walls may contribute to localize damage to 'unexpected' parts of building, due to irregularities in elevation (Galasco, Lagomarsino, & Penna, 2006). On the other hand, this method has the possibility to use a specific acceleration time-history as a demand spectrum on the method as this way it is possible to take into account the hysteretic behavior.

In general there are some limitations of the static pushover analysis for it is a time-independent analysis, but also it is providing important data, as the structure's strength and ductility, that one cannot obtain using simply linear static analysis. In order to overcome this time-independent issue some new approaches have been suggested as the adaptive pushover.

2.4.4 Dynamic non linear analysis – *Time-History*

The non linear dynamic analysis is applied on building models by using as input not a conventional seismic action, but directly artificial acelerograms, natural or simulated.

The nonlinear dynamic procedure provides an accurate calculation of the structural response to strong ground shaking, since it incorporates inelastic member behavior under cyclic earthquake ground motions. The nonlinear dynamic procedure explicitly simulates hysteretic energy dissipation in the nonlinear range.

Nonlinear dynamic analysis provides a more reliable assessment of earthquake performance than nonlinear static analysis. Nonlinear static analysis is restricted and it is not able to capture transient dynamic behavior with cyclic loading and degradation. Nevertheless, the nonlinear static approach provides a useful method for structures whose dynamic response is governed by first mode shapes. In general, the nonlinear static procedure works well for low-rise buildings with symmetrical regular configurations. In any case, nonlinear static analysis is always a helpful design tool.

3. PREPARATION OF THE NUMERICAL MODEL

3.1 INTRODUCTION

The correct structural modeling is essential for the design of new structures and to reproduce the structural strength of existing structures and, if necessary, to design an effective structural rehabilitation of the building. In the case of seismic analysis one should have extra careful on choosing the nonlinear parameters and assumptions. The seismic action corresponds to an imposed displacement at the base of the structure and not to the effect of direct application of forces to the structure; as a consequence, it is possible to consider the nonlinear behavior of the materials - the restitution forces depend on the constitutive stress and strain relations of the materials. By admitting non linear behavior, the structure can achieve higher displacements than its yield displacement without reaching the collapse. When subjected to an imposed displacement, after entering into the non linear field of response, the structure will have lower forces than those in linear regime.

In the present thesis the buildings will be modeled using the software DIANA using the macro-model approach to simplify the analysis and to reduce the computational time needed to perform it.

3.2 MICRO AND MACRO MODELING APPROACH

Masonry is one of the oldest and most used materials but is still difficult to exactly understand and model its complex behavior. Presently, macro-modeling and micro-modeling (detailed micro-modeling and simplified micro-modeling) are the two major ways to possibly model masonry material and buildings (see Figure 26). Both modeling are valid and use for different purposes, for example, micro-modeling is necessary to arrive to a better understanding about the local behavior of masonry structures and macro-models are the best tool to study masonry buildings in a bigger scale.

In macro-models the interaction between units and mortar is not taken into account as there is no distinction between units, mortar and unit–mortar interfaces. The masonry will be represented as a continuum material with average properties and the parameters to define it are the elastic modulus, the shear modulus, the compressive strength, the tangential shear strength and the tensile strength - which will influence flexural behavior in the 3D Macro models and the diagonal shear domain in the 1D models (Marques & Lourenço, 2010). Homogenization “permit to establish constitutive relations in terms of averaged stresses and strains from the geometry and constitutive relations of the individual components, can represent a step forward in masonry modeling, mostly because of the possibility to use standard material models and software codes for isotropic materials” (Zucchini & Lourenço, 2004). On the other hand, this homogenization process comprise difficulties in accounting the intrinsic complexity of formulating anisotropic inelastic behavior, which means

that it is not easy to define different inelastic criteria for tension and compression using this method. Macro-models are applicable when the dimensions of a structure are sufficiently large so that the relationship between average stresses and average strains is acceptable (Chaimoon & Attard, 2006). Also, this modeling strategy is more user-friendly to generate the mesh and provides a good compromise between accuracy and efficiency.

Micro-modeling is probably the best tool available to analyze and understand the real behavior of masonry, particularly concerning its local response. Using this kind of modeling will assure very accurate results, but on the other hand its very time consuming. The typical micro-modeling aim to characterize separately mortar, blocks and their interfaces and the constitutive laws and mechanical behavior are defined for each of the three components. For both mortar and units the Young's modulus and Poisson's ratio and its inelastic properties need to be defined. The interface represents a potential crack/slip plane with initial dummy stiffness to avoid interpenetration of the continuum. Presently, some effort is being made in order to try to overcome the high computational effort involved on the micro-modeling by trying to simplify the procedure using an intermediate approach: in each joint (consisting of mortar and the two unit–mortar interfaces), the properties of mortar and the unit/mortar interface are clamped into a common element, while expanded elements are used to represent the brick units (as a way to keep the same geometry). With this type of modeling masonry is considered as a set of elastic blocks bonded by potential fracture/ slip lines at the joints but the general accuracy is spoiled since Poisson's effect of the mortar on the joints is not included (Berto, Saetta, Scotta, & Vitaliani, 2004) and (Zucchini & Lourenço, 2004).

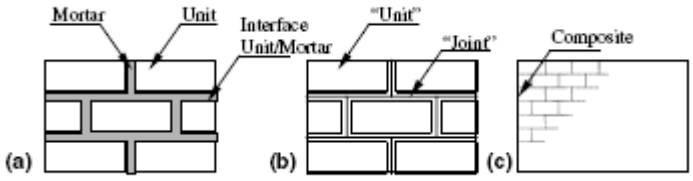

Figure 26 – Modeling masonry types: a) detailed micro-modeling; b) simplified micro-modeling; (c) macro-modeling. (Zucchini & Lourenço, 2004)

For the building's model studied on the present thesis, a macro-modeling approach was applied since the resisting masonry walls were considered with only one material. Different materials were considered to take into account the pavements and the floors' joists.

3.3 NON LINEAR MACRO MODELING OF THE STRUCTURE

In problems of nonlinear dynamic analysis of structures, dynamic equilibrium equation (equation of motion) can be written according to Eq. (4):

$$M\ddot{u} + C\dot{u} + Ku = -m\ddot{u}g \quad (4)$$

Where,

$M\ddot{u}$ – represents the inertial forces;

$C\dot{u}$ - represents the damping forces;

Ku – are the restitution forces;

The structural behaviour is nonlinear, characterised by non-proportional variation of displacements with loading, particularly in case of large displacements or high material nonlinearities. The dynamic response of a system when it is no longer responding in its linearly elastic range is not conformable to linear analytical solution, even if the excitation can be described through a simple function. As a consequence, it is necessary to apply numerical models to solve the nonlinear equation of motion as well as incremental iterative procedure, whereby loads are applied in pre-defined increments and equilibrated through an iterative procedure.

3.3.1 Integration method

The numerical integration method to solve the equation of motion consists in the direct integration of the equation of motion to obtain the response along the time in terms of displacement, velocity or acceleration, using incremental procedures - integration step-by-step. The numerical integration methods are able to consider the stiffness variation of the system during time as well as the damping variation and as a consequence, they can take into account the physical nonlinear behavior. Multi step integration is performed so as to satisfy the equation of dynamic equilibrium incrementally, so that at the end of each step, equilibrium is maintained, and displacement u, velocity $\dot{u}$ and acceleration $\ddot{u}$ are used as initial conditions for the next increment.

The integration methods can be divided into explicit methods and implicit methods. In explicit methods, the response $u_{t+\Delta t}$ at a generic instant $t + \Delta t$ is obtained from the equations, establishing at time t. In implicit methods – for example, Wilson-θ method, Newmark method and method of Hilber-Hughes-Taylor - the integration scheme is based on consideration of hypotheses for the variation of displacements, velocities or accelerations between the instants t and t + Δt. The response at time t e $t + \Delta t$ depends on the values of the displacements, velocities and accelerations corresponding to the instant t ($u_t, \dot{u}_t$ e $\ddot{u}_t$) and also $u_{t+\Delta t}$.

The Newmark's method is based on the establishment of a structural response to the variation in acceleration. The differential equations to be solved are presented in Eq. (5) and Eq. (6):

$$\dot{u}_{t+\Delta t} = \dot{u}_t + [(1-\gamma) + \gamma\ddot{u}_{t+\Delta t}]\Delta t \quad (5)$$

$$u_{t+\Delta t} = u_t + \Delta t\dot{u}_t + \left[\left(\frac{1}{2} - \beta\right)\ddot{u}_t + \beta\ddot{u}_{t+\Delta+}\right]\Delta t^2 \quad (6)$$

If β=1/6 and $\gamma = 1/2$ the method is unconditionally stable since, for these values, the method corresponds to an integration scheme which is considered a constant acceleration in the interval Δt with value equal to the average between $\ddot{u}_t$ e $\ddot{u}_{t+\Delta t}$.

The Hilber–Hughes–Taylor (HHT) method is a one parameter multi-step implicit method specifically designed to solve second-order differential equations. The HHT method uses the same finite difference equations as the Newmark method and its main property is the possibility of introducing numerical damping of higher frequencies preserving a second-order accuracy. This algorithm was the one used on this thesis and it requires the characterization of as extra parameter, α, used to control the numerical dissipation.

In order to conserve the second-order accuracy of the method, the parameters are related as described in Eq. (7):

$$\beta = \frac{1}{4}(1-\propto)^2, \qquad \gamma = \frac{1}{2}(1-2\propto), \qquad \propto \in \left[-\frac{1}{3}, 0\right] \tag{7}$$

For α equal to zero the HHT method reduces to the Newmark's method. Decreasing α means increasing the numerical damping, and the adopted damping is usually low for the low frequency modes and high for the high frequency modes (TNO DIANA, 2011). The parameters assumed in this study were $\propto = -0.1$, $\beta = 0.3025$ and $\gamma = 0.6$.

3.3.2 Time stepping

In a non linear dynamic analysis the reliability of the solution depends on the robustness of the algorithm used in the software, number and types of elements used, the definition of the boundary conditions and the size of the time steps, etc. In what concerns definition of the time steps, the time scale is divided into a series of time steps, usually of constant duration and they should be considered sufficiently small in comparison with the total duration of the analysis. Each the time step should be small enough to resolve the motion of the structure. The time step it is controlled by the mode with the lowest period with contribution for the dynamic behavior Tj (Eq. (8)):

$$\Delta t = \frac{T_j}{20} \tag{8}$$

3.3.3 Iterative procedures

The equilibrium of the equations in each step of the non linear analysis is obtained through iterative solution methods. In FEM (Finite Element Method) models the solution algorithm has the possibility to employ different methods as the Regular Newton-Raphson, the Modified Newton-Raphson and Linear Stiffness.

In a Newton-Raphson method, the stiffness matrix $\mathbf{K}_i$ represents the tangential stiffness of the structure. The difference between the Regular and the Modified Newton-Raphson method is the point at which the stiffness matrix is evaluated. The definition of the number of stiffness updates is related to the times the tangent stiffness matrix of the structure is recalculated and updated. In the Regular Newton-Raphson method, the

stiffness matrix is evaluated every iteration (Figure 27). This means that the prediction of the stiffness matrix is based on the last iteration (TNO DIANA, 2011). The computational savings in the formation and assembly of the stiffness matrix during the iterative process can be significant when using the Modified Newton-Raphson method, in which the stiffness matrix is not updated for each time integration (Figure 28). However, more iterations are often required with the modified Newton-Raphson, leading in some cases to an excessive computational effort.

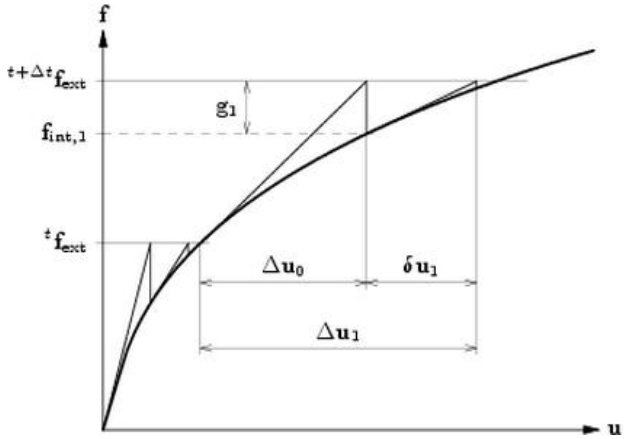

Figure 27 –Regular Newton-Raphson iterative method. (TNO DIANA, 2011)

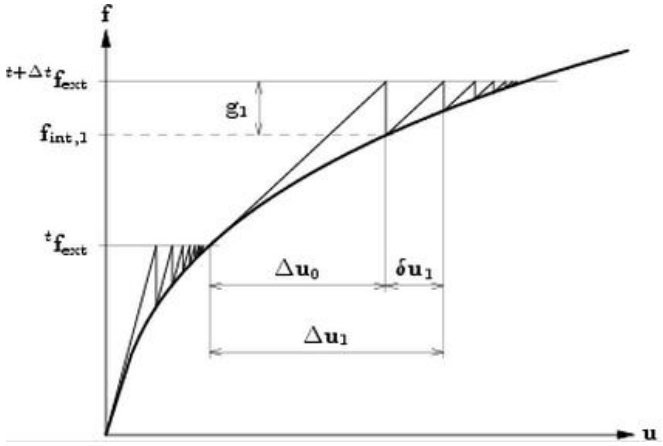

Figure 28 - Modified Newton-Raphson iterative method. (TNO DIANA, 2011)

For the non linear dynamic analysis performed in this thesis the iterative method applied was the Linear Stiffness method, which uses the linear stiffness matrix for the entire analysis. This method potentially has the slowest convergence, but it costs the least time per iteration since the stiffness matrix needs to be set up only once. Moreover, in case of a direct linear solver, the costly decomposition has to be performed only once. The Linear Stiffness method (Figure 29) can also be advantageous if it is desirable that the stiffness matrix remains symmetric where the tangential stiffness matrix would become non-symmetric. The Linear Stiffness method is usually very robust, but it is very well possible that it follows unstable equilibrium paths after bifurcations.

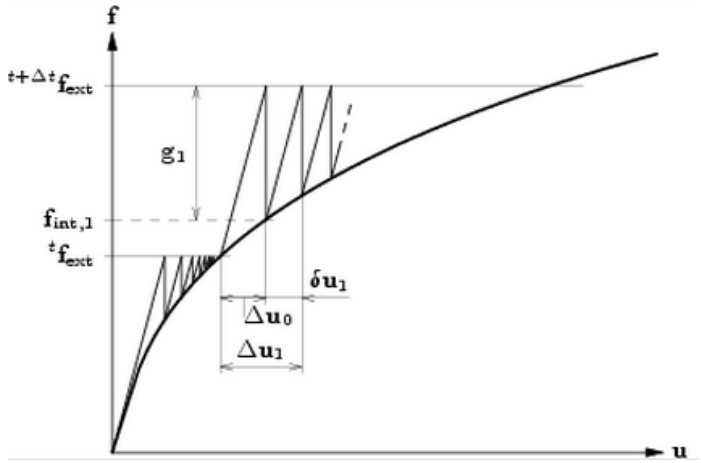

Figure 29 – Linear Stiffness iterative method. (TNO DIANA, 2011)

Generally, during the iterative process the internal forces, corresponding to a displacement increment, are computed and convergence is checked. If no convergence is achieved, then the out-of-balance forces (difference between applied load vector and equilibrated internal forces) are applied to the structure, and the new displacement increment is computed. Such loop proceeds until convergence has been achieved or the maximum number of iterations has been reached. The possibility of the solution becoming numerically unstable is checked every iteration, right from the start of any given loading increment, by comparing the Euclidean norm of out-of-balance with a pre-defined maximum tolerance. If the out-of-balance norm exceeds this tolerance, then the solution is assumed as numerically unstable and the analysis is restarted from the last point of equilibrium. In the iterative method, the detection of divergence is based on the same norms as the detection of convergence and in this case the convergence criterion was based on the internal energy with tolerance equal to 10^{-3}.

3.3.4 Damping

The damping depends on many factors specific to a given building. Therefore it is difficult to generalize the appropriate amount of damping to use in a nonlinear analysis. Normally, measurements of total damping, expressed in terms of percent critical damping in the first translational mode, range from low values of 0.5 % to 1 % in buildings under wind and ambient vibrations up to 10 % in buildings subjected to earthquakes. However, in the latter case, the measured damping of 10 % is likely to reflect energy dissipation due to both nonlinear hysteretic and inherent damping. It is suggested to specify equivalent viscous damping in the range of 1 % to 5 % of critical (Deierlein, Reinhorn, & Willfor, 2010).

In the present thesis the viscous damping for all the structural elements, which is a form of damping proportional to the velocity, was defined as Raleigh damping with the value of 3.3%. The Rayleigh damping matrix, C, is obtained by a linear combination of the mass matrix M, stiffness K of the structure (Chopra, 1995), as shown Eq. (9)

$$C = \propto M + \beta K \quad (9)$$

The introduction of a small amount of viscous damping can be beneficial in terms of numerical stability of highly inelastic dynamic analysis, since the damping matrix will have a stabilizing effect on the system of equations. (Chopra, 1995)

3.3.5 Material modeling

In order to take advantage of the deformation capacity of the structure, it is necessary to give it the ability to deform after the initial cracking (failure) without the total loss of capacity load (ductile behavior). In the case of masonry buildings the capacity to dissipate energy is achieved by cracking mechanisms. When modeling the hysteretic properties of elements, the initial stiffness, strength, and post-yield force-displacement response of cross sections should be determined, based on principles of mechanics and/or experimental data. Under large inelastic cyclic deformations, the stiffness and strength of the elements suffer deterioration (Figure 30) due to phenomena like fracture, cracking, crushing, local buckling, bond slip, or other phenomena. The degradations of the elements during cyclic loading should be included, through appropriate modifiers to the stiffness and internal forces, so that the model can simulate materials experiencing hysteretic behavior (Deierlein, Reinhorn, & Willfor, 2010).

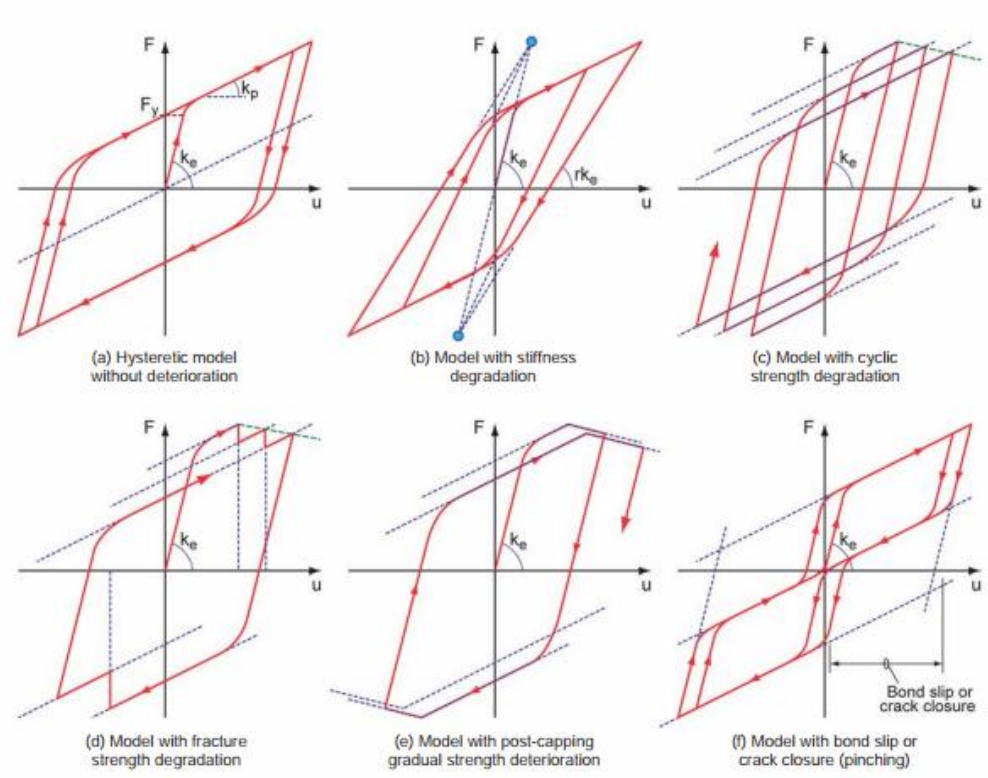

Figure 30 – Types of possible hysteretic modeling (Deierlein, Reinhorn, & Willfor, 2010).

For the hysteretic behavior of masonry, the Total Strain Fixed Crack model was selected (TNO, 2011). In compression, a parabolic stress-strain relation was adopted with no lateral confinement and no lateral crack reduction (Figure 31). In tension, an exponential tension-softening diagram with a tensile strength of f_t = 0.2 N/mm^2 and a tensile fracture energy of G_f = 0.05 N/mm were adopted. For compression the maximum values were taken ino account: f_c = 1.0 N/mm^2 and tensile fracture energy of G_c = 1.0 N/mm

In the Total Strain Fixed Crack model the tensile and compressive behavior of a material is described using only one stress-strain relationship and these types of models cannot be combined with other constitutive models. However, they are very well suited for Serviceability Limit State (SLS) and Ultimate Limit State (ULS) analyses which are predominantly governed by cracking or crushing of the material (TNO DIANA, 2011).

In the Total Strain Fixed Crack model the strain transformation matrix is fixed upon cracking and is evaluated in the fixed coordinate system determined by the principal strain directions. On the other hand, in the rotating crack model commonly used for reinforced concrete modeling, the cracks do not remain invariant during the loading.

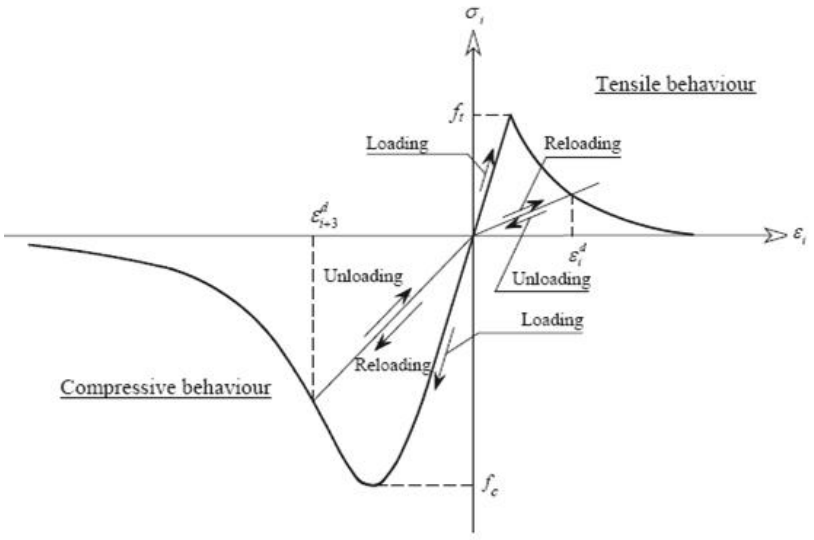

Figure 31 – Damage model considered for the modeling of masonry walls.

For the total strain fixed model, in each integration point a maximum of two orthogonal cracks can open; for the case of multi-fixed crack model more than two cracks can develop per integration point. As a consequence, fixed cracks can have a strength capacity slightly higher than the real ones in shear dominated application and multi-fixed material models provide lower strength capacity than the real ones, since the deterioration of the stiffness increases due to the possibility of the cracks to rotate according to the directions of the principal strains (Póvoas R, 1991).

The shear stress develops along the crack surface and the post-cracked shear stiffness is defined by taking into account the retention factor of its linear behavior, which reduces its shear capacity according to equation Eq. (10).

$$G^{cr} = \beta G \tag{10}$$

where,

β - is the retention factor 0< β ≤1 and it is reduced with the increasing of crack width;

G - is the shear modulus of the undamaged material.

The shear retention factor β was assumed equal to 0. 10. This means that the shear strength of the material will be reduced to ten percent of the original shear strength when cracks form.

3.4 ELEMENT MODELING

In the numerical model, quadratic shell elements with eight nodes (CQ40S) were used for simulating the masonry walls and MDF panels of the floors, which allows the simulation of the in plane deformability. The CQ40S element (Figure 32) is an eight-node quadrilateral isoparametric curve shell element and it is based on quadratic interpolation and Gauss integration over the element area. The integration in thickness may be made using Gauss or Simpson. In the case of a rectangular element the strain ε_{xx} , the curvature k_{xx} , the moment m_{xx} , the membrane force n_{xx} and the shear force q_{xz} vary linearly in *x* direction and quadratically in *y* direction. The strain ε_{yy} , the curvature k_{yy} , the moment m_{yy} , the membrane force n_{yy} and the shear force q_{yz} vary linearly in *y* direction and quadratically in *x* direction (TNO DIANA, 2011). All the finite elements are based on the theory of Mindlin-Reissner, in which the shear deformation is taken into account. In the modeling of the floors, shell elements were used aiming at simulating the in plane deformability**.** The masonry walls is the only the material considered as non linear. Each element presents 20 points of integration (5 points of integration on the thickness).

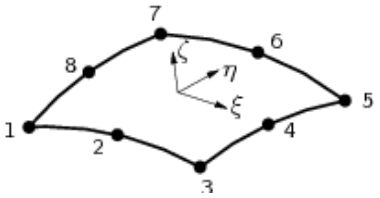

Figure 32 – The eight element node. (TNO DIANA, 2011)

Beam elements with three nodes (CL18b) were used for simulating the timber joists. The CL18B element is a three-node and three-dimensional beam element, with translation variables u_x, u_y, u_z, and the rotational variables ϕ_x, ϕ_y, ϕ_z in the nodes (Figure 33). The strains vary linearly along the center line of the beam. By default the program applies a 2-point Gauss integration scheme along the bar axis and it was what it was considered in the numerical model (TNO DIANA, 2011).

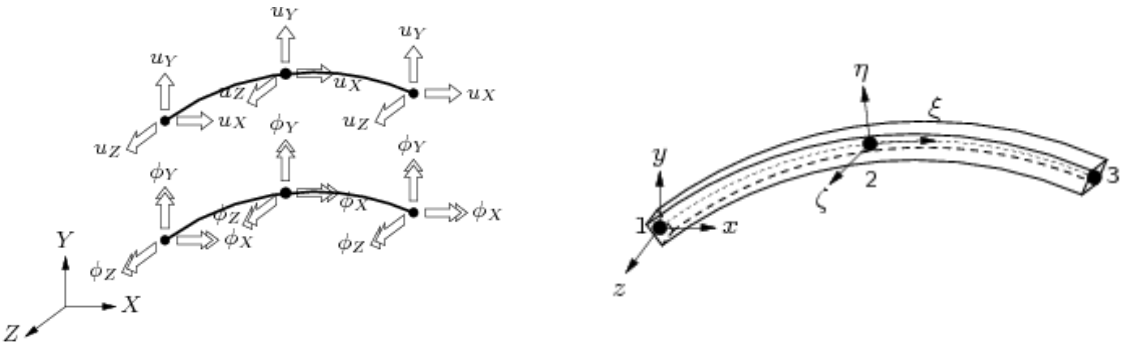

Figure 33 – The beam element.(TNO DIANA, 2011).

3.5 SUPPORT CONDITIONS

The model defined on this thesis is representative of an isolated building and so the boundary conditions were only defined for the foundations. Also, as there are not any interior or partition walls, the supports were only defined for the foundation of all the external masonry walls. In order to eliminate the variation of the soil influence in the response of the building and as it is not very relevant for the present study, the structure was considered pinned to the soil with the restriction of the rotations and translation e in all directions.

3.6 LOADS DEFINITION

3.6.1 Definition of permanent loads

The determination of the total mass of the building is fundamental for the total response of the building and mode shapes; bigger masses lead to lower natural frequencies of the building. As a consequence, the study of the masses involved, as well as their distribution, should be carefully studied. The inertial forces of current masonry buildings are mainly related with the mass of the masonry walls. Nevertheless, considering the guidelines provided by NP EN 1990 (2009) and NP EN 1991-1-1 (2009) the weight of the partition walls and live loads are, in general, unfavorable during an earthquake and so they should be considered. The reference model adopted in Mendes (2012) did not include either the mass of the partition walls nor live loads, due to the necessity to compare with a previous mock-up tested in shaking table.

In the new models studied in the present thesis these loads are considered, and turned out to increase the total weight in approximately 10%. Although these walls are not usually considered as load-bearing elements, the mass increment can be relevant for the seismic analysis.

The load combination considered for the Ultimate State is presented in Eq. (11). According to NP EN 1991-1-1 (2009), the seismic loads should not be multiplied by any safety factor; the self-weight should be also

considered with a safety factor of 1.0 and the live loads should be multiply by ψ_2, which is equal to 0.3 for the case of current buildings.

$$S_d = \sum_{i=1}^{m} S_{Gik} + S_{Ek} + \sum_{j=2}^{n} \psi_{2j} S_{Qjk} \quad (11)$$

There are generally two types of partition walls in a *gaioleiro* building: brick and lath and plaster walls. In the present work, all the partition walls will be considered to be all made of lath and plaster and the value is obtained by multiplying the weight of lath and plaster walls, which was assumed equal to 100 kg/m^2 (Branco, 2007), by the total length of lath and plaster walls in plan, by the inter-story height (3.6 m), and dividing it per the total floor area (108 m^2). Based on the example of *gaioleiro* building's plan presented in Branco (2007) and Gomes (2011), the weight distributed uniformly on the floors due to partition walls is 1.0 kN/m^2. The live load referenced in NP EN 1991-1-1 (2009) for a current building is equal to 2.0 kN/m^2 and will also be considered uniformly distributed on the pavements.

3.6.2 Definition of seismic loads

In order to perform a dynamic time history analysis, a ground acceleration time history (accelerogram) is required as an input. An accelerogram may represent a real earthquake record or it may be artificially generated to have specific characteristics. In the present study only the seismic horizontal action will be taken into account. The seismic vertical parcel will be neglected since does not have a relevant impact on the structure seismic behavior and since the objective is not to analyze the behavior of the floors but the behavior of the building's walls which present a very high stiffness for the vertical direction. According to Eurocode 8 and the Portuguese Annex (NP EN 1998-1-1, 2009), for Lisbon it is necessary to consider the far-field (type 1) and near-field (type 2) earthquake scenario, as it is shown in Figure 34. However, in this study only the type 1 earthquake was considered.

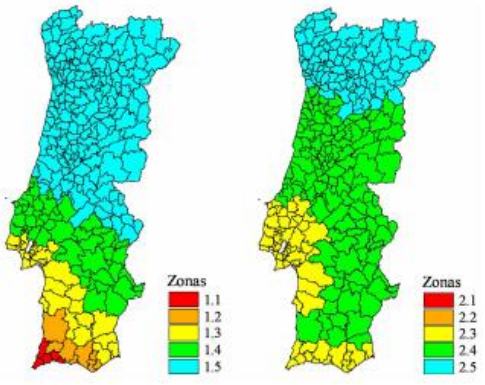

a) b)

Figure 34 – Seismic zonation for Mainland Portugal: a) Far-field earthquake (type 1); b) Near-Field earthquake (type 2).

The earthquake signals applied to the structure (history of accelerations in time) are the ones presents in Figure 37 and correspond to input signals used by Mendes (2012) and mesured in the shaking table tests. Two artificial accelerograms were generated and applied in the shaking table tests, based on stochastic methods and techniques of finite fault modeling. The accelerograms used (Figure 37) are compatible with the type 1 design response spectra (Figure 35) defined by Eurocode 8 (NP EN 1998-1-1, 2009) and Portuguese National Annex for Lisbon (a_{gr} = 1.5 m/s^2), with a damping ratio equal to 5% and a type *A* soil (rock, *S* = 1). Table 2 presents the parameters for Lisbon.

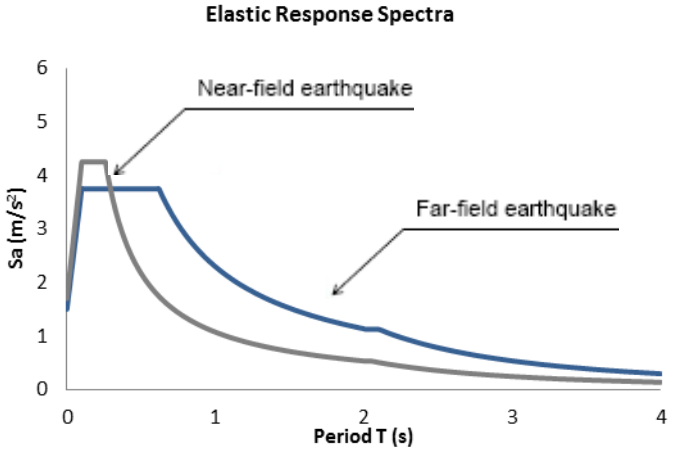

Figure 36 – Acceleration response spectra for far-field and near-field earthquake in Lisbon.

Table 2 – Parameters of the spectra for Lisbon.

Soil A	Zone 1.3 Earthquake 1	Zone 2.3 Earthquake2
a_g (m/s^2)	1.5	1.7
S	1	1
TB (s)	0.1	0,1
TC (s)	0.6	0.25
TD (s)	2	2

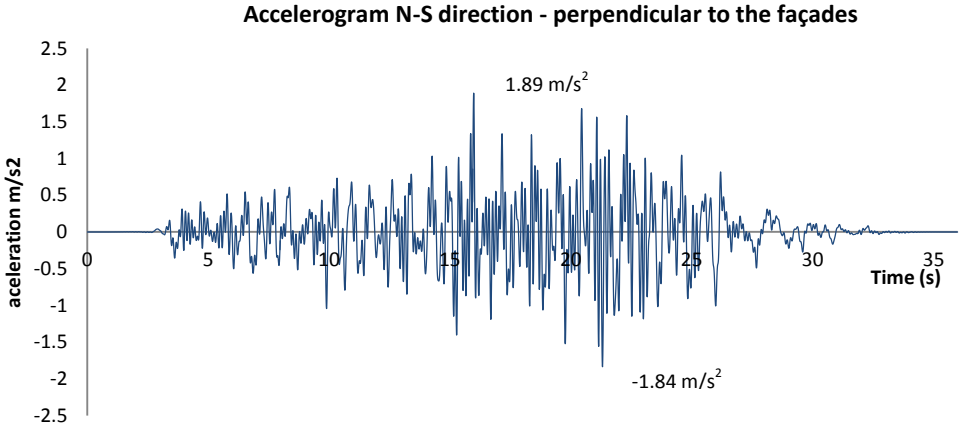

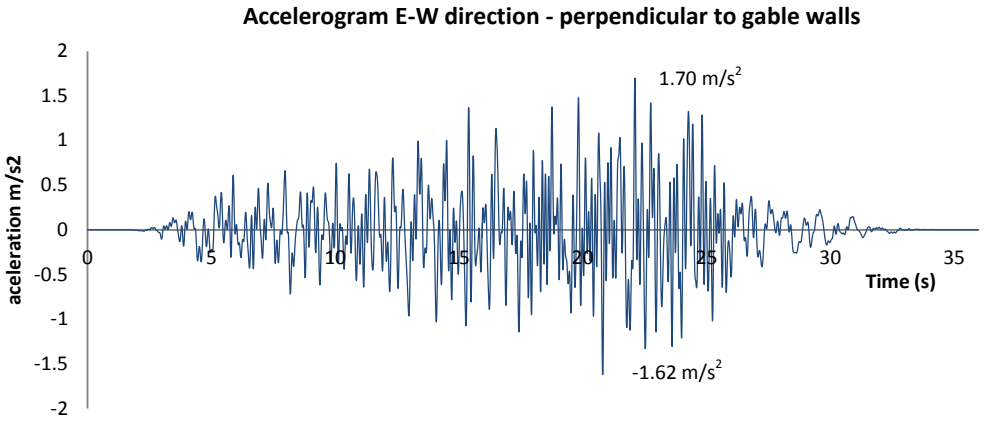

Figure 37 – Signals applies to the structure. a) North-South direction; b) East-West direction.

3.7 REFERENCE MODEL

The reference model (Model 0) will be taken into account, in order to derivate the sensitivity of *gaioleiro* buildings to seismic actions, is based on the real scale model and mock-up used in (Mendes, 2012). In the work carried out by Mendes (2012), a non-strengthened mock-up with a reduced scale of 1:3 was tested on a shaking table. After, a numerical model was prepared, also with a scale of 1:3, using the numerical program DIANA in order to be possible the calibration considering directly the experimental results obtain previously. Furthermore, using the scale factors of the Cauchy similitude law, a numerical model with the real scale was prepared.

The mock-up aim to reproduce the characteristics of a *gaioleiro* building and was defined according with its main properties. Nevertheless, some properties and construction methods had to be changed due to the limits of the shaking table. The mock-up was built in National Laboratory of Civil Engineering (LNEC), in Lisbon, with the following characteristics: four windows in each level, which is equivalent to have the two facades with 28.6% of opening area, two gable walls without openings, masonry walls of 0.17m thickness, MDF panels with 0.012 m, wooden joists parallel to the façades with 0.100x0.075 m^2 and the floors have and inter-storey height of 1.20 m.

The reduced scale is not favoring the construction of all joists and so the joists have the dimensions of three joists put together. This will be also reproduced on the numerical model, where the width of the wooden beams will be bigger than its height. Some pictures of the mock-up with a reduced scale of 1:3 are presented in Figure 38.

As noted before, starting from some of the previous considerations, a numerical model with reduced scale was made and calibrated and the real scale model was prepared at last. The full model has four floors, with an

inter-storey high of 3.60 m and with four windows in each level, which is equivalent to have both façades equal and with 28% of opening areas. The gables are perpendicular to the façades and do not have any openings. The façades and gables have 0.51 walls thickness which is not changing with height. The floors are considered flexible and made of MDF wood panels with thickness equal to 0.036m connected to timber joists parallel to the façades. The total are of the building in plan is equal to 9.45x12.45 m2.

Due to the difficulties in reproducing the gable roof in the experimental reduced mock-up, this was also not considered in the numerical model. As a consequence, the effect of the horizontal forces transferred from the roof to the walls under an earthquake, which can aggravate the out-of-plane mechanism of walls, were not taken into account. Balancing this unfavorable effect, the corresponding vertical component of the self-weight of the roof, which normally increases the compressive stress in the masonry walls, was also not considered meaning that the simplification is not expected to provide a major change in the response (Mendes, 2012).

Figure 38 – Non-strengthened mock-up used in the shaking table of LNEC. (Mendes, 2012)

3.7.1 Reference model description

The reference model will be symmetric in the two perpendicular directions, creating a regular model. The model has 12x9 m^2 of implantation area and four floors, each one with 3.60m high. The wall openings will appear only on the façades and have dimensions of 2.70x0.900 m^2, representing 28% of the façade's area. The piers have 1.20x2.70 m^2 and the spandrels on top of the windows 0.90mx0.90m. All the external walls will be composed of masonry with 0.51m thickness which is not varying in height. The internal walls were only considered by their weight on the floors. The floors are deformable, made of MDF wood panels with a thickness of 0.036 m, and are supported in a system of wood joist with 0.225x0.300 m^2 spaced of 0.525 m between each other. The connection between walls and floors was modeled as perfectly pinned. The building is

pinned to the soil. The reference model has a weight of 649 ton. In Figure 39 presents the geometry of the numerical model as well as the mesh.

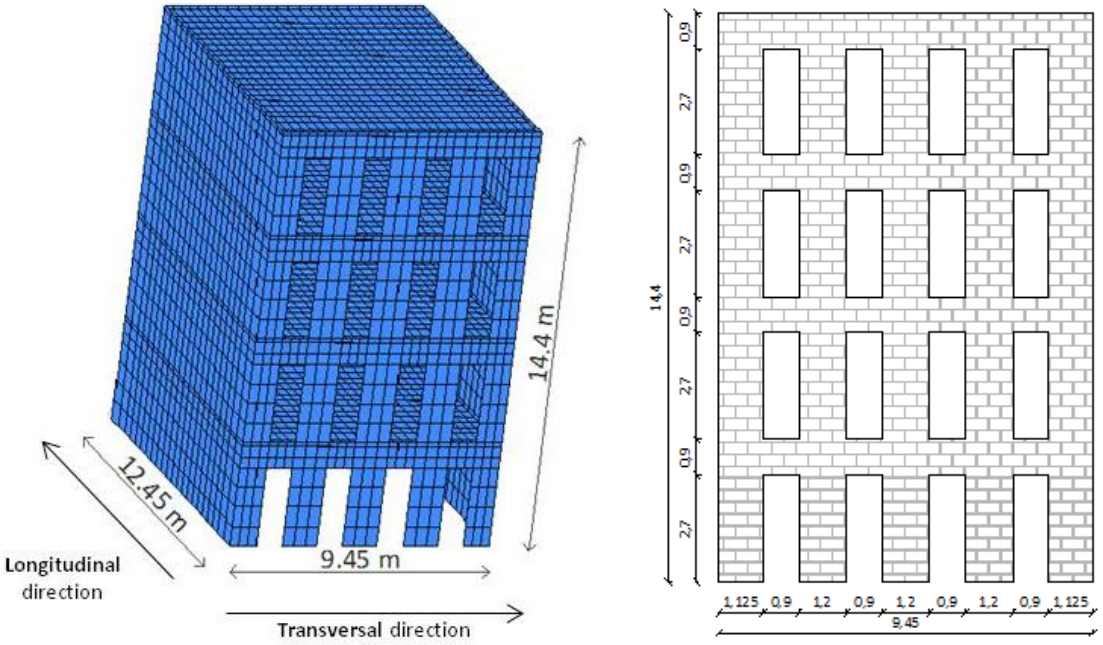

Figure 39 – Reference Model. a) Model and mesh of the walls and floors; b) Geometry.

The material characteristics that have been used as the reference for the modeling are given in Table 3.

Table 3 – Material properties.

	Young's Modulus *E* [GPa]	Density (kN/m^3)	Compressive strength *fc* [MPa]	Compressive fracture energy *Gc* [N/mm]	Tensile strength *ft* [MPa]	Mode I – Tensile Fracture energy *Gf* [N/mm]
Masonry walls	1.00	21.5	1.00	1.60	0.10	0.05
MDF panels	0.16	7.6	-	-	-	-
Wooden joists	12	5.8	-	-	-	-

4. REFERENCE MODEL RESULTS

4.1 INTRODUCTION

In this chapter the geometry, properties and results of the reference model which will be used as comparison for all the others will be presented.

Using the non linear dynamic analysis the damage associated with different earthquake intensities was tested for this model by applying increasing percentages of the code's seismic action - 25%, 50%, 100%, 150%, 200%, 250%, 300% . These analyses were done separately without considering the cumulative damage in between analysis.

4.2 DYNAMIC PROPERTIES

The results obtained for the reference model are presented in Table 4 and the deformed mode shapes are in Figure 40. The mode shapes presented in Figure 40 are intrinsic to the structure and represent in a way the deformed shape the structure will adopt during a dynamic excitation, as an earthquake. By the analysis of the results it is possible to see that the first mode (fundamental mode shape) has a frequency of 1.59 Hz and it will be a translation on the transversal direction, as it was expected since it is the less stiff direction; The presence of the openings on the façade walls and the lower dimensions of the walls in the transversal direction is contributing for the decrease of stiffness. A clear distortional mode with a frequency of 2.80 Hz will take place confirming the presence of flexible floors. This mode shape doesn't have any participation factor in both directions since the walls are rotating and distorting in opposite ways which means that the masses of the walls are "cancelling" the effect of each other. After the first mode in the transversal direction the structure will present a longitudinal mode shape with a frequency of 3.4 Hz and a mass participation factor of 19% on this direction (z direction); this is a local mode shape with a low contribution of the lateral walls and showing a single curvature of the façades. The second mode on the longitudinal direction is again a mode involving almost exclusively the façades but they are having an out-of-plane behaviour in out-of-phase. The 3rd Longitudinal mode f=4.89 Hz, 4th Longitudinal f=5.62 Hz and 5th Longitudinal f=6.09Hz are three modes showing the displacement and out-of-plane behavior of the façade all with a second degree curvature. The 4th Transversal mode (f=5.63Hz), however, is presenting finally a mode involving the deformation of the gable walls with a third curvature.

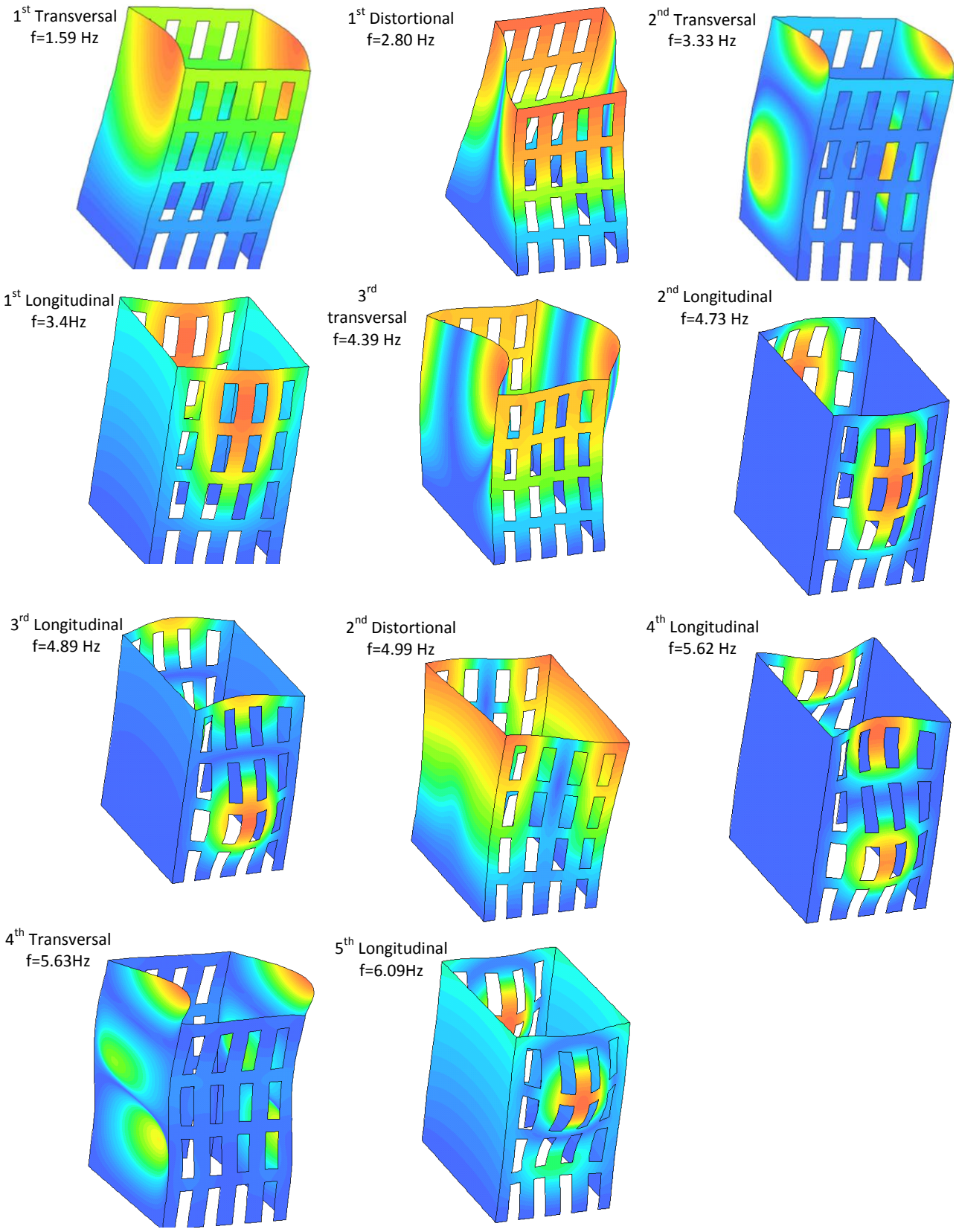

Figure 40 - Modes and frequencies obtained for the reference model.

Table 4 – dynamic analysis results for the reference model.

Mode shapes	Frequency (Hz)	Modal Participation Factor	
		TX %	TZ %
1st Transversal	1.59	21.98	0.00
1st Distortional	2.80	0.00	0.00
2nd Transversal	3.33	5.82	0.00
1st Longitudinal	3.40	0.00	19.72
2nd Longitudinal	4.73	0.00	0.00

Due to its deformable floors the structure is presenting a huge number of local mode shapes, associated with the vertical deformation of the floors, that will have no mass participation in the X (transversal) and Z (longitudinal) direction. These modes are not analyzed because they are not relevant. Thus, it is difficult to detect global translational or rotational modes of the structure as they will happen for a very high frequency – global modes are the stiffest ones. If they are happening for very high frequencies it means that the structure will not behave on this way, it will deform in different ways and, in the hypothesis of having a strong earthquake, it will collapse following the pattern of the mechanisms related with the first mode shapes. Some of the local modes are related with the curvature and out-of-plane of the façades. The curvature along the height of the building can be single, double or triple (similar with the global deformation of MDOF reinforced concrete structures).

4.3 NON LINEAR STATIC ANALYSIS

As discussed before, there are two methods to perform the Pushover analysis: Proportional to the mass of the structure and proportional to the first mode shape. Also, these two types of analysis were carried out in each orthogonal direction since there is expected a very different behavior and different seismic capacity in the longitudinal and transversal direction.

In Figure 41 the capacity curves in the two orthogonal directions are presented. When the two curves are put together in the same graph it is easy to directly detect the differences between the capacity of the structure to resist force in each direction. Independently from the method used to perform the non linear static analysis the longitudinal direction (along the gable walls) is much stiffer and resistant than the transversal direction; this difference is approximately 4 times more in the longitudinal direction comparing with the transversal one. This relative difference between both directions is the same using the forces proportional to the mass or to the first modal shape in each direction but the information about the maximum value of force capacity (seismic coefficient) is different.

In addition, it is perceptible by looking at the same graphs (Figure 41) that in the transversal direction the slope in the elastic and non elastic range is smoother than in the longitudinal direction. The initial slope of the graphs is indicating the elastic stiffness of the building. In the present case, the façade walls are much less resisting

and the initial stiffness in the transversal direction is K_1=43121 kN/m and K_1=27863 kN/m (first value for mass distribution second to modal shape distribution). After the first cracks these values are falling to K_2=15430 kN/m and K_2= 9809 kN/m; the slopes of the curves are different between the two approaches but the reduction from the linear state to the non linear with the presence of the first cracks is of about 65%.

On the contrary, the long gable walls without any openings have a initial stiffness of K_1=177559 kN/m and K_1=963207 kN/m (first value for mass distribution second to modal shape distribution) and are dropping to K_2=50308 kN/m and K_2= 33237 kN/m. So, it is possible to conclude that the initial stiffness in the longitudinal direction is almost 4 times higher than the transversal one, and after cracking the gable walls are losing around 70% of the original stiffness. The gable walls have the capacity to resist to very high values of horizontal load but, after reaching the maximum force, the walls will break suddenly and the collapse in this direction is fragile while the mechanism of In plane diagonal cracking of the façades in the transversal direction is much more ductile.

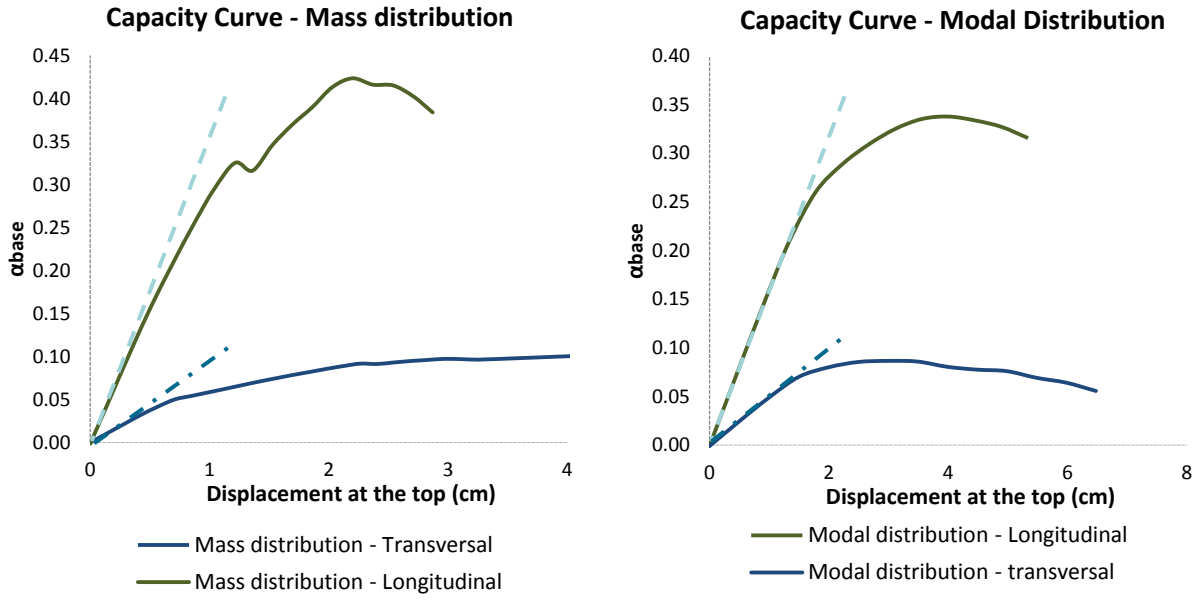

Figure 41 – Capacity curves obtained with the two different methods in each direction. a)Force proportional to the mass; b) Force proportional to the first mode.

The direct comparison between the two possible distributions of horizontal loads in the pushover method, on the two directions, is presented in Figure 42. Analyzing the results for the transversal direction, the maximum seismic force that the structure can resist using the modal force distribution is around 8.6% of the self-weight of the structure while with the forces proportional to the mass is just above 10%. When performing the pushover in the longitudinal direction and using the forces proportional to mass the resistance is over 42% and with the modal distribution is only 34%. The difference between the two methods is close to 20% which is noteworthy. What is concerning the displacement for the maximum force in the longitudinal direction, the

modal distribution approach is pointing a higher value, 3.9 cm, than the mass distribution approach, 2.2 cm. This difference is around 40%. The same happens in the analysis of the transversal pushover curve.

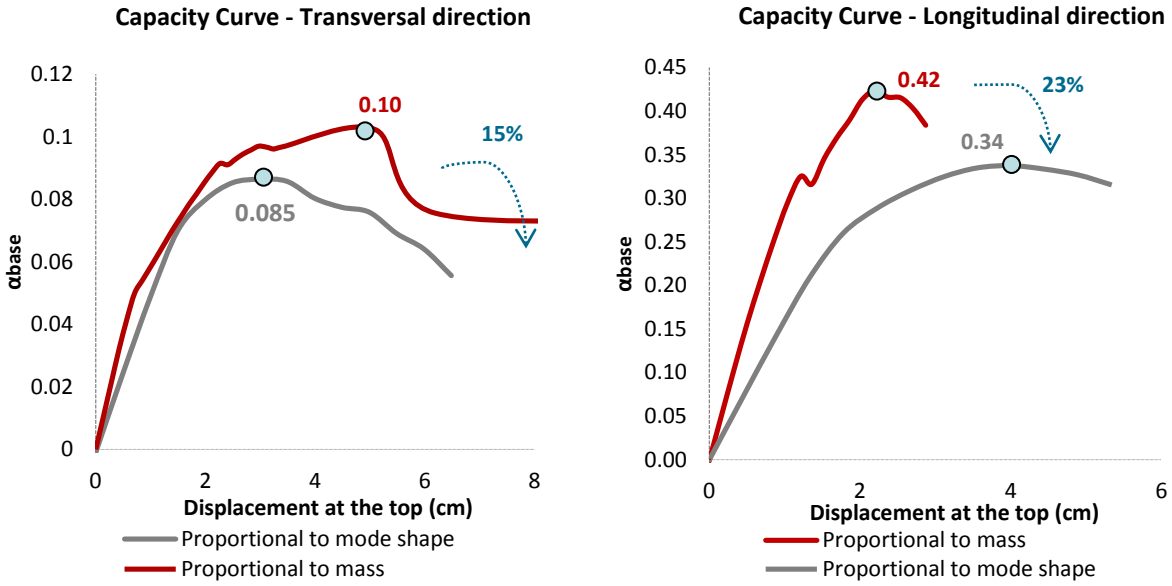

Figure 42 – Capacity curves for each pushover method. a)Transversal direction; b) Longitudinal direction.

In order to better understand the failure mechanism involved on the pushover analysis, the principal strain where studied, especially on the steps of the method where there was stiffness modifications. In Figure 43 the principal events of the pushover proportional to the mass in the transversal direction are indicated and in Figure 44 the correspondent principal strains are shown.

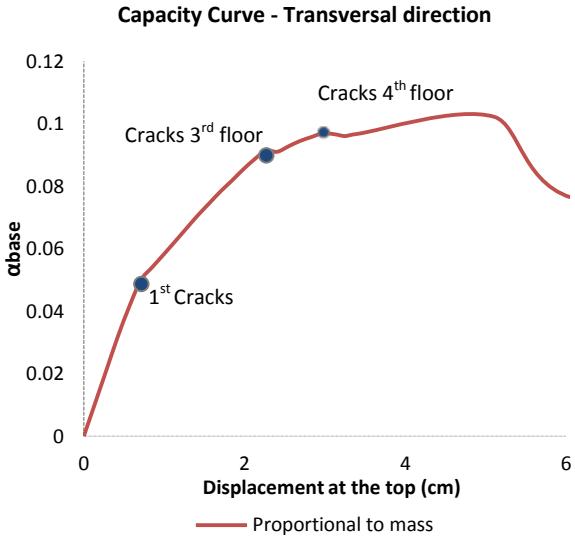

Figure 43 – Capacity curve and identification of failure points on the Transversal direction of the reference model.

The first stiffness slump is due to the formation of the first cracks on the bottom levels. These cracks are starting on the edges of the openings. After these cracks, the second slump is due to the continued development of the previous cracks and development of others on the 3rd floor (and one beginning in the last one). The stiffness will decrease again due to the formation of the cracks in the last floor; these cracks have different pattern and are spreading more on the horizontal – the in plane failure of this part will be by rocking and not diagonal cracking of the spandrels. In the end of the analysis the structure is not globally working anymore since the diagonal cracks located in the spandrels will take all the stiffness and resisting capacity of these elements and the piers will start working as cantilevers. As a consequence the stresses will increase at the base of these slender walls (Figure 44 c).

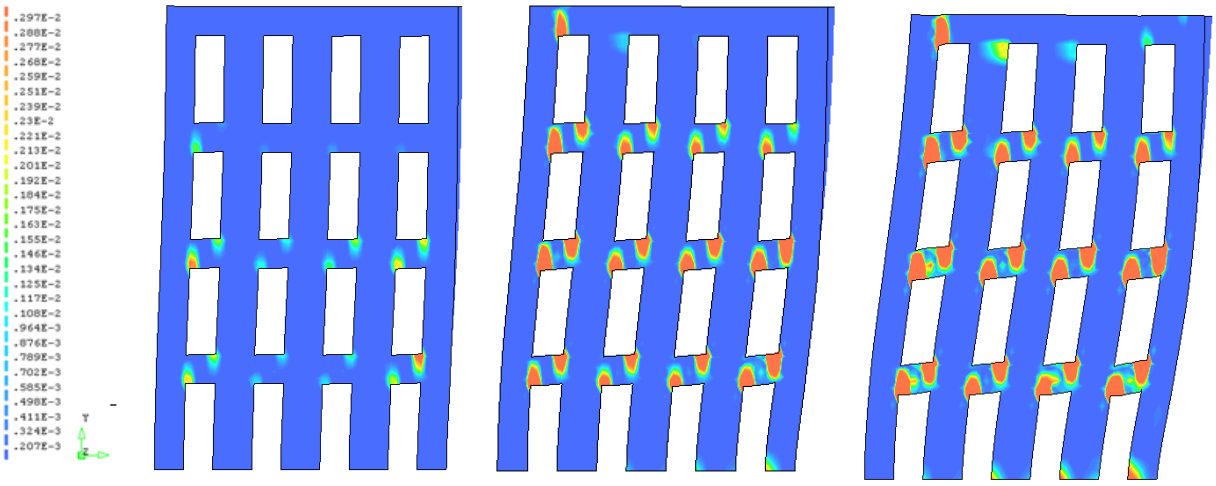

Figure 44 – Deformation and location of cracks. a)First cracks; b)cracks on the 3rd floor; c)cracks on 4th floor and base piers.

In Figure 46 the points of the pushover proportional to the mass in the longitudinal direction are exhibited and in Figure 44 the correspondent principal strains are presented. When one is applying increasing forces parallel to the gable walls, the first damage to become visible is a marked vertical crack going through almost al the height of the building located next to the corners; the gable wall is not able to follow the simple curvature out-of-plane deformation of the façade and the crack will start developing next to the corners due to compability problems between macro elements with very different stiffness. The vertical crack on the gable walls will allow the out-of-plane of the façade which is a similar mechanism of the one represented in Figure 45 b) .

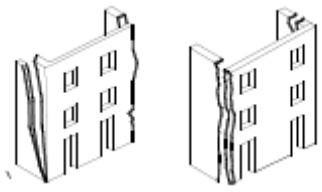

Figure 45 – Failure mechanisms associated with the façade. a) Out-of-plane of the façade; b) Detachment of the façade.

Some steps after another crack will develop on the opposite part of the gable wall (Figure 47 a). This crack will be concentrated on the bottom part and can be explained due to the boundary conditions defined. The walls are pinned to the soil and so they cannot rotate and when the façade is forcing this rotation damage is taking place. The extensive diagonal crack on the gable wall (represented in Figure 47) going from the middle height of the gable wall to the base of the gable wall can be a consequence of the same mechanism: the rotation of the opposite façade and the boundary condition will make the crack to appear. This last crack will incite the division of the structure into two macro elements and one can rotate with the center of rotation located on the bottom corner of the gable wall (see Figure 45 a).

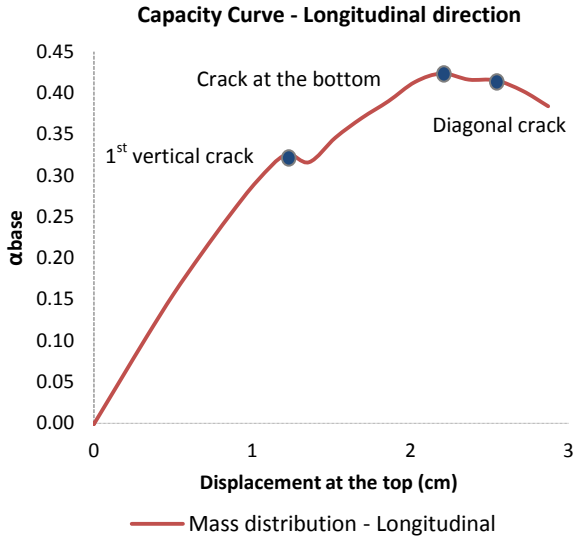

Figure 46 - Capacity curve and identification of failure points on the longitudinal direction of the reference model.

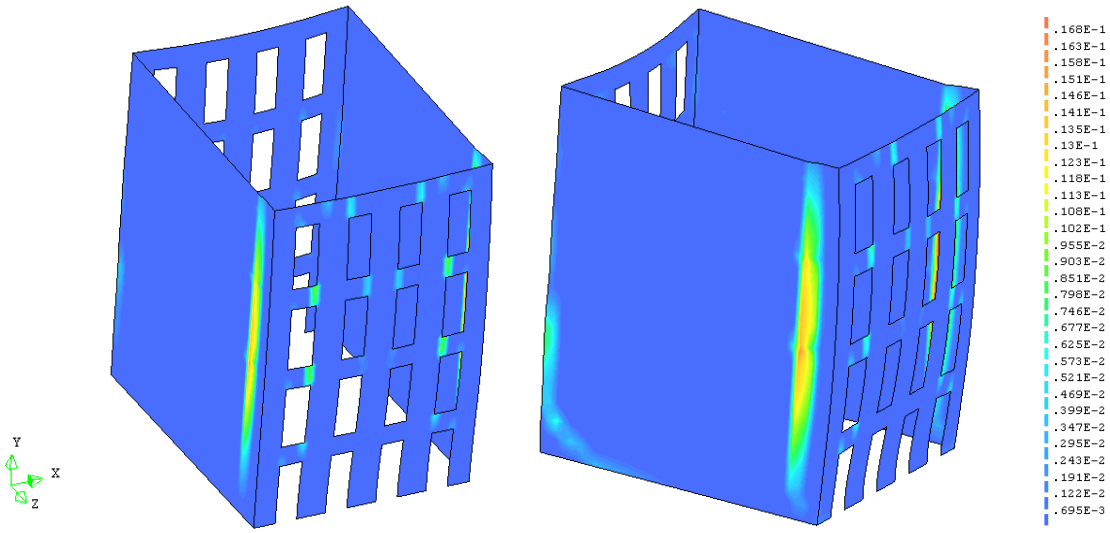

Figure 47 - Deformation and location of cracks. a)1st Vertical crack; b) Crack at the bottom.

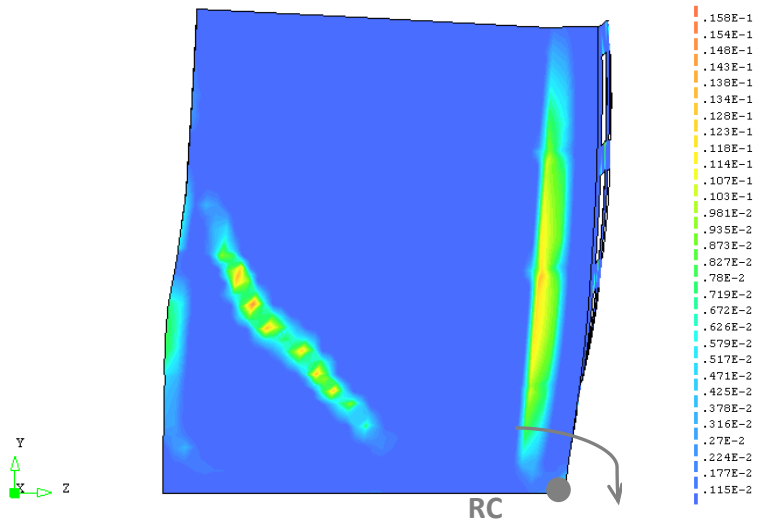

Figure 48 – Pattern and location of the diagonal crack on the gable wall. Rotation center of the macro element.

4.4 NON LINEAR DYNAMIC ANALYSIS

As the structure is symmetrical the results obtained for the out-of-plane displacement of both façades and gable walls is similar; consequently, it will only be presented the results referent to one façade and one gable wall.

The North Façade's out-of-plane displacement profiles are presented in Figure 49. The values of the displacements are, as expected, rising with due to the increasing earthquake loads. This increasing tendency is bigger from 50% to 100% and from 150% to 200%: the first gap is related with the development of the first cracks and the second one can be explained due to the accumulation of a lot of damage. The shape of the displacements profiles are following the deformed shape corresponding with the first longitudinal mode, which means that the displacement on the 3rd floor is bigger than the displacement at the top floor. After entering clearly on the non linear behaviour in height is changing and for 2, 2.5 and 3 times the code Earthquake the displacements is increasing almost linearly in height. According to the out-of-plane displacement profile of the façade the most relevant displacement variation is at the level base. This tendency is confirmed by the out-of-plane drift of the façade: the first level is the one with higher deformations.

The displacement of the top floor for 100% Earthquake is approximately 2.0 cm and this displacement will increase a lot until it reaches 8cm displacement for the biggest earthquake.

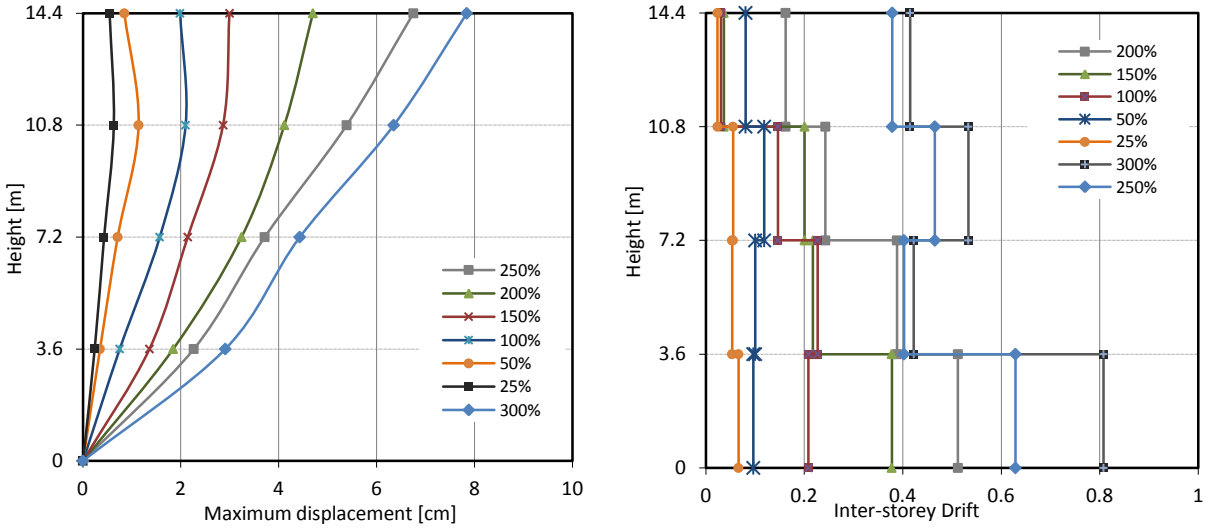

Figure 49 – a) Out-of-plane displacement of the North façade; b) Inter-storey Drift of the North Façade.

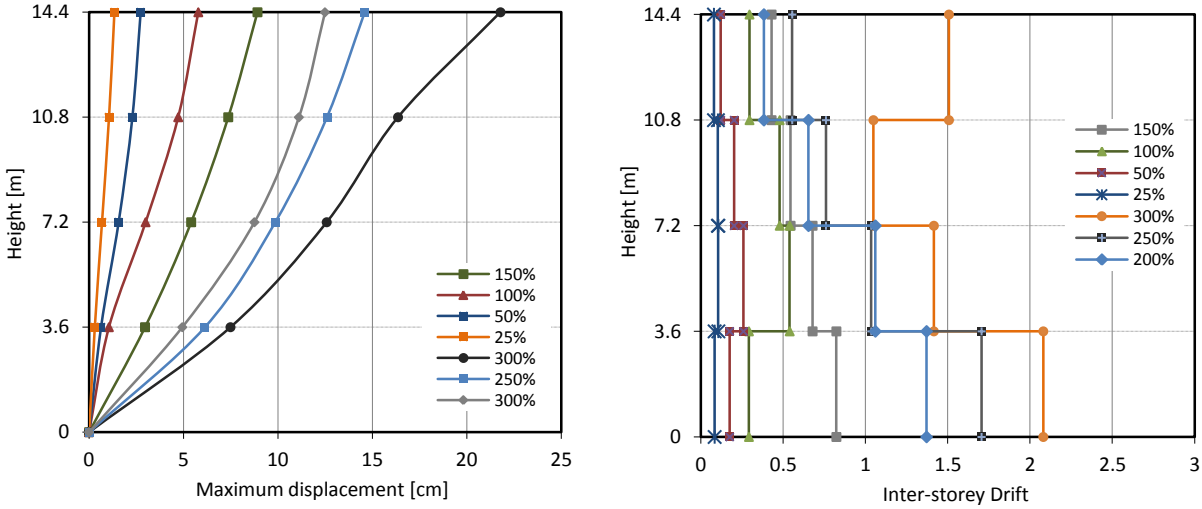

Figure 50 – a) Out-of-plane displacement of the East gable wall; b)Inter-storey Drift of the East Gable wall.

The out-of-plane displacement of the gable walls compared with the façades is significantly bigger: for 100%Earthquake the structure is reaching a displacement of approximately 5.80cm which is almost 3 times the displacement of the façades. This out-of-plane displacement of the gable walls is the result of a global behavior of the structure: the total displacement is the sum of the in plane transversal displacement of the façades plus the out-of-plane displacement of the lateral walls of the building. The façade walls are very flexible and are deforming and in a way “pushing” and forcing the gable walls to deform on the out-of-plane direction. Also it is necessary to consider the effect of the weight of the floors which is being supported by the lateral walls – more weight means more inertial forces and so more seismic forces on the walls.

The results of the in plane behaviour of gable walls and façades are the opposite of the out-of-plane since the in plane displacement profile of the façade is reaching much higher values than the in plane displacements of the gable walls. The top in plane displacement of the façade is, 2.2 for 50% Earthquake, 5.15cm for 100% and 8.1cm for 150% (see Figure 51 a). The structure is already presenting damage on the façades for 100% earthquake which means that the spandrels are already cracked for 5.15cm of in plane deformation. The displacements regarding the application of 200%, 250% and 300% are higher than 10cm (the maximum is 26 cm) which is too high; the structure will be completely damaged and deformed for this level of loads.

For lower values of horizontal load the inter-storey drifts are increasing from the base until the top but after having the damage, and being the damage concentrated more at the base, the inter-storey drifts at this level are the highest ones (Figure 51 b). After the 100% earthquake the increasing of the drifts is not proportional to the increasing of the horizontal loads which means that the structure is damaged and behaving in a non linear way.

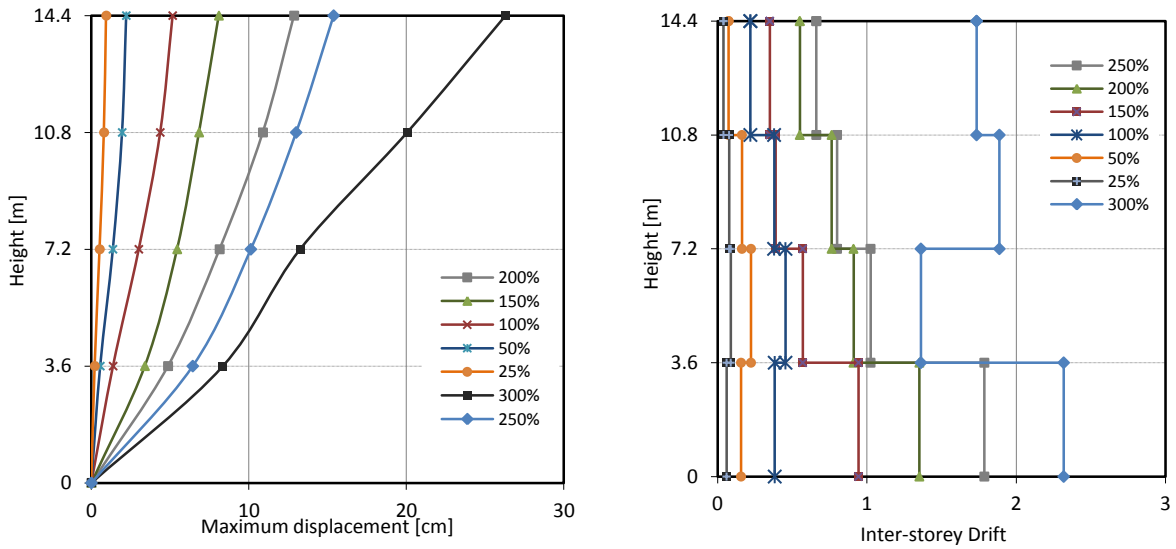

Figure 51 – a) In plane displacement of the North façade; b) Inter-storey Drift of the North Façade.

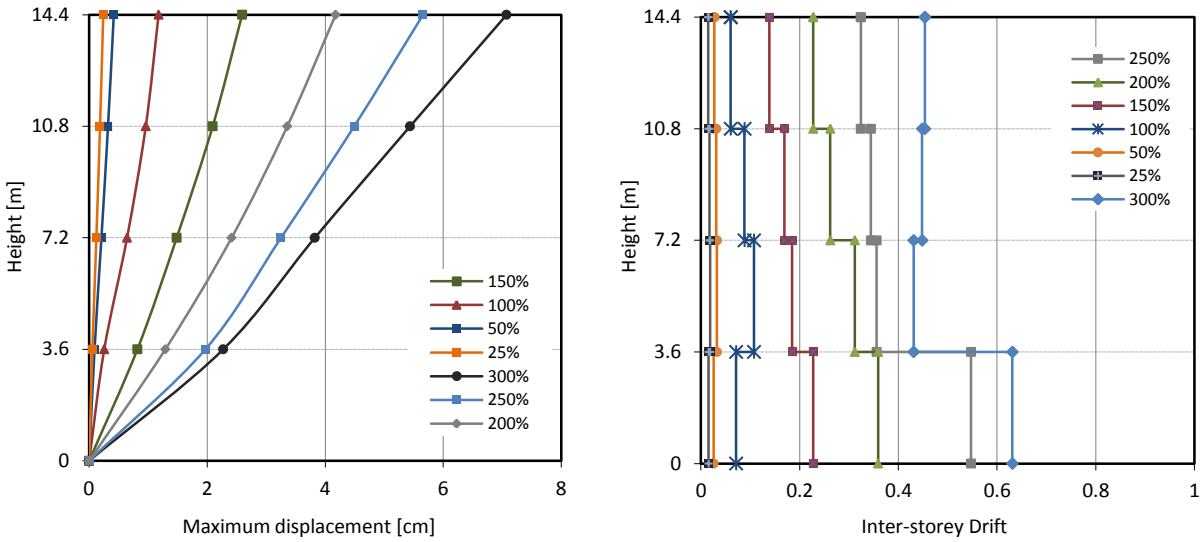

Figure 52 – a) In plane displacement of the East gable wall; b) Inter-storey Drift of the East Gable wall.

The in plane displacements profiles of the gable walls are linear as the first mode shape in this direction but are much lower (Figure 52 a). On this direction the gable walls are much stiffer than in the orthogonal direction because it is a long wall without any opening which is the opposite of what is happening with the in plane behavior of the façades. As a consequence, these lateral walls are only having a maximum displacement of less than 7.1 cm. Also the inter-storey drift is almost 4 times lower than the inter-storey drifts of the façades. These walls are still able to resist to more lateral loads and will only have damage for much higher seismic loads.

The results shown in Figure 53 and Figure 54 are the envelopes of the hysteretic behaviour relating the displacement of the node on the top floor with the horizontal seismic forces ($\alpha_{base} = \sum V_{base}/Weigh_{structure}$).

Figure 53 shows that in the transversal direction, for α_b approximately equal 0.10, the structure is reaching its maximum capacity to resist the seismic forces. This means that, for a seismic force of more than 10% of the self-weight, the structure is reaching the inelastic behavior and from that point onwards only the displacement of the structure is rising. As a consequence, one can conclude that for the transversal direction (less stiff one), the maximum capacity of the structure is reached for the earthquake indicated in the codes (horizontal load equal to 100% of the earthquake). The top displacement of the structure is suffering a dramatic growth from the 100% earthquake on, showing a clearly non linear relation between the variation of the force applied and the consequent displacement, which means that the structure is clearly already damaged from the 100% earthquake.

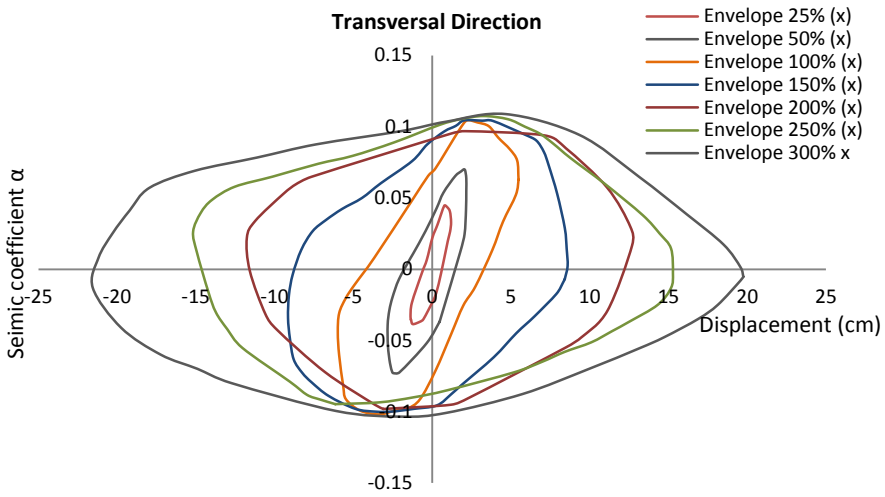

Figure 53 – Envelope of α_b results in the transversal direction.

The behaviour on the longitudinal direction is noticeably different from the transversal one, as it is visible in Figure 54. The gable walls are much more resistant than the façades and as a consequence, they are still capable to absorb much bigger earthquake loads. The damage will occur not for 100% earthquake but for approximately 200% earthquake, which is equivalent to α_b approximately equal to 0.35 (30% of the self weight of the structure).

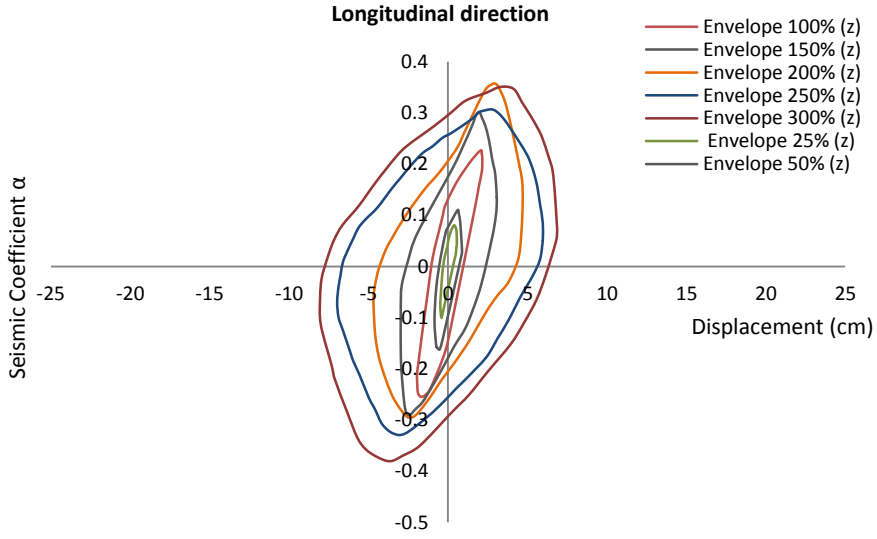

Figure 54 - Envelope of α_b results in the longitudinal direction

From the previous seismic coefficients envelopes' analysis it was concluded that the structure was already responding in a non linear range from the 100%Earthquake load onwards. This conclusion was taken since the structure from 0.10 of the self-weight was no longer absorbing more horizontal forces but was still deforming.

With the analysis of the maximum principal strains it is possible to detect where and how the structure has reached the failure and which points had achieved the tensile strength and cracked; from looking at Figure 55 it

is visible that the structural elements of the façade were already cracked for the 100% Earthquake load (on the transversal direction): the spandrels have experimented diagonal cracking which is more severe on the lower floors than on the upper floors. In Figure 55 it is possible to detect a change on the cracking patterns of the piers: the trend is changing from pure diagonal cracking (on the bottom piers) to horizontal cracking between the corners of two openings; the horizontal cracks are an indication of the in plane rocking behaviour of the top piers, due to low compressive stresses. Comparing with the experimental works this trend is a little bit less obvious since the weight of the roof was considered on the present numerical model.

After the cracking of the spandrels the structure is no longer working as a whole and the stresses and strains are now being only absorbed by the piers. If the spandrels are cracked the walls will have to work separately as cantilever walls with the dimensions of the piers. The walls are now working as cantilevers and so it is natural that the damage will be concentrated at the base, next to the foundations. This fact is evident on the image with the maximum principal strains of the structure subjected to 150%Earthquake; the huge difference on the regarding the damage accumulation from the 100%Earthquake to 150%Earthquake is precisely a consequence of the cracking of the spandrels on the previous stage of load – 100%Earthquake.

The damage at the base is a consequence of the boundary condition defined for the models; when the structure is subjected to the horizontal load the deformation at the base of the walls will be restricted (perfectly pinned to the soil) and the stresses will tend to accumulate here. This damage is severely increased from the 100%Earthquake to the 150%Earthquake.

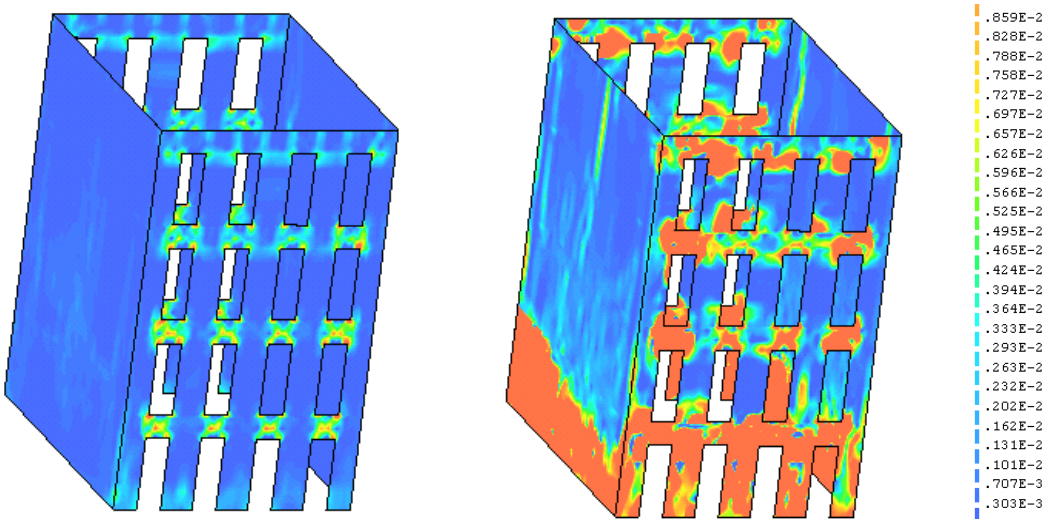

Figure 55 - Principal Strains (external surfaces of the walls) in the reference model. a) 100%Earthquake load; b) 150%Earthquake load.

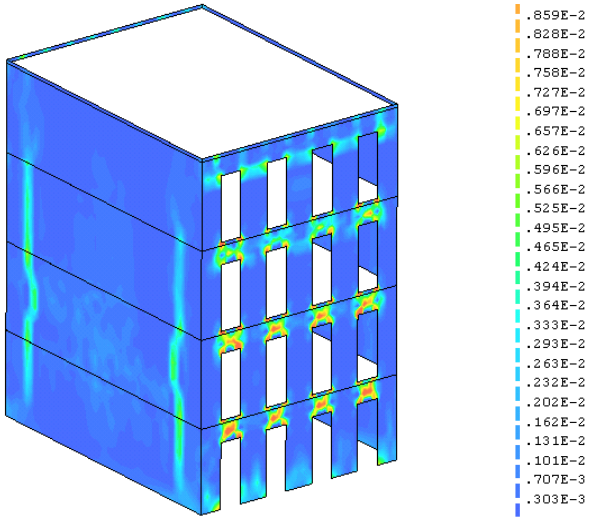

Figure 56 – Maximum Principal strains on the interior surface of the masonry walls for 100%Earthquake load.

In what concerns the behavior of the gable walls, it is possible to observe some still light vertical cracks in the external surface of the walls when the 100%Earthquake load is being applied but this damage gets evident on Figure 55 b). The gable walls are concentrating an evident damage on the base level, due to the same reason presented before. The analysis of the interior surface of the gable walls presents a concentration of damage next to the connection points between wooden floors' beams and the lateral walls (the connections were defined on the numerical model as perfect connections). The Young's Modulus of the floors is much lower than the masonry's Young's Modulus and so the deformation of the pavements and wooden joists is much higher creating a concentration of stresses on this connection points. The vertical cracks and concentration of stresses is higher next to the extreme beams since these wood joists are the ones having more weight.

Another qualitative analysis of the damage can be done using The European Macroseismic Scale (EMS): This scale denotes how strongly an earthquake affects a specific place. The classification is presented in Figure 57.

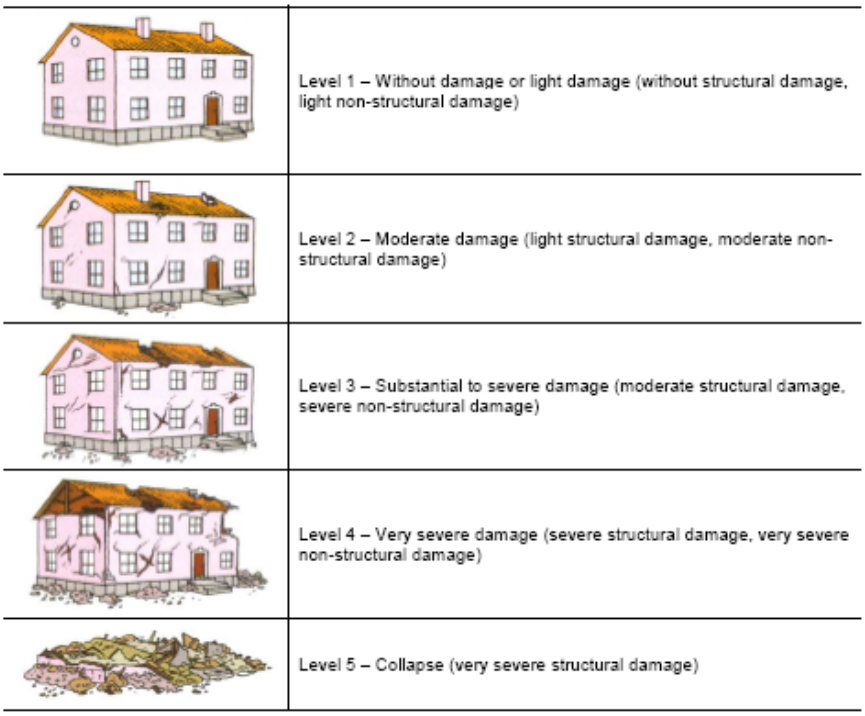

Figure 57 – Classification of damage on masonry buildings to be used in the calculation of EMS 98 intensities. (Simões & Bento, 2012) e (Lopes M. , 2008)

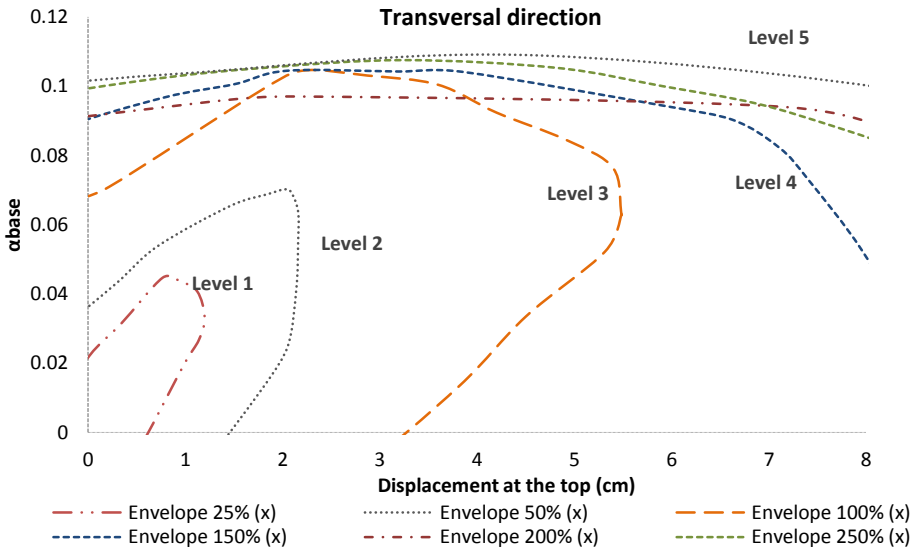

Figure 58 –DNL envelopes for different seismic intensities and grades of damage according to the European Macroseismic Scale 1998.

From the qualitative analysis of the principal strain the structure presents level 1 of damage for 25%, level 2 for 50%Earthquake, Level 3 for 100%Earthquake, level 4 for 150% and 200% earthquake and level 5 for 250% and 300%Earthquake, as represented in Figure 58.

4.5 COMPARISON BETWEEN NON LINEAR DYNAMIC AND STATIC ANALYSIS

The complexity involved on a non linear dynamic analysis and the numerical power needed to perform it was already pointed before. Nevertheless, this is still the best available seismic analysis, more accurate and close to the true behavior of the structure because it is able to consider the interaction between parameters and their variations are evaluated along the time. The question is if it is worth to use all this numerical power and time to get better results. Depending on the objective of the analysis, the accuracy of the static non linear analysis can be satisfying. For the static non linear analysis to be considered correct it should be close enough to the real behavior and resistance of the structure – obtained with experimental tests or numerically using the Time – History approach. The objective of this sub chapter is to compare the results of both analyzes in terms of resistance, displacement and failure mechanisms.

In terms of maximum resistance in the transversal direction the differences between non linear analyses are not very important (Figure 59), especially in the case of the pushover with forces proportional to the mass. The initial stiffness of both pushover analyzes are quite similar but the pushover with forces proportional to the mode shapes are too conservative. On the other hand, the pushover proportional to the mass is showing already some damage for horizontal loads equivalent to less than 50%Earthquake and the other approach is in elastic range on this point

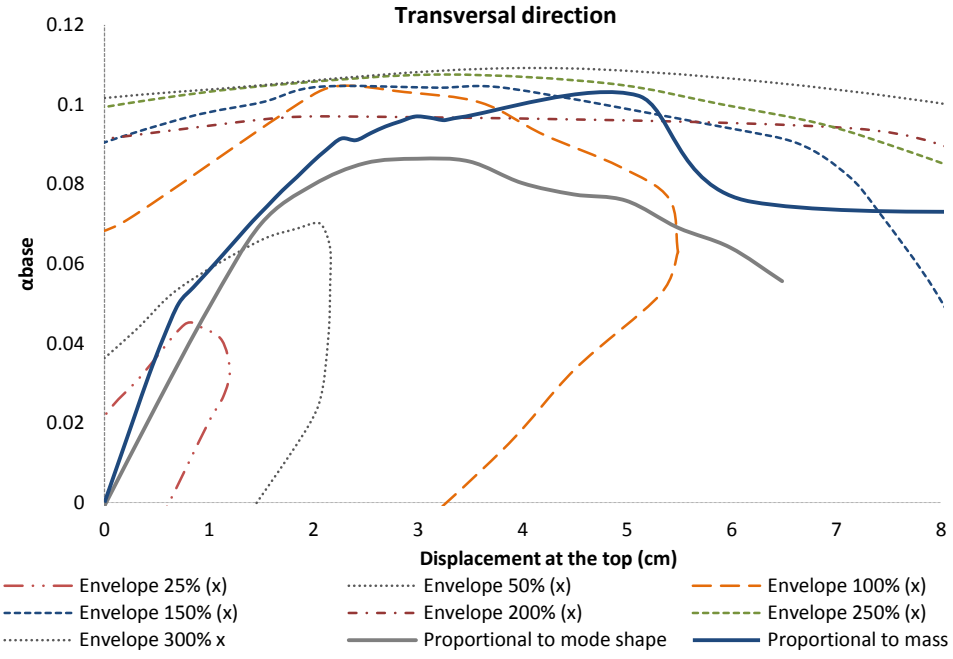

Figure 59 - Comparison between the pushover and time-history analysis' envelopes in the transversal direction.

In Figure 61 the principal strain state of the reference model for 300% earthquake is presented in order to compare the damage with the final step damage of the pushover analysis, presented before in Figure 44 and

Figure 48 (to compare qualitatively the results the scales are the same). From the images it is possible to see that the damage pattern is different, especially for the damage in the gable walls. The vertical cracks that are visible right on the first steps of the pushover analysis are also present for the non linear dynamic analysis applying the higher seismic intensity. In the non linear dynamic results two vertical cracks are presented because the loads are applied in both directions and with repeated cycles of loading and unloading and not only loading of the structure. The cumulative damage on the bottom part of the structure is also perceptible on both seismic analyses (even if there is more damage on the dynamic one). However, the vertical crack producing the out-of-plane of the façade and half the gable walls is not existent in the time-history analysis. Apparently there is an extra failure mechanism considered in the pushover analysis. In what concerns the damage and cracking of the façade, the pushover analysis seems to be construing the right failure mechanisms: the concentration of damage on the piers, the diagonal cracking of the spandrels and the horizontal cracks on the top floors due to the lower compressive stress on that part and consequent in plane rocking mechanism.

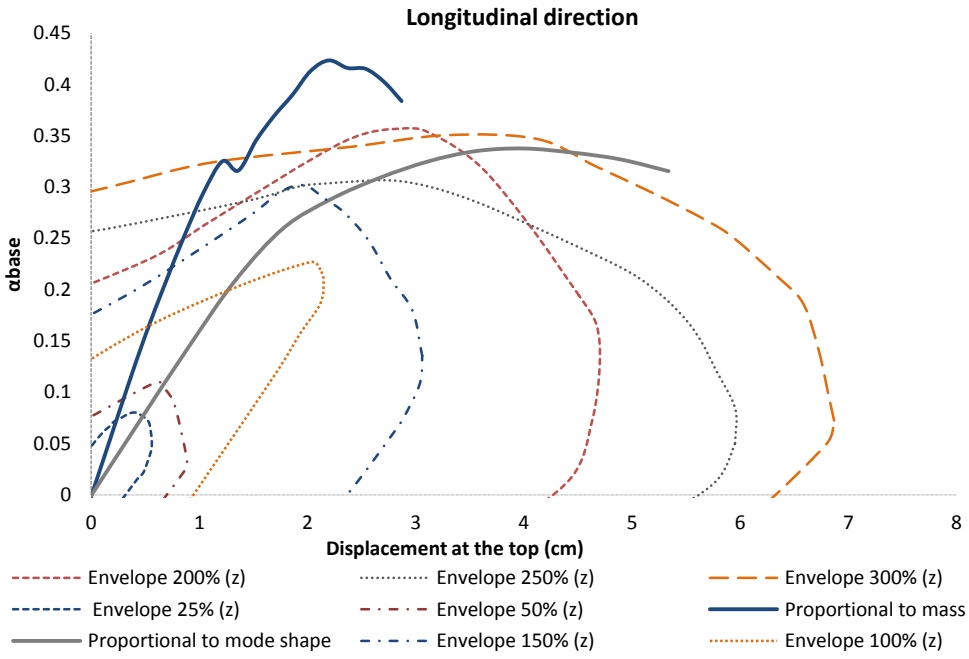

Figure 60 - Comparison between the pushover and time-history analysis' envelopes in the longitudinal direction.

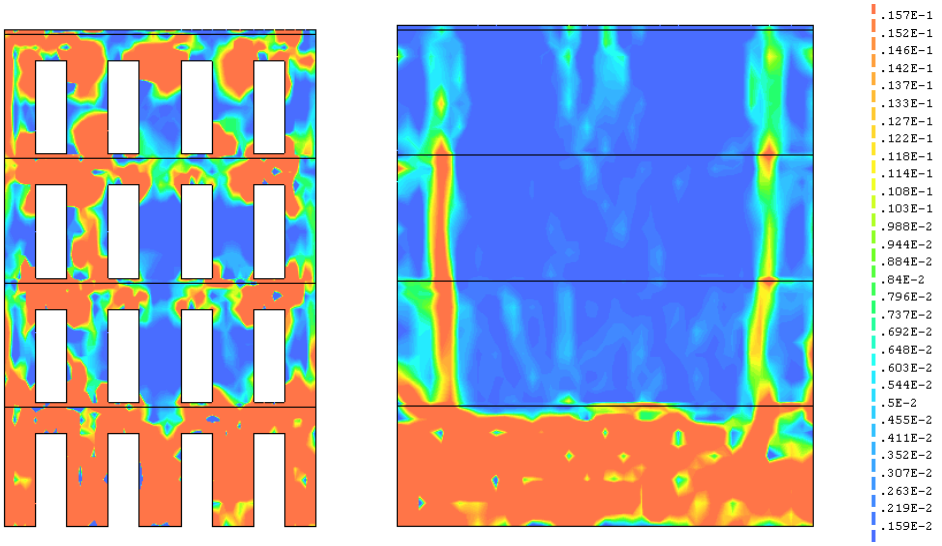

Figure 61 - Principal Strains (external surfaces of the walls) in the reference model for 300% Earthquake. a) Damage on the façade; b) Damage on the gable wall.

Generally, the dynamic non linear analysis seems to have more damage for the same applied force since the deformation is higher. This response and results are normal since on the Time-History the structure is being pushed and pulled in both directions. As a consequence, the damaged produced is more global and the structure will have simultaneously in plane and out-of-plane damage. Nevertheless, the pushover seems to reproduce adequately the behavior in the transverse direction (most vulnerable one), specially the pushover using the uniform load pattern.

5. SENSITIVITY ANALYSIS

5.1 INTRODUCTION

In the present chapter a parametric analysis will be carried out, aiming at determining the seismic sensitivity of the *gaioleiro b*uilding to different properties and geometries. Thus, the results obtained for the numerical models with variation of the geometry - model with 5 floors, model with 6 floors, model with short spandrels and model with slender piers – and the results regarding the models with different material properties will be presented and discussed. In the sensitivity analysis, the dynamic behavior was compared with respect to the results obtained from the non linear dynamic analysis of the reference model for 100% Earthquake. Based on the geometry of the reference model, described in the Section 3.7.1, the young's modulus of the walls and floors changed.

The results evaluated in each model are: the out-of-plane displacement in the middle vertical alignment of the façades and gable walls, the in plane displacement in the extreme vertical alignment of façades and gable walls, and the envelopes of the dynamic response (seismic coefficient at the base versus displacement at the top of the structure). In addition, the maximum principal tensile strains were also analyzed, in order to identify the points of the structure that present damage.

A factor taking into account the total weight of the structure, named on this thesis as *seismic coefficient* - α_{base}, was calculated presented in equation (12). This factor will be related with the maximum displacements reached during the non linear dynamic analysis to define the maximum force resistance of the different models and structures.

$$\alpha_{base} = \frac{\sum V_{base}}{Weight_{structure}} \tag{12}$$

All the models were prepared based on reference model, by changing in each model only one parameter of the geometry so that it would be possible to understand the influence of each parameter on the seismic behavior of the structure. The definition of the new parameters was based on the characteristics that can be observed on the *gaioleiros* buildings and are described in Candeias (2008) and Appleton (2005).

The geometry variations happened only on the façades. The gable walls were kept the same thickness (0.51m) and without any openings. The implantation area was also not changed 12.45x9.45m^2. The height, on the other hand, changed in order to study the behavior of higher buildings. The geometry of the floors, composed of MDF panels, remained the same for all the models except for the case where the objective is to analyze the sensibility of the structure to the variation of the Young's Modulus of the floors. Several solutions for the floors

were evaluated, namely: building without floors, increasing of the thickness of the floors by including an extra layer of wood panels (double thickness), and replacement of the wooden slab by a RC slab.

The reference model, presented in the previous chapter, has 649 ton. The maximum value for masonry's compressive strength defined on the model is 1.0 MPa. Subjected only to permanent loads and live loads (for the service load combination) the maximum stresses at the base of the reference model is 330 kPa, which corresponds to 33% of the maximum compression strength. To determine the stress at the base of the models, a linear static analysis was carried out and the vertical stress where considered at the middle of the gable wall. This value allows the determination of the percentage of maximum compressive force is being explored when applying only the self weight and live loads. The results are presented in Table 5.

Table 5 – Stresses at the base for the different models (Linear static analysis).

Model	Weight (ton)	σy (KPa)	Compressive strength fc (kPa)	σy/fc (%)
Reference	649	330	1000	33.0
Model with 5 floors	831	445	1000	44.5
Model with 6 floors	999	533	1000	53.3
Model with short spandrels	687	356	1000	35.6
Model with slender piers	625	363	1000	36.3

5.2 NUMERICAL RESULTS AND ANALYSIS

5.2.1 Variation of the number of floors

The numerical model with 5 floors has exactly the same properties and characteristics of the reference model, but one extra floor was added. As consequence, the self-weight of the structure increased for 831.36 ton. The generated mesh was also the same as the one generated for the reference model and it is presented in Figure 62 along with the geometry.

The next model has 6 floors, a total high of 21.6 m and a total self-weight of 999 ton. By observation of the current *gaioleiro* stock buildings in Lisbon, there are a lot of tall buildings with 6 floors, two more than it was considered for the reference model, and so it was considered to be important to study also the response for 6 floors. Nevertheless, to say that this is the current situation does not mean that the buildings were like that originally; some of the floors that one can see presently could be added later. The mesh followed the same strategy of the one explained before (Figure 63).

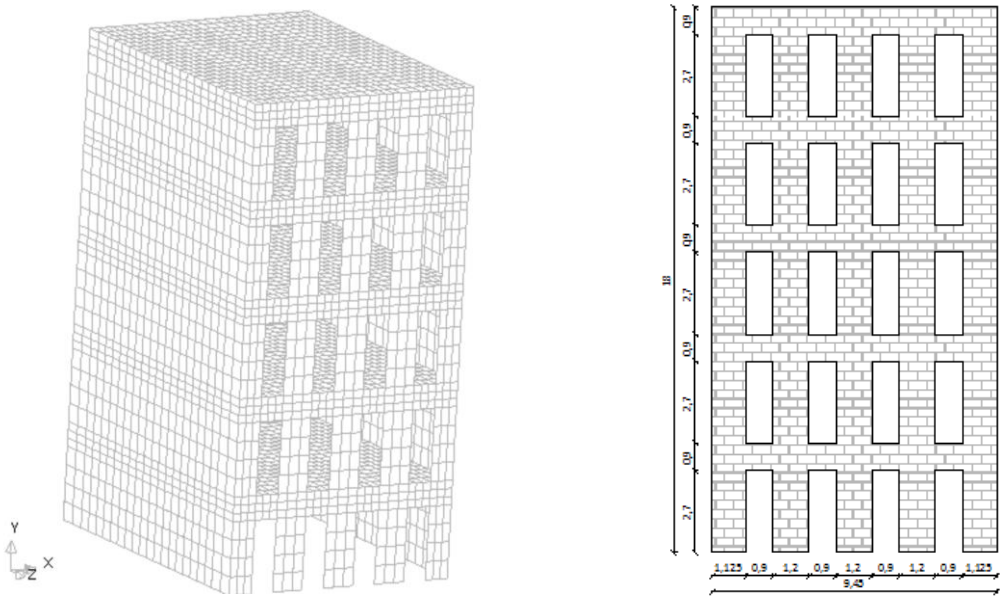

Figure 62 – Model with 5 floors. a) Model and mesh of the walls and floors; b) Geometry.

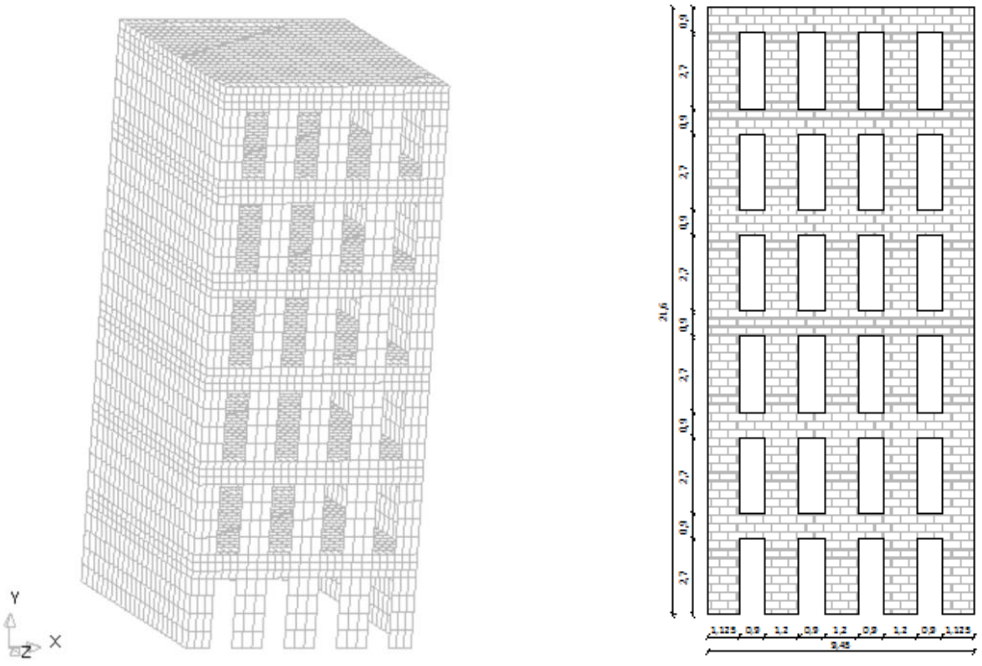

Figure 63 – Model with 6 floors. a) Model and mesh of the walls and floors; b) Geometry.

5.2.1.1 Dynamic properties

Different geometry means variation of the masses and different stiffness of the structure, which will influence directly the dynamic properties. From the values presented in Table 6Table 6 and by the mode shapes presented in Figure 64 some conclusions maybe taken.

Table 6 – Mode shapes, frequencies and modal participation factors of each model type.

	Mode shapes	Frequency (Hz)	Modal participation factor TX %	TZ %
Model with 5 floors	1st Transversal	1.29	25.59	0.00
	1st Longitudinal	2.80	0.00	0.24
	1st Combined	2.82	7.94	0.00
	2nd Transversal	4.16	5.04	0.00
	1st Distortional	4.46	1.14	0.00
	2nd Longitudinal	4.75	0.00	6.39
Model with 6 floors	1st Transversal	1.07	27.97	0.00
	1st Longitudinal	2.21	0.00	25.86
	1st Distortional	2.26	0.00	0.00
	2nd Transversal	2.50	9.40	0.00
	1st Combined	3.41	0.00	0.00
	2nd Longitudinal	4.52	0.00	9.13

The models with a higher number of floors are presenting a lower frequency value as expected. In the case of the 5 floors model and 6 floors model, the 1st longitudinal is equal to f=2.82 Hz and f=2.21 Hz, respectively. Similarly to the reference model, the new model present distortional shape modes. These mode shapes are associated to the deformable wood floors. Due to the same reason, there are a lot of local mode shapes that are associated with the vertical behavior of the floors.

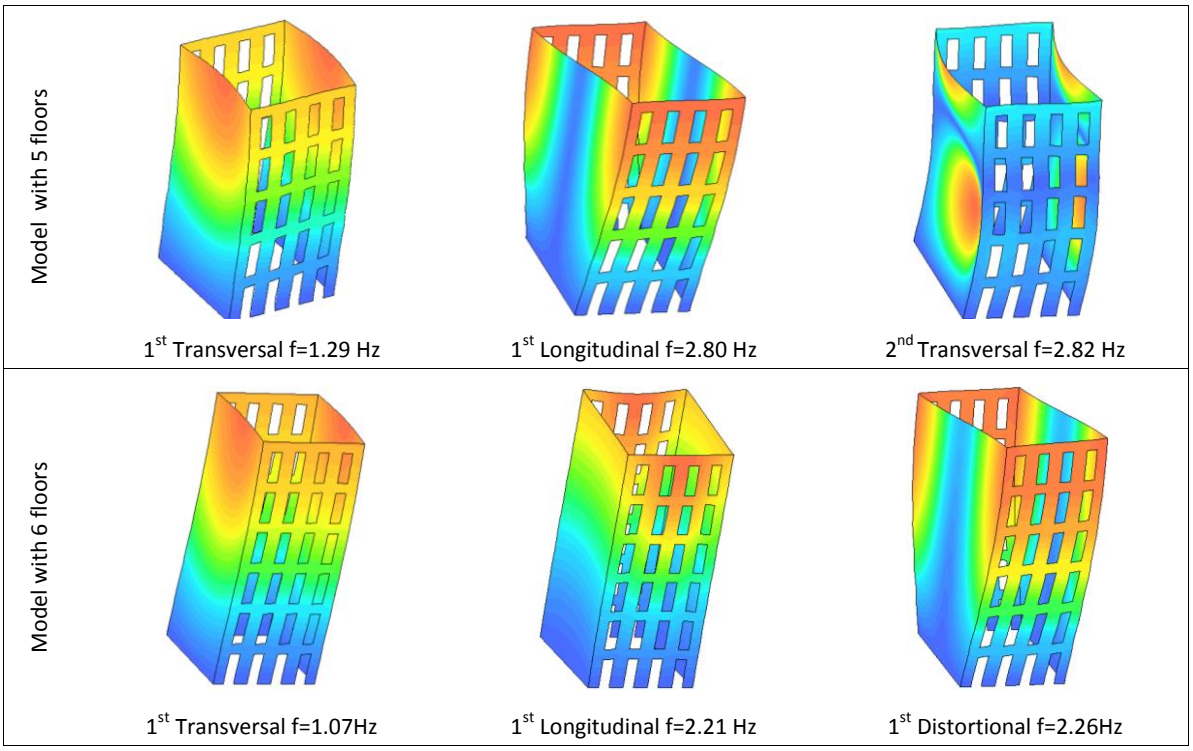

Figure 64- Mode Shapes of model with 5 floors and 6 floors.

5.2.1.2 Dynamic non linear analysis results

As expected, the damage produced by the 100% Earthquake is higher for the tallest building. The façade's out-of-plane behavior is showing a significantly high displacement of the structure presenting 6 floors. For the same model, a peculiar displacement profile was obtained with a very high inter-storey drift in the first two floors. This was a consequence of the concentration of damage (see also Figure 69) on the two first floors and so the top floors had the possibility to deform more easily. This behaviour was not repeated for the reference model nor for the model with 5 floors. Both models have similar in plane displacements of the façade and are higher than the ones obtained for the reference model. The gable walls are also having high displacements but, as discussed before for the case of the reference model, this is a global displacement.

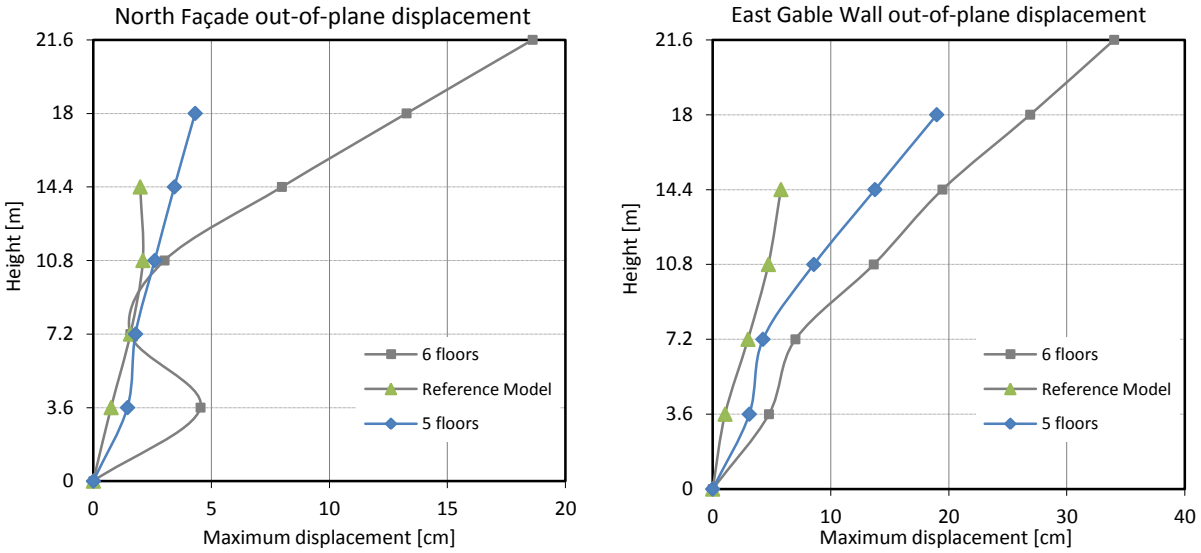

Figure 65 - Out-of-plane displacements at middle of the walls for models with different number of floors. a) Out-of-plane displacement of the North façade; b) Out-of-plane displacement of the East gable wall.

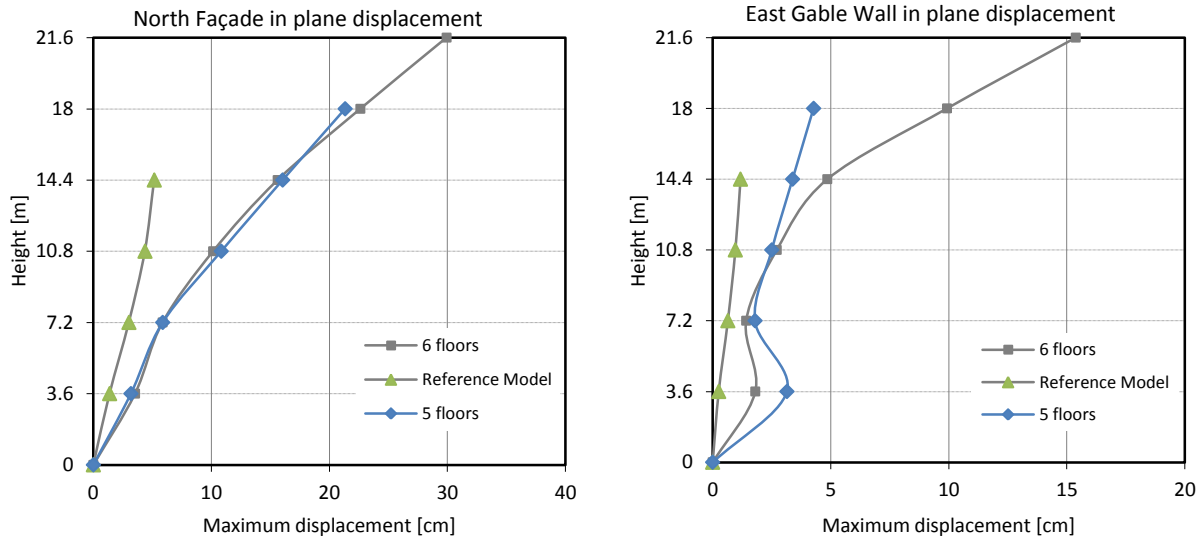

Figure 66 – In plane displacements for models with different number of floors. a) In plane displacement of the North façade; b) In plane displacement of the East gable wall.

The envelopes of the response (Figure 67 and Figure 68), in terms of displacement, are showing a considerable increase both in the transversal and longitudinal direction (more deformable structure). The displacements for 100% Earthquake are already too high showing that the structure is no longer presenting a linear response. The increase of mass in height increase the inertial forces and the capacity of the structure in force changed, in the transversal direction (Figure 67), to about 50% of the value obtained with the reference model. This difference is even bigger for the model with 6 floors (decrease until 0.04). In the longitudinal direction (Figure 68) the

force capacity has also decrease a lot (from 0.23 to 0.14 in the case of the model with 5 floors and 0.12 in the case with 6 floors).

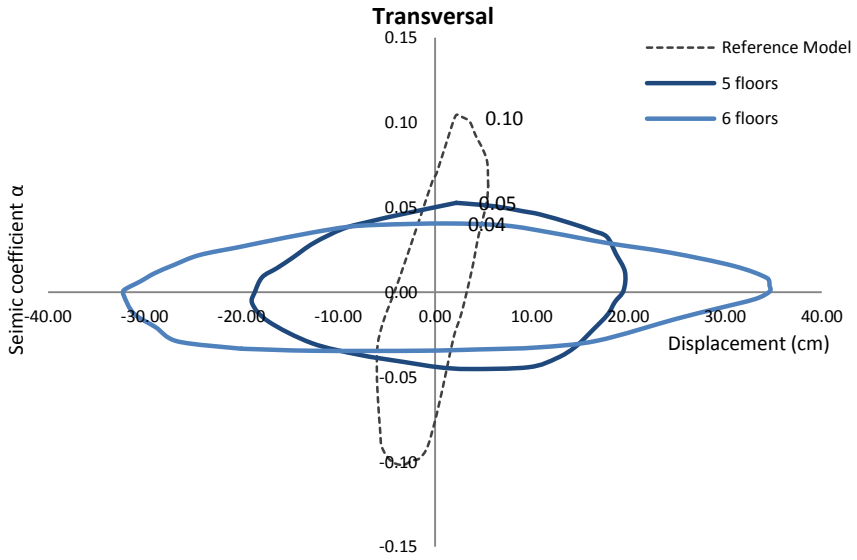

Figure 67 - Envelope of the response obtained from the non linear dynamic analysis in the transversal direction. Variation of the number of floors.

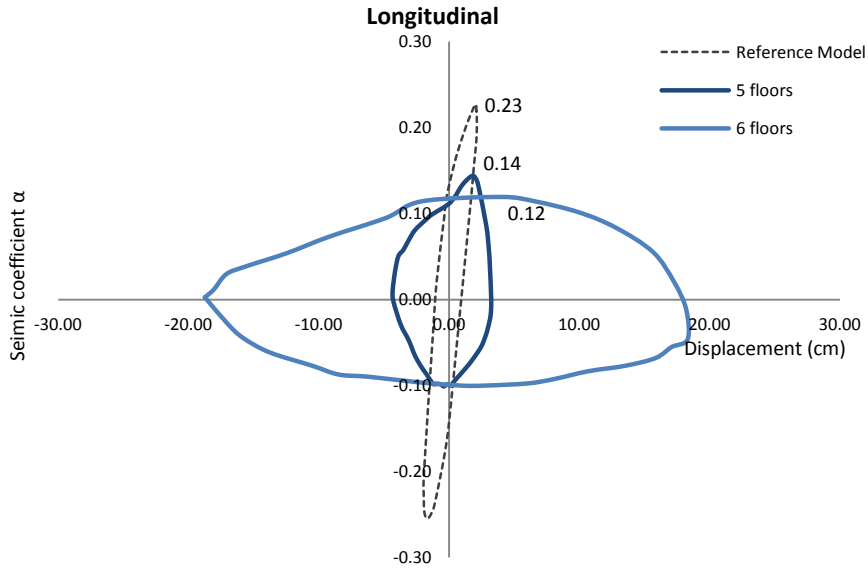

Figure 68 - Envelope of the response obtained from the non linear dynamic analysis in the longitudinal direction. Variation of the number of floors.

The model with 6 floors presents, for the horizontal loads equivalent to the 100% Earthquake, a concentration of damage at the base. The piers at the top level are already presenting damage, showing the beginning of the in plane rocking mechanism – the high damage on the spandrels is making the piers to work alone and to carry all the loads. As a consequence the loads have to be redistributed only through the piers going to the

foundation. The reference model for this level of load is not presenting this high damage concentration at the base, even if the failure mode seems to be the same because the model is lighter.

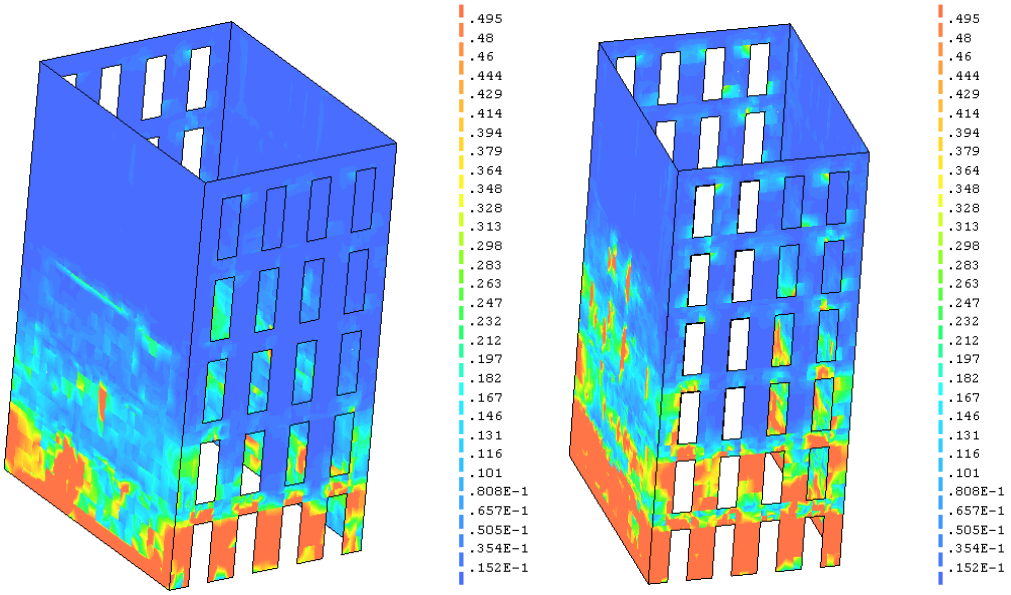

Figure 69 – Maximum tensile principal strains obtained from the dynamic non linear analysis. a) Model with 5 floors; b) Model with 6 floors.

5.2.2 Variation of the spandrel ratio

The ratio between high and length of piers and spandrels of the reference model is equal to 2.25 and 1.00 Eq. (13) and Eq. (14), respectively. For studying the influence of the spandrel ratio, two new models were prepared: model with short spandrels (Figure 70) and model with slender piers (Figure 71). For the in plane behavior of unreinforced masonry buildings, the ratio between the height and the length of spandrels and the geometry of these structural elements is very important, since they effluence the type of collapse mechanism.

$$Ratio\ of\ piers = \frac{Height}{Length} = \frac{2.7}{1.2} = 2.25 \quad (13)$$

$$Ratio\ of\ spandrels = \frac{Height}{Length} = \frac{0.9}{0.9} = 1.00 \quad (14)$$

It is well known that these parameters are controlling the response and, if the pier is weak and the spandrels strong, the cracks are concentrated in the piers and vice-versa. Nevertheless, it is important to understand the influence of these ratios, in the particular case of this structure. For the model with short spandrels (model 3) the ratios applied are the ones presented in Eq. (15) and the generated mesh and geometry is presented in Figure 70. For the case of model 3 the height of the spandrels were increased significantly. The total weight of the model is 687.2 ton.

$$Ratio\ Piers = \frac{Height\ Piers}{Length\ Piers} = \frac{2.0}{1.2} = 1.67 \quad (15)$$

$$Ration\ Spandrels = \frac{Height\ Spandrels}{Length\ Spandrels} = \frac{1.6}{0.9} = 1.78 \quad (16)$$

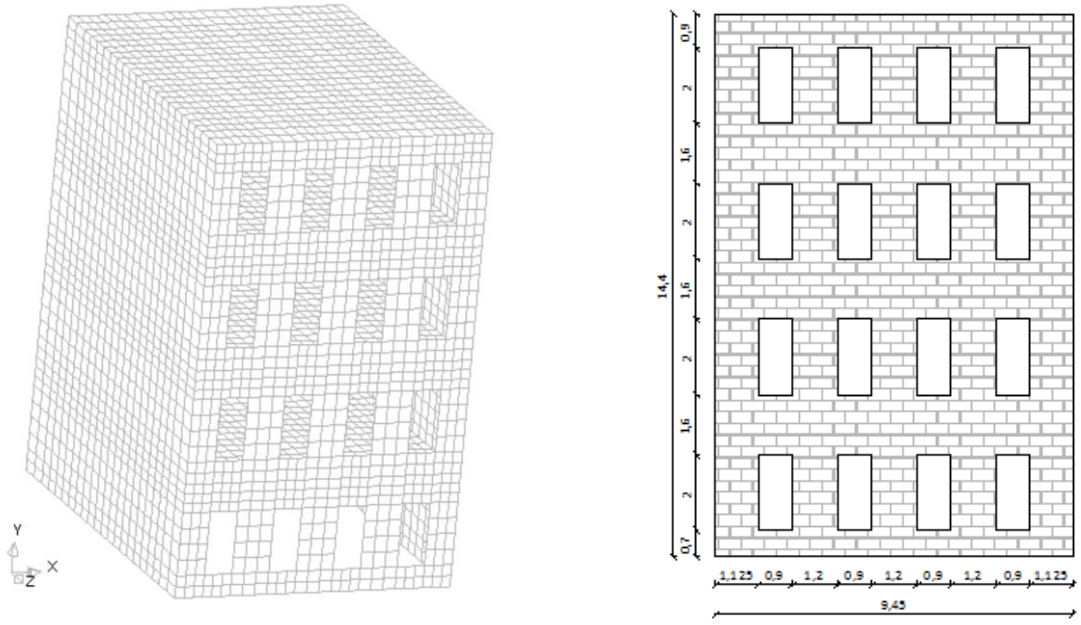

Figure 70 – Model with short spandrels. a) Model and mesh of the walls and floors; b) Geometry.

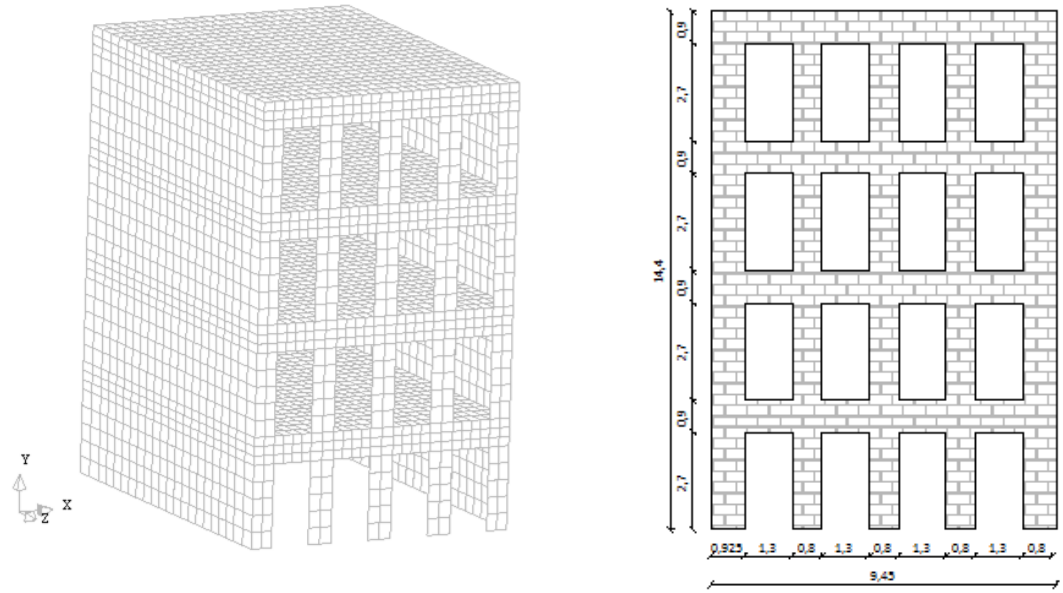

Figure 71 – Model with slender piers. a) Model and mesh of the walls and floors; b) Geometry.

For the case of the model with slender piers the percentage of openings increased and the piers became much more slender, as it is shown in Eq. (17) and Eq. (18). The total weight of the model is 625.2 ton. As the geometry changed the mesh had to change also, but the strategy to define it remained the same..

$$Ratio\ of\ piers \quad = \frac{Height}{Length} \quad = \frac{2.7}{0.8} = 3.38 \tag{17}$$

$$Ration\ of\ spandrels \quad = \frac{Height}{Length} = \frac{0.9}{1.3} = 0.69 \tag{18}$$

5.2.2.1 Dynamic properties

Different geometry means variation of the masses and different stiffness of the structure, which influence directly the dynamic properties. From the values presented in Table 7 and by the mode shapes presented in Figure 72 some conclusions were made.

In what concerns the fundamental mode shape, most stiff is the one presenting robust spandrels, due to the reduction of openings on the façade. The frequency of this model increased, meanings that the short spandrels and the variation of the openings are giving to the structure more stiffness comparing with the relative adding of the mass. The reference model presents stiffness in between the model with strong resisting in plane elements (short spandrels) and the one having weak piers (slender piers).

Table 7 – Mode shapes, frequencies and modal participation factors of each model type.

	Mode shapes	Frequency (Hz)	Modal participation factor TX %	TZ %
Model with short spandrels	1st Transversal	1.92	22.81	0.00
	1st Distortional	3.41	0.41	1.50
	2nd Transversal	3.44	0.00	0.00
	1st Longitudinal	3.56	0.00	19.30
	1st Combined	4.94	6.27	0.17
	2nd Longitudinal	5.23	0.15	3.59
Model with slender piers	1st Transversal	1.21	22.46	0.00
	1st Distortional	2.53	0.69	0.00
	2nd Transversal	2.99	6.79	0.00
	1st Longitudianal	3.56	0.00	17.41
	3rd Transversal	4.54	3.54	0.00
	2nd Longitudianal	5.24	0.00	3.64

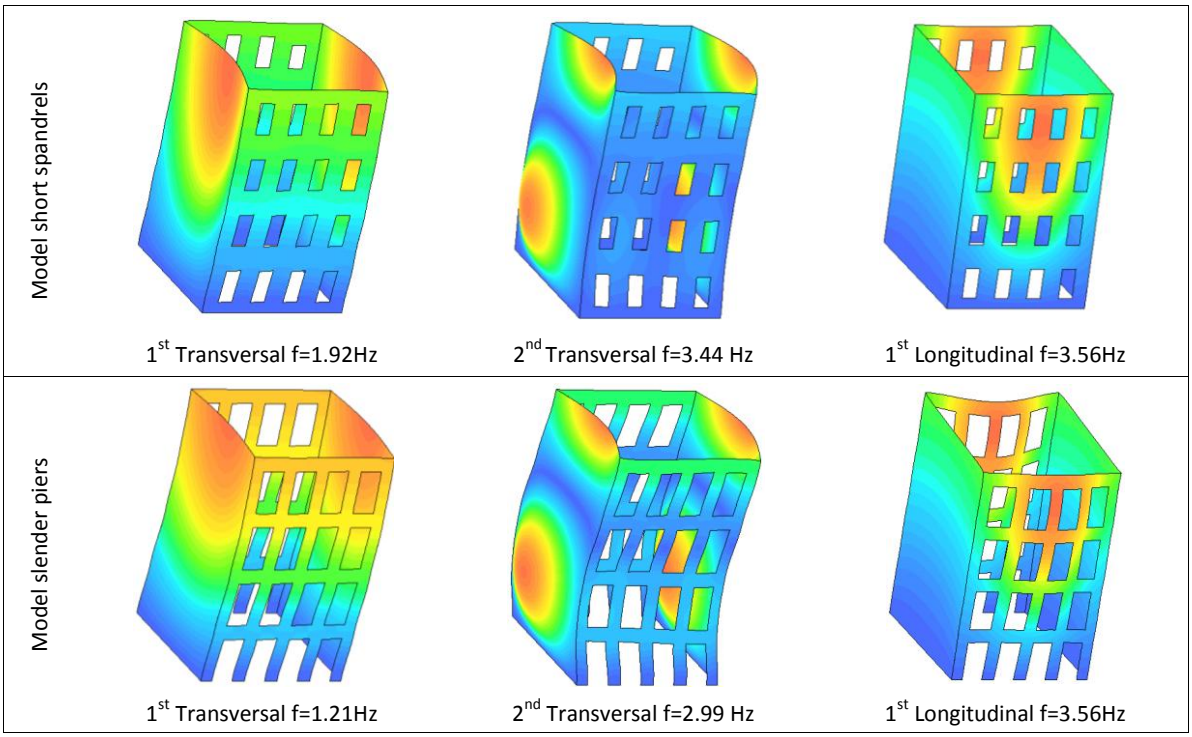

Figure 72 – First mode shapes of model with short spandrels and model with slender piers.

For both geometries, the modes in the transversal direction are connected simultaneously with local behavior of the gable walls like the out-of-plane and the curvature in elevation: first mode in transversal direction is presenting a simple curvature of the gable walls, second mode shape in the transversal direction shows a double curvature of the gable walls and the third one a triple curvature of the gable walls in height. Comparing the results obtained for the models with 4 floors, the frequency of the 1st longitudinal mode is not being much influenced by the geometry of the façades because the stiffness along the gable walls is the same and it is not influenced by the variation of the percentage of openings on the façades. The longitudinal mode shapes are producing the curvature of the façades: first longitudinal mode shape is happening along with the first curvature in phase of the façades, second one simple curvature of the façades vibrating in out of phase, and so on.

Similarly to the reference model, some distortional shape modes are detectable. These mode shapes are due to the deformable wood floors. Due to the same reason there are a lot of local mode shapes that are associated with the vertical behavior of the floors.

5.2.2.2 Dynamic non linear analysis results

In Figure 73 the North Façade's out-of-plane displacements in height are presented. The comparison between the maximum top displacements of the three models is giving very similar results. As a consequence, one can conclude that the different spandrel ratios are not having a fundamental influence on the top maximum displacement. The model with short spandrels and the reference model are having the same top displacements

and even analogous displacements profiles – both to the first longitudinal modal shape deformation. This means that, in the longitudinal direction, the stronger spandrels are not making a huge difference. If the control point was in the third floor a bigger difference would be noticed.

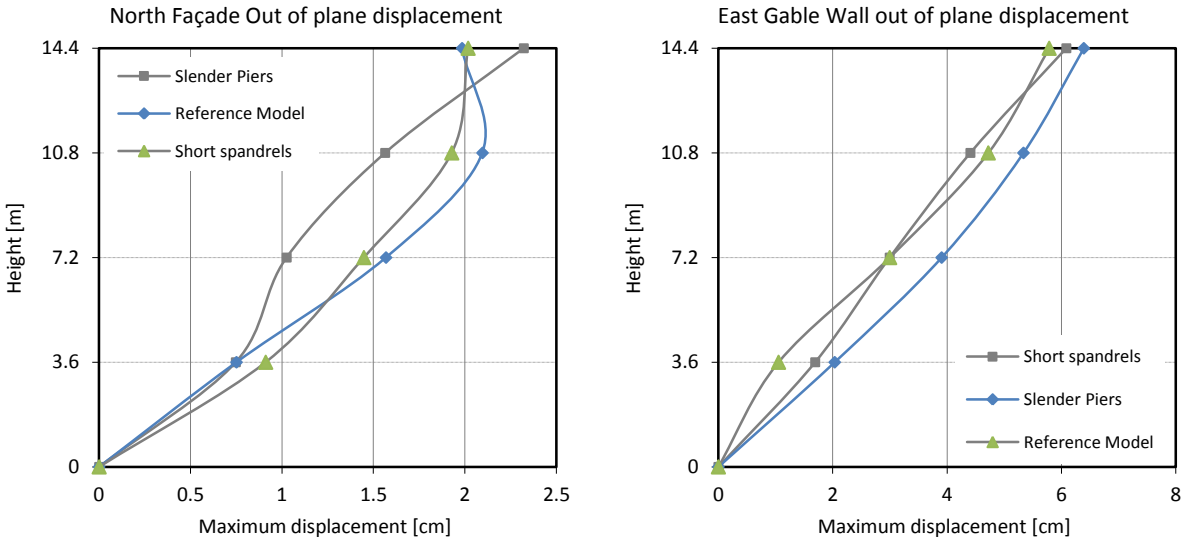

Figure 73 – Out-of-plane displacements at the middle of the walls for variation of the spandrel ratio. a) Out-of-plane displacement of the North façade; b) Out-of-plane displacement of the East gable wall.

The values obtained for the out-of-plane behavior of the gable walls are more than three times bigger than the out-of-plane of the façades. Even if the gable walls are exactly the same for the three analyzed models the values and behavior is different, because this displacement is highly influence by the in plane behavior on the transversal direction. The out-of-plane is depending on the in plane deformation of the façades, which means that the model with the bigger percentage of openings is having also a bigger out-of-plane of the gabble walls. This phenomenon was already commented in Section 4.4. Nevertheless, the difference between the three top values is around 5% which is not very meaningful.

For the in plane behaviour, the percentage of the openings is influencing slightly more the difference on the top displacements of the structure. However, for the in plane maximum displacement of the façade the difference is between 5.15 cm and 6.57 cm (less than 1 cm). The reference structure and the structure with slender piers are presenting a closer curvature in elevation and it was expected that the reference structure would have a displacement in between the other two values. The drift is experience a decrease value on height for the slender piers and also for the reference model but the short spandrels' drift is actually higher on the top (Figure 74).

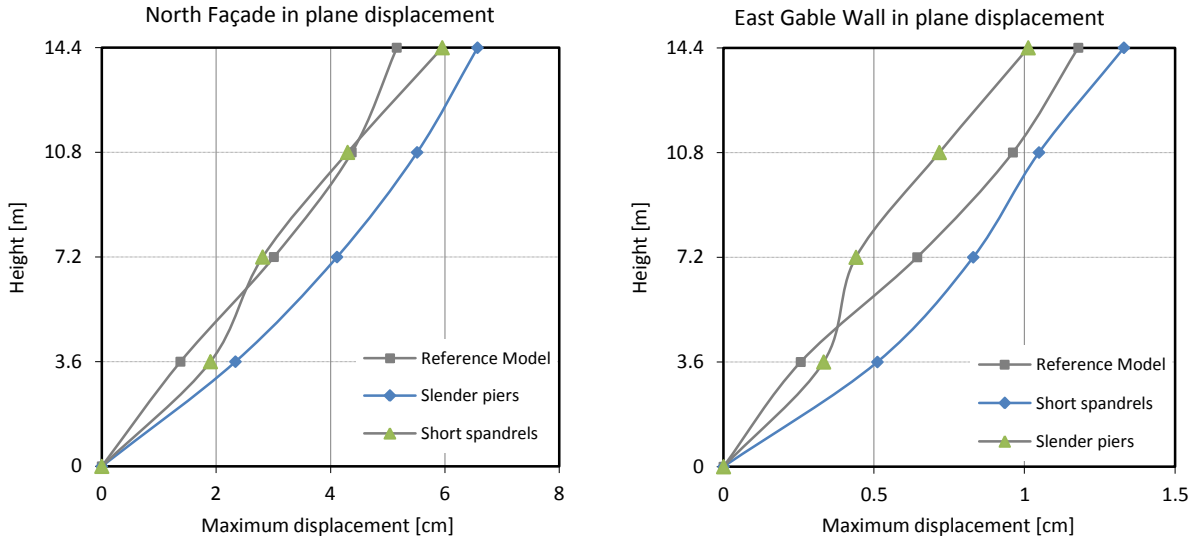

Figure 74 – In plane displacements for variation of the spandrel ratio.a) In plane displacement. of the North façade; b) In plane displacement of the East gable wall.

Figure 75 and Figure 76are showing the envelopes of the hysteretic non linear dynamic response of the three models, where the influence of the spandrel ratio and percentage of openings was analysed. In Figure 75 it is possible to observe that the value of the maximum strength is higher for the model with the short spandrels and much lower for the model with slender piers, as it was expected. In the transversal direction the most important structural elements giving resistance to the structure are the spandrels and the piers, as a consequence, if the model is presenting a bigger spandrels it will have more capacity to take loads before presenting the diagonal cracks (in plane failure of the façades). The maximum seismic coefficient for the most resisting model is equal to 0.12 (12% of the self weight) and for the model with more area of openings is 0.05 (4.9%), which means that the value changed for half. The structure with slender piers is much less stiff and will crack much earlier, developing a mechanism where the piers have to work individually as cantilevers and will only deform and not take any more horizontal loads (model presenting a top displacement of 6.58 cm, which is the highest of the three). Consequently the in plane resistance of this type of structure is extremely dependent of the spandrel ratio and slenderness of the piers.

In what concerns the behaviour of the structure in the longitudinal direction, by looking at the graph presented in Figure 77 it seems like the behaviour both in terms of maximum force and maximum displacement is not very influences by this parameter; but to a level of loads of 100% it is not possible to be sure since the structure is still not reaching the failure.

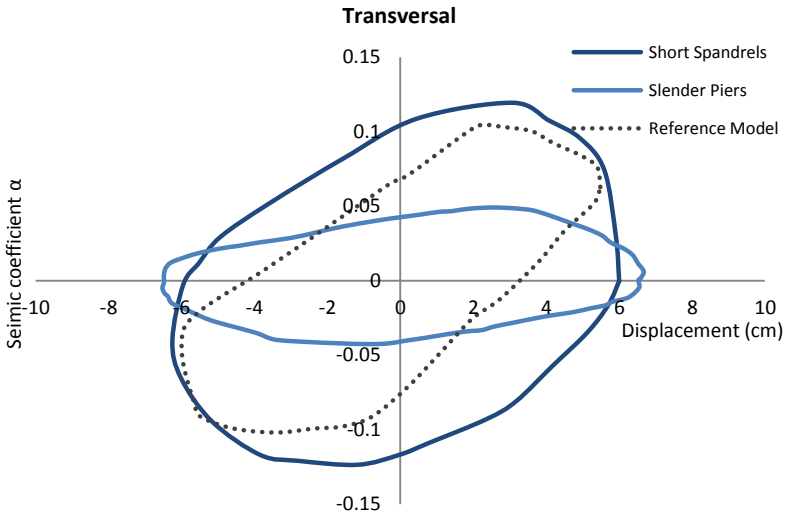

Figure 75 - Envelope of the response obtained from the non linear dynamic analysis in the transversal direction: Variation of the spandrel ratio.

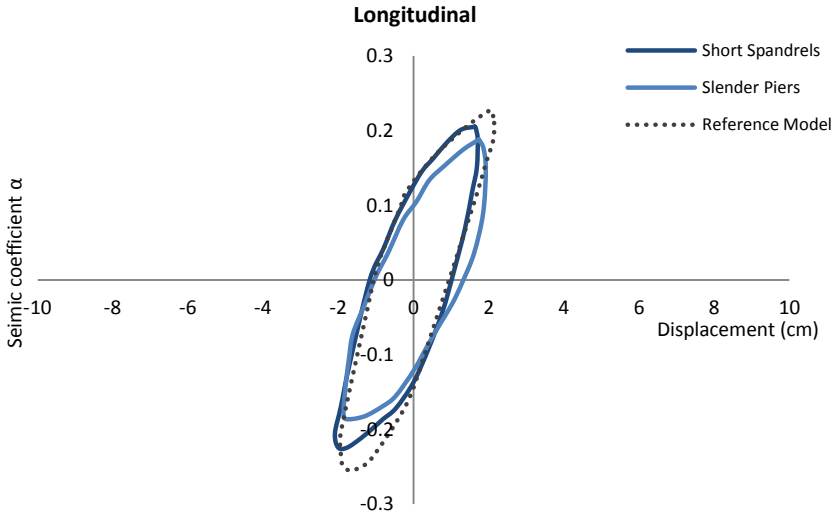

Figure 76 - Envelope of the response obtained from the non linear dynamic analysis in the longitudinal direction: Variation of the spandrel ratio.

The principal tensile strains are presented in Figure 77. For the model with short spandrels the diagonal cracks are still not obvious while in the model with slender piers the concentration of damage is starting in all the singular points as the corners of the windows. The damage is higher in the gable wall of the stiffer model. However the piers of the façade show an accumulation of damage at the base. It is possible to conclude that the dynamic response of the short spandrel model is better for the in plane failure of the façade and it is presenting more damage in an element which has more resistance.

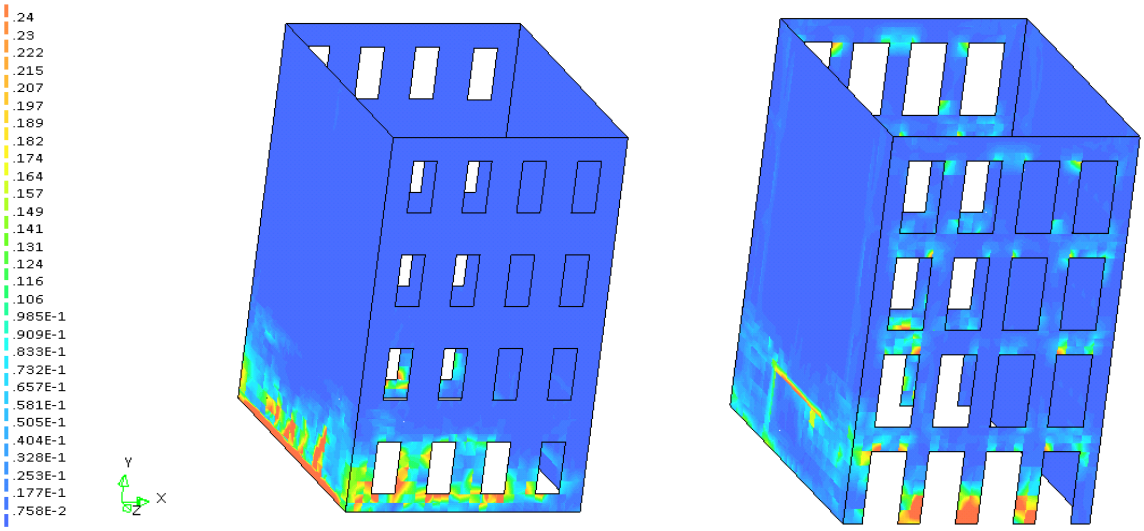

Figure 77 – Maximum tensile principal strains obtained from the dynamic non linear analysis. a) Model with short spandrels; b) Model slender piers.

5.2.3 Variation of the Young's modulus of the walls (Ewalls)

In this sub-chapter the influence of the stiffness of the masonry walls on the behavior of the structure under a seismic action will be analyzed. This way the two new models, one with E_{walls}=0.5 MPa and the other E_{walls}= 4.0 MPa will be compared with respect to the reference situation. The lower value is characteristic of low quality masonry and the higher one is close to the value obtained by (Mendes, 2012) on the experimental tests of masonry walls.

5.2.3.1 Dynamic properties

The stiffer model is the one with higher Young's modulus as expected and the one with the higher frequency or the first mode. The first frequency of the reference model is equal to 1.59 Hz. When the E_{walls} is changing to 0.5 MPa the frequency becomes 1.17 Hz and when E_{walls}=4.0 MPa the frequency is increasing to f=2.02 Hz. For both variations the first mode is still a mode on the transversal direction.

5.2.3.2 Dynamic non linear analysis results

The value of the Young's modulus has influence on the deformability of the walls and consequently the global deformability of the structure. The variation of the Young's modulus is not making the displacements to decrease or increase proportionally to the variation in respect to the reference model, but it is highly influencing the response. For example, if the E_{walls} is four times higher then the top out-of-plane displacement of the façade is approximately decreasing to 60% and if the E_{walls} is half it becomes me 70% higher. From the displacements profiles (Figure 78 and Figure 79) it is possible to notice that all the walls, in both directions, are highly influenced by this parameter, as expected. Nevertheless, it the façade's in plane displacement is the one changing more.

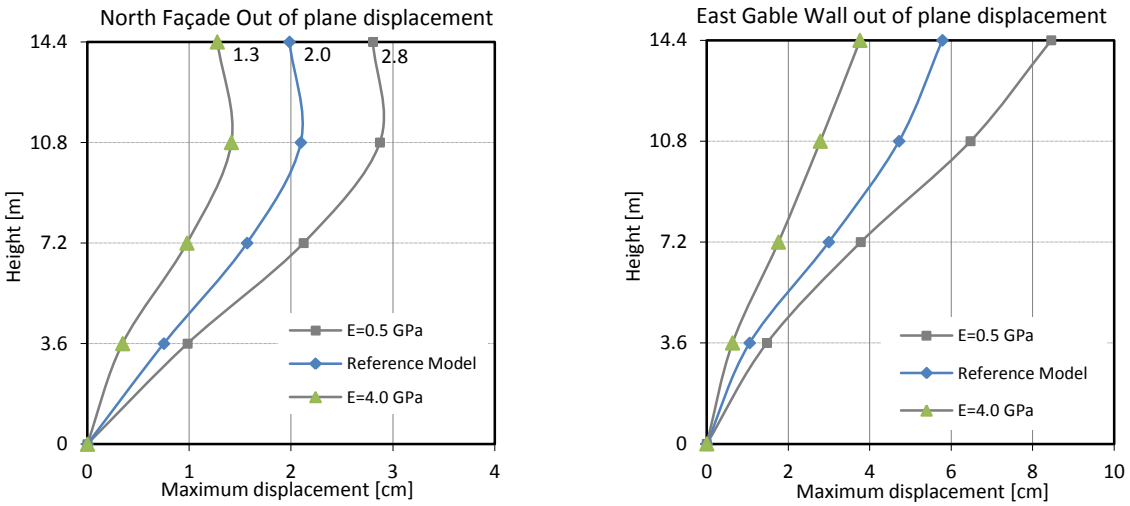

Figure 78 — Out-of-plane displacements at the middle of the walls for models with variation of the Young's modulus of the walls. a) Out-of-plane displacement of the North façade; b) Out-of-plane displacement of the East gable wall.

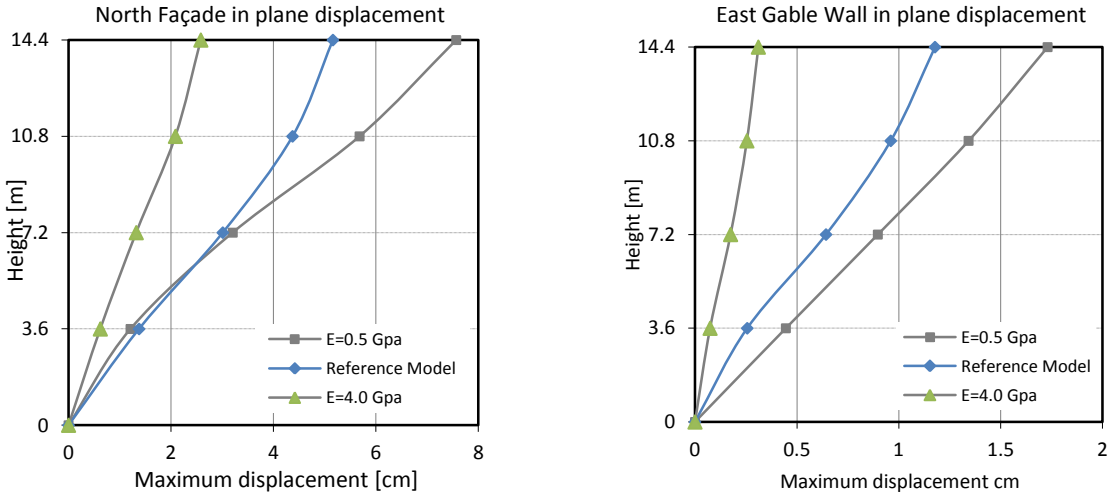

Figure 79 – In plane displacements for models with variation of the Young's modulus of the walls. a) In plane displacement of the North façade; b) In plane displacement of the East gable wall.

Higher stiffness means less deformation but not necessarily more resistance of the structure. In the transversal direction (Figure 80), the increase of the E_{walls} to 4.0 MPa lead the structure to resist 30% more of the total weight comparing with the reference model. At the same time, in the transversal direction, the less stiff structure is presenting approximately three times the maximum displacement of the structure with E=4.0 MPa.

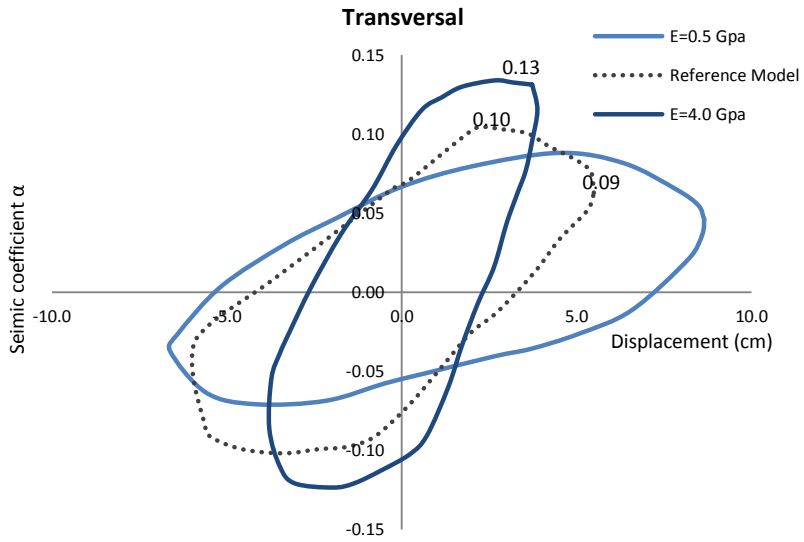

Figure 80 - Envelope of the response obtained from the non linear dynamic analysis in the transversal direction. Variation of the stiffness of the masonry walls.

On the other hand, in the longitudinal direction (Figure 81) the inverse happened. The capacity in force of the structure for the lower value of E_{walls} got higher. A possible explanation lies on the fact that the structure with so low value of Young's modulus will have a considerable deformation and, after exploiting all the capacity of the walls in the transversal direction, the structure can try to use the extra force capacity on the longitudinal direction. As discussed before, the reference structure is very close to the failure when subjected to the 100% Earthquake. Nevertheless, in the longitudinal direction, the structure is still far from its maximum capacity in force. As a result, the more deformable structure (E=0.5 MPa) is taking advantage of the resistance of the gable walls and the α_{base} got 30% bigger in respect to the reference value (Figure 81).

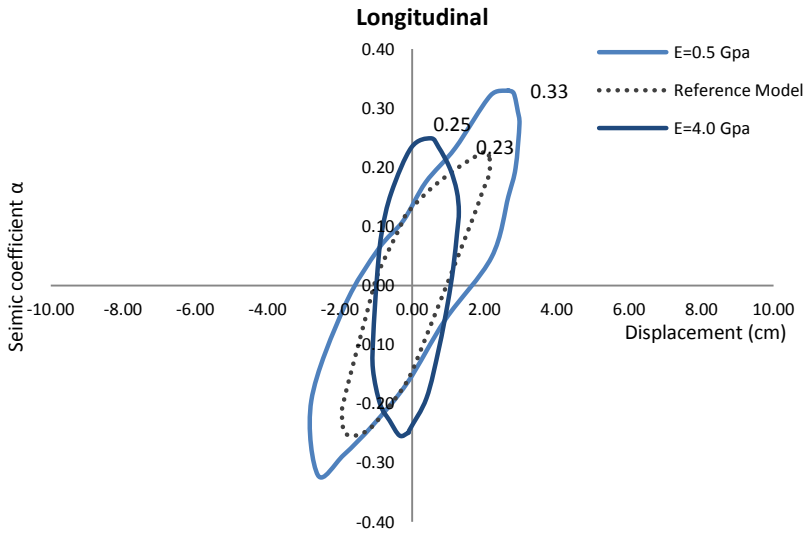

Figure 81 - Envelope of the response obtained from the non linear dynamic analysis in the longitudinal direction. Variation of the Young's modulus of the masonry walls.

From the analysis of Figure 82, it is possible to observe a similar damage pattern for both the limit values, as they are presenting diagonal cracking at the spandrels of the first, second and third level (connecting the corners of the openings). The difference is that the more deformable model (*E*=0.5MPa) is having more damage for the same level of horizontal loads. Both have similar collapse mechanisms of the reference model. Also, for the more flexible model, it is possible to observe that the piers' bases are already having the accumulation of damage and so they are allowing more deformations and displacements in the plane of the façades. The gable walls for the stiffer model are experiencing the slight development of three vertical cracks, but this damage is not severe. The gable walls of the more deformable model have a concentration of damage at the base and a concentration of damage really at the top due to the high deformation of the structure.

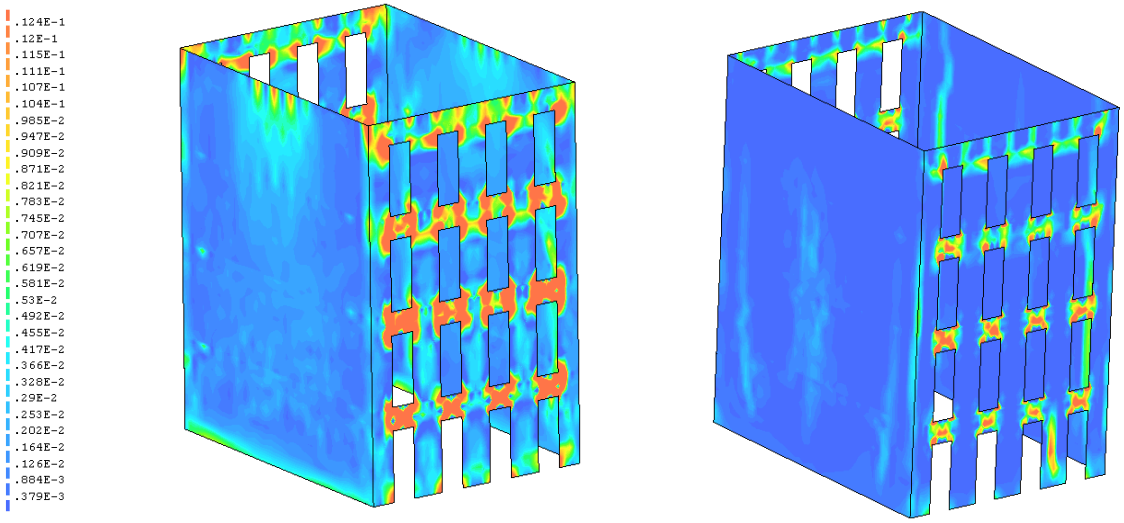

Figure 82 – Maximum tensile principal strains obtained from the dynamic non linear analysis. a) Model considering E_{walls}=0.5 GPa; b) Model considering E_{walls}=4.0 GPa

5.2.4 Variation of the Young's Modulus of the floors (Efloors)

In ancient masonry buildings, the strengthening of the floors, in order to guarantee diaphragm properties, is essential to impose a global behavior of the structure. Its main advantage is to assume compatible horizontal displacements in every point of each floor and therefore to allow the distribution of the seismic forces in accordance to the stiffness of the resistant vertical elements.

In general, the ancient masonry buildings can be improved to resist seismic actions by increasing its horizontal force capacity, its stiffness (reducing displacement demands), or its ability to undergo higher seismic displacement demands without collapsing (improvement of ductile capacity). To a certain extent, and according to the type of structural system deemed to be strengthened, the different approaches can be applied simultaneously or independently, in what is generally referred as selective intervention techniques (Pinho 2001).

For the present thesis four different situations were studied: an extreme situation without the floors, deformable wooden floors with a thickness of 3.6 cm (reference model), one where the thickness of the wooden floor is the double of reference model (final thickness of 7.2 cm) and a last one where the wooden floors were replaced by a reinforced concrete slab.

In the first situation the floors were not included but the weight of the floors and partition walls were included in the weight of the gable walls through the application of concentration walls. As a consequence, the total weight of the structure is the same of the reference model.

The second solution used is based on a common one where normally the floors are strengthened with the superposition of an extra layer of wood, normally, with the joints in the orthogonal direction of the joints of the original floor. Also, in order to improve the flexural capacity of the floor another solution can be used: one extra layer is used but it is supported in a steel profile beam instead on directly supported in the previous floor. The thickness enlarge of the floors had as a consequence the increase of the total weight of the structure of around 2%.

The other stiffening technique tested was based on the substitution of the wooden floor by a reinforced concrete slab with 0.20 m thick. This solution has the obvious advantage of increasing the stiffness of the floor diaphragm and as a result the forces are much more effectively distributed to the load bearing walls. However, the new slab is much heavier (more 23% of weight comparing with the reference model), producing the increase of the inertial forces during an earthquake and also will produce the increase of the vertical stresses on the masonry walls.

5.2.4.1 Dynamic properties

The dynamic properties of the structure are changing significantly varying the stiffness of the floors. For the case of the structure without the floors, the first frequency is equal to 1.29 Hz (transversal direction). The first mode shape in the longitudinal direction has a frequency of 2.48 Hz, which means that the longitudinal direction has almost the double of the stiffness. In the case of double thickness of the floors, the first mode is in the transversal direction with a frequency of 1.59 Hz. The frequency of the first longitudinal mode is equal to 3.40 Hz. The first frequency model with the reinforced concrete slab is equal to 1.64 Hz (transversal direction). The difference is that the second mode shape is already a longitudinal mode with a frequency of 3.59 Hz and the distortional mode very typical from buildings with deformable floors is being replaced by a torsional mode with f=4.03 Hz (the angles between orthogonal walls are kept the same). The local mode shapes related with the vertical deformation are no longer present in the beginning (now they are higher modes).

5.2.4.2 Dynamic non linear analysis results

The model showing the highest out-of-plane displacements is the one without any floors, as it was expected (Figure 83). Even the wooden joists were removed on this model, which means that the stiffness in the

transversal direction decreased. As a consequence, it is expected that the out-of-plane displacement of the gable walls increase, since there is no connection between the walls. In Figure 83 b) and Figure 84 a) a high displacement of the model with RC slab is observed, which can be explained due to an excessive concentration of damage on the first floor. As a consequence, the first and second floors are presenting a high drift and deformation, while the other floors are not moving in respect with each other. This effect can be better analysed with the comparison between the principal tensile stresses (Figure 82). The model with the double floor thickness and axial stiffness is the one having less out-of-plane deformations (Figure 83 a). If the analysis is focused on the second and third floors the presence of the double wood floor is improving the results.

The out-of-plane behavior of the gable walls is presenting a maximum for the model with reinforced concrete slab. Actually, the maximum top displacements are increasing with the increasing of the inertial forces.

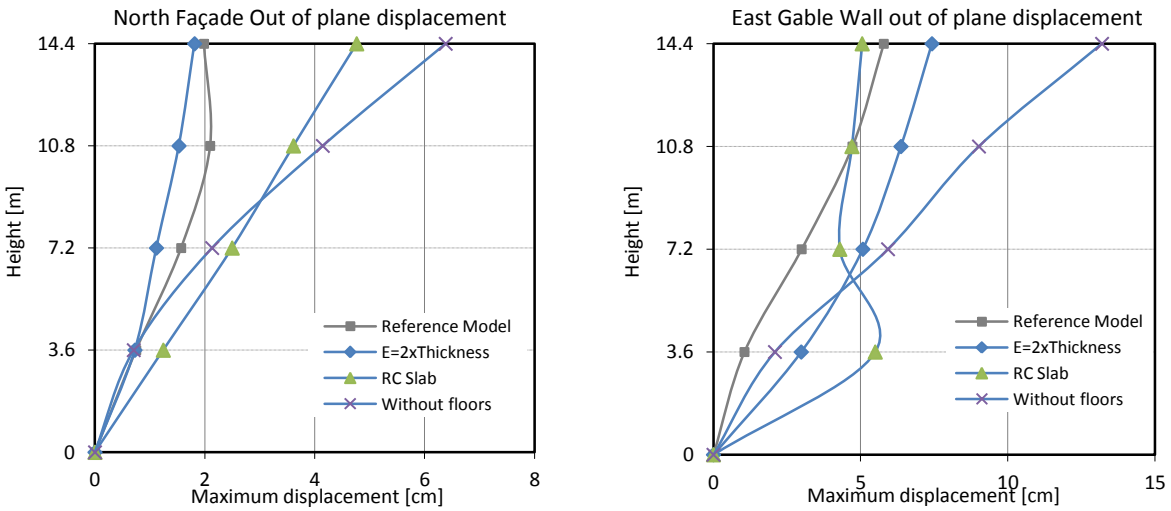

Figure 83 – Variation of the floor Young's modulus. a) In plane displacement of the North façade; b) In plane displacement of the East gable wall.

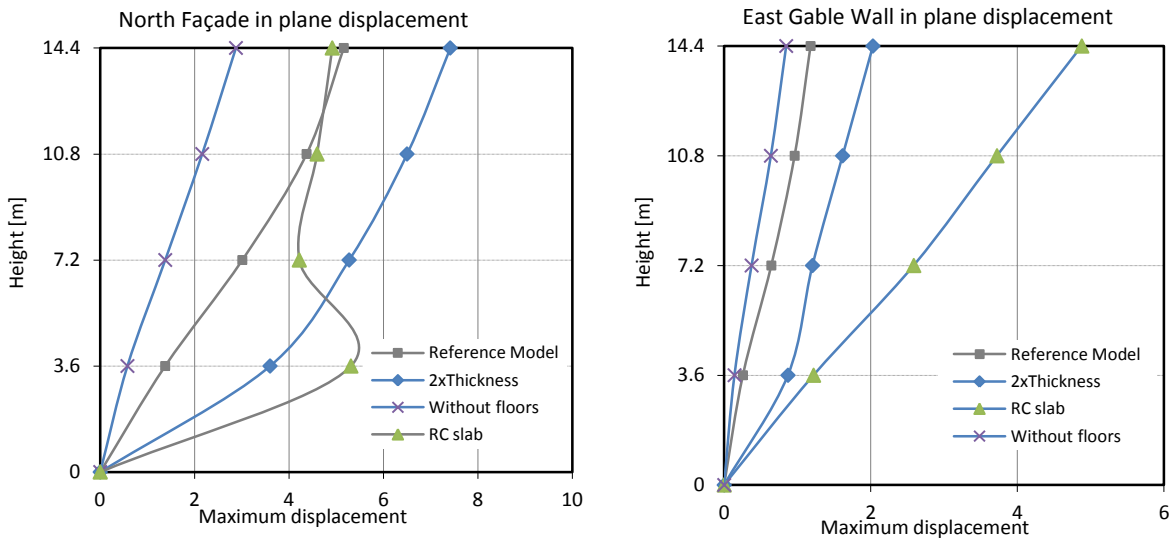

Figure 84 – Variation of the floor Young's modulus. a) Out-of-plane displacement at the middle of the North façade; b) Out-of-plane displacement at the middle of the East gable wall.

The envelopes of the responses for the three new models, varying the Young´s modulus of the floors, are presented in Figure 85 and Figure 86. The results in both directions are contradicting the general initial idea that the strengthening of masonry building floors using a RC slab is an appropriate method. The α_b decreased in this situation from 10% to 60% (40% difference). In the transversal direction, only the solution including the two layers of floors is allowing a better result in what concerns the force capacity.

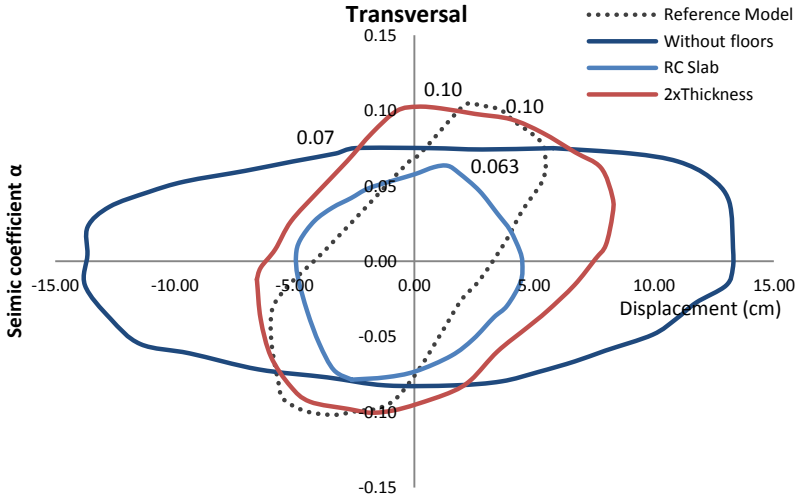

Figure 85 - Envelope of the response obtained from the non linear dynamic analysis in the transversal direction. Variation of the *E* of the floors.

The extreme case of the structure without floors has significant difference on the dynamic behavior of this type of buildings, both in terms of force capacity and maximum displacement. The maximum displacement is higher for the model without floors (almost 3 times the reference value). This means that even if the wooden floors

are deformable and very thin (in this case the thickness of the panels is 3.6 cm) they are improving clearly the behavior of the structure. The wood beams parallel to the façade are controlling the deformation of the floors and transferring the forces from the floors to the walls and between gable walls, preventing the high out-of-plane displacements of the gable walls.

In the longitudinal direction, the better solution is the model with the two layers of MDF panels. The reinforced concrete slab model is equivalent in force of not having floors; nevertheless the slab is preventing bigger displacements.

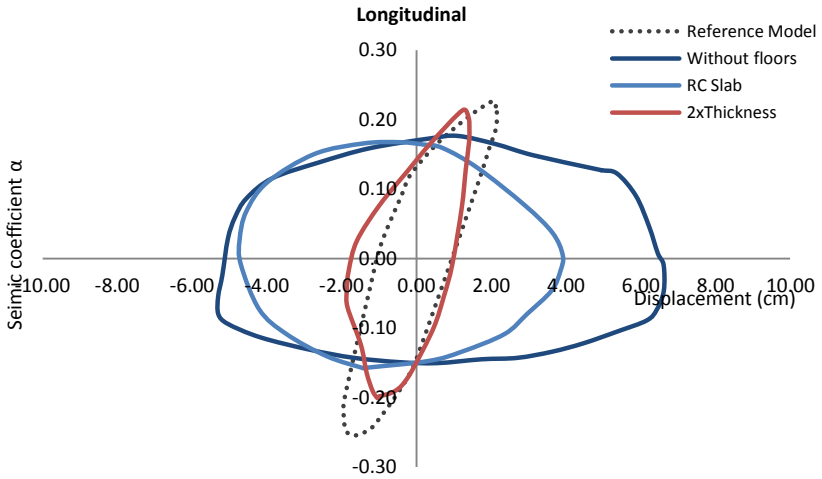

Figure 86 - Envelope of the response obtained from the non linear dynamic analysis in the longitudinal direction. Variation of the *E* of the floors.

To better understand the values and behavior of the structures, it is necessary to analyze the damage that the structure is presenting after being subjected to an earthquake. The maximum tensile principal strains obtained from the dynamic non linear analysis for each model is presented in Figure 82. The different models present different collapse mechanisms and damage. The reference structure is presenting diagonal cracks at the spandrels and also at the top floor, due to the in plane forces, as it can be seen in Figure 82 a). The model without walls presents a vertical crack located in the top of the gable wall and serious damage at the top of the façades (Figure 82 b). This damage is very typical of structures with flexible floors. When increasing the stiffness of the floors these start to be able to distribute the horizontal forces between the load bearing walls and this located damage starts to fade. The structure with the thickness of the floor equal to 7.2 cm is presenting a behavior in between the reference model and the reinforced concrete slab model, because it has the properties in between the two structures.

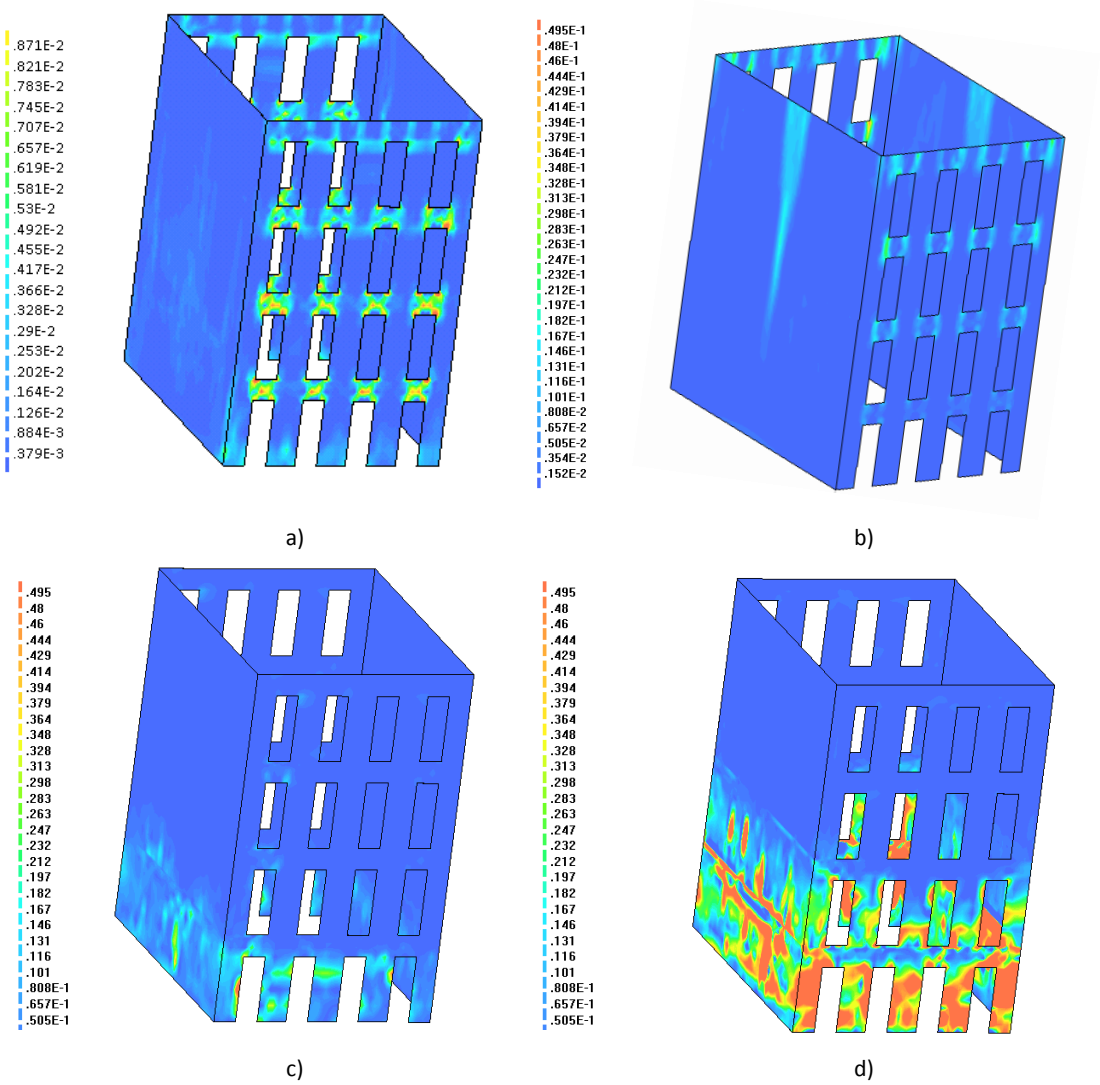

Figure 87 – Maximum tensile principal strains obtained from the dynamic non linear analysis. a) Reference Model; b) Model without floors; c) Model 2xthickness; d) Model with RC slab.

The lower value of the maximum force capacity of the model with a concrete slab is a consequence of the increasing of the inertial forces and consequent high concentration of stresses at the lower level. The floors are now much stiffer and much heavy, which will produce the increase of the inertial forces. After all this forces absorbed during the earthquake have to be redirected for the foundations passing through the masonry buildings, spandrels and piers that did not had any improvements in the material properties or geometry. Thus, the damage is all concentrated in the lower part and the rest of the structure is not showing almost no damage. The lower part is too damaged and, even if the top part can work, the structure is not able to increase the seismic coefficient (see Figure 84 a).

Furthermore non linear dynamic analyses using different earthquake amplitudes (50%, 100% and 150%) were carried out. From Figure 88 to Figure 90 the envelopes of the hysteretic behaviour varying the stiffness of

floors, relating the displacement of the node on the top floor with the horizontal seismic forces at the base (α_b), are presented. In Figure 88 the behavior of the structure without floors is presented; it is possible to understand the high deformable capacity of the structure. The displacements are more or less changing for the double each time the seismic intensity is changing which means that the structure is very deformable. Nevertheless, the structure is still increasing the response in terms of force capacity achieving a value of 10% the total weight in the transversal direction. In the opposite direction both the force and the displacement are still increasing. The maximum force in this direction is about 20%. The fundamental frequency is 20% less comparing with the fundamental frequency of the reference model in the transversal direction.

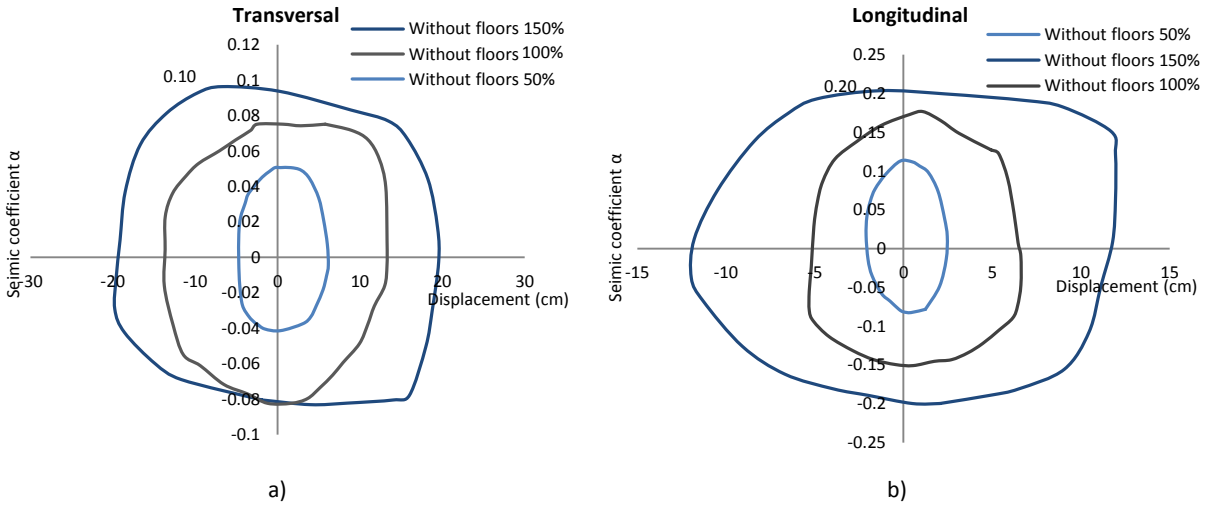

a) b)

Figure 88 - Envelope of response of the model without floors. a) Transversal direction; b) Longitudinal direction.

In Figure 89 the behavior of the structure with the reinforced concrete slab is presented. In the transversal direction the structure seems to achieve the failure to the 100% Earthquake (0.08) since it cannot absorb any more loads and it is only deforming. Even between the results obtained with the 50% Earthquake and 100% earthquake the displacements are the triple and it can mean that even for the 50% Earthquake the structure is already presenting severe damage. The maximum value in force in the transversal direction is reached for the 50% Earthquake (0.08) but still lower than the capacity of the reference model. As expected, the longitudinal direction is much stiffer than the transversal (the maximum value is 0.20) but even with the stiffer diaphragm the displacements are very high. As said before, the high total self-weight will has consequence the high inertial forces that damage highly the bottom levels; the top displacements are mainly due to the displacements at the base and the top floors have a global displacement.

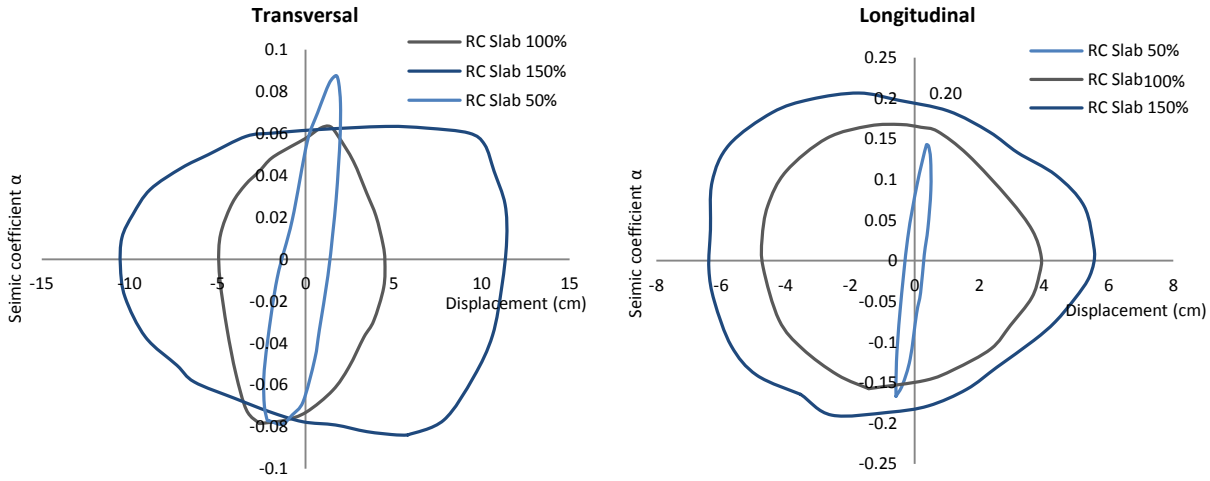

a) b)

Figure 89 - Envelope of response of the model with reinforced concrete slab. a) Transversal direction; b) Longitudinal direction.

The force capacity in the transversal direction (Figure 90 a) is achieved for the 100% Earthquake. In the longitudinal direction, the model is also very stiff (more than the double of the orthogonal direction). In the longitudinal direction (Figure 90 b) the model is probably starting to accumulate damage from the 100% to 150% Earthquake since the displacements increased significantly and the absorbed force stayed almost the same.

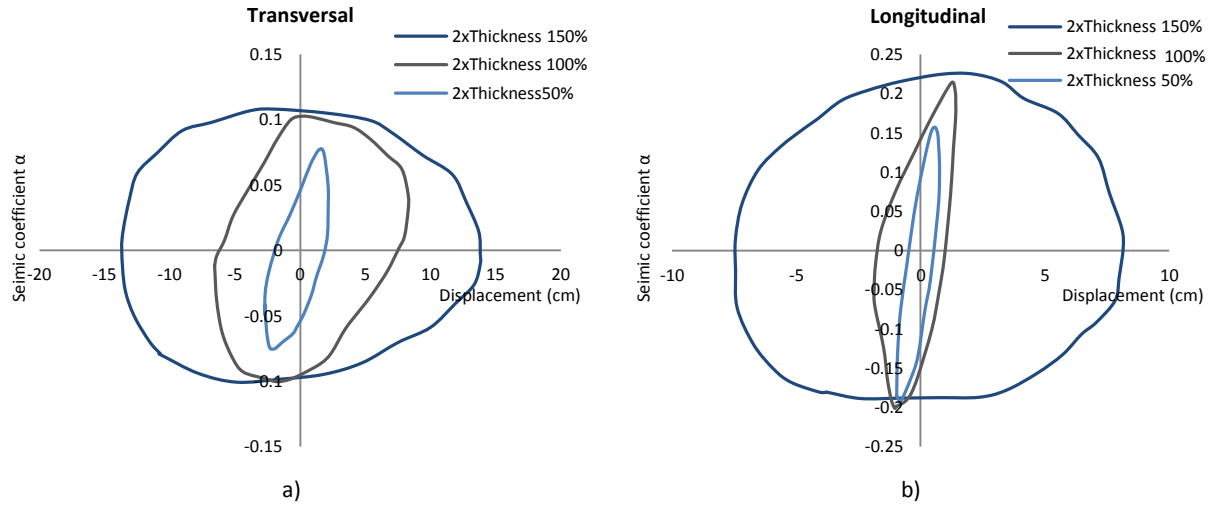

a) b)

Figure 90 - Envelope of response of the model with two times thickness floor. a) Transversal direction; b) Longitudinal direction.

5.2.4.1 Static non linear analysis results

A non linear static analysis was performed with the objective of comparing its accuracy and suitability. The capacity curves, obtained with the pushover analysis proportional to the mass, are presented in the same graph along with the envelopes of Earthquake 50%, 100% and 150%; the pushover analysis proportional to the mode was not carried out since the results of the pushover using the mass were more accurate.

The graphs in Figure 91 are showing that the pushover curves are not matching the deformation capacity nor the force capacity that one can determine with the non linear dynamic analysis. Even if the non linear dynamic analysis did not find the true force capacity of the structure (because the envelopes are not still giving sign of being 'saturated' in force) the pushover is supposed to take the structure until the limit. The pushover curve is estimating the force capacity in around 0.04 which is two times less the value of force capacity of this model. Regarding the longitudinal direction, the pushover curve is having a lot of stiffness variations and is accumulating a lot of damage not reaching again the value in force determined with the dynamic non linear analysis. The pushover curve is reaching a pick at α=0.15 but to a correspondent top displacement of 0.30m which is not admissible; the structure will collapse before that point.

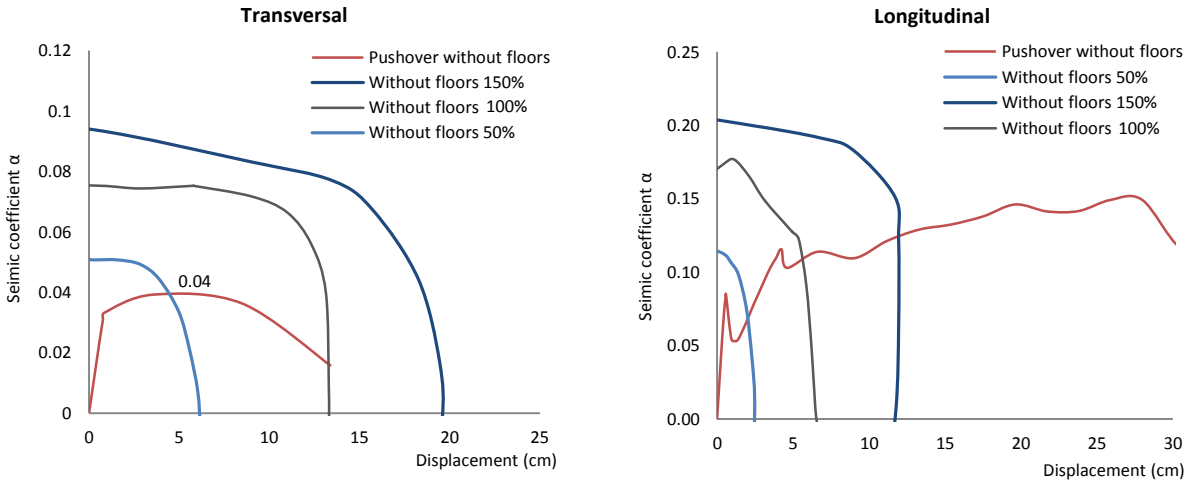

a) b)

Figure 91 - Envelope of response of the model without floors. a) Transversal direction; b) Longitudinal direction.

The capacity curve, presented in Figure 92 a), has a maximum of around 10% of the total weight of the structure, which is less that the value obtained with the non linear dynamic analysis and 150% Earthquake. In the longitudinal direction (see Figure 92 b)), the force capacity determined with the pushover is 45% of the total weight which means that more non linear dynamic tests should have been done in order to get take the structure more close to the collapse. In what concerns the displacement, the pushover is presenting a much more fragile collapse, while the non linear dynamic analysis results, without even getting close to the maximum force capacity of the structure, are showing more or less four times the maximum displacement obtained with the pushover method.

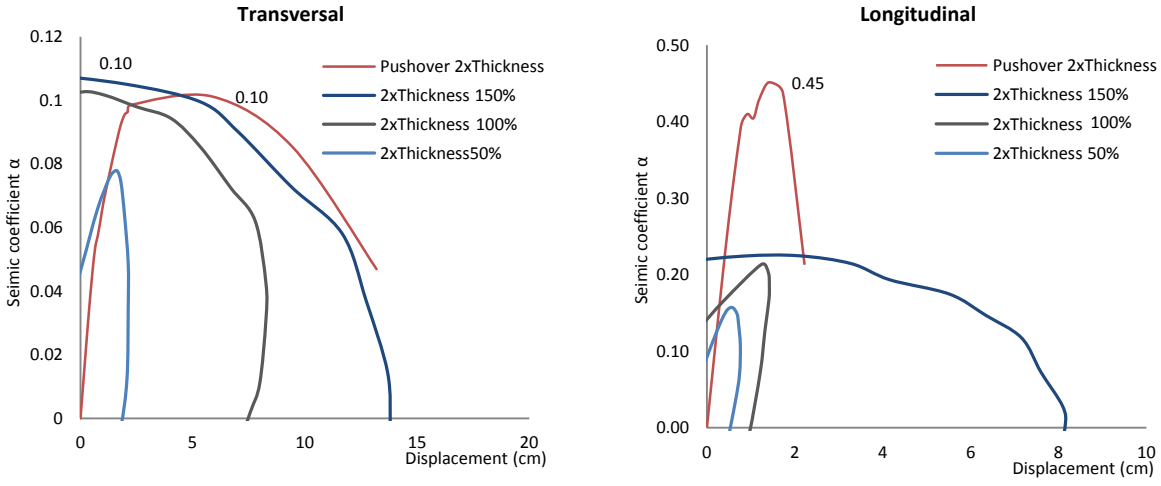

a) b)

Figure 92 - Envelope of response of the model with two times thickness floor. a) Transversal direction; b) Longitudinal direction.

The pushover results for the model with a concrete slab is computing very high values for the force capacity both in the transversal (Figure 93 a) and longitudinal (Figure 93 b) directions. In Figure 87 d) a plot of the maximum principal strains for 100% earthquake is exhibiting a lot of damage, especially concentrated at the base; this means that the pushover is overestimating the force capacity of the structure, on the other hand is underestimation its capacity to deform since both curves have a very steep slope.

The pushover analysis is a static analysis, meaning that is applying the force monotonically and only in one direction. In reality the horizontal seismic force is being applied in both directions in a quick way. The dynamic effect is increasing a lot the forces at the base and so there is more damage than the one computed with the pushover analysis.

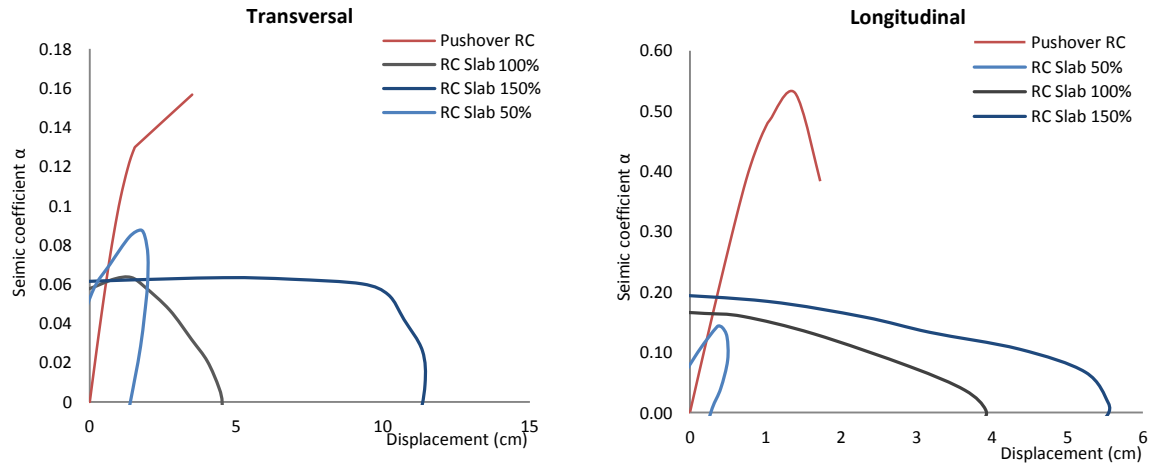

a) b)

Figure 93 - Envelope of response of the model with RC slab. a) Transversal direction; b) Longitudinal direction.

The pushover analysis is not giving such good results even with this last model that has a much stiffer diaphragm and a lot more concentration of masses at the floors levels. Nevertheless, the major part of the masses is still distributed on the walls. As a consequence, there are still not the perfect conditions to apply the pushover analysis.

6. CONCLUSIONS

6.1 FINAL CONCLUSIONS

The objectives of the present study is to define the seismic behavior of the a masonry ancient building *gaioleiro* typology and its sensibility to the changing of some parameters as the number of floors, percentage of openings of the façade and also the variation of the Young's modulus of the floors and masonry walls. The analysis of the performance of this particular typology was carried out using a non linear dynamic analysis and also a non linear static analysis. Furthermore, a brief study of the applicability of the non linear static analysis to this type of buildings was made.

The comparison and the sensitivity seismic analysis will be based on a reference model, with a total high of 14.4 m (4 floors), implantation area of 9x12m2 and flexible floors made of MDF panels supported in wood joists connected to the masonry walls. The most important data analyzed was the top displacements – both in plane and out-of-plane – the envelope of the dynamic non linear response relating the total base shear divided by the total weight and the top displacement and the principal tensile strains in the exterior surface of the walls. The main failure mechanisms of this model are associated with the diagonal cracking of the spandrels, creating a discontinuity between the structural elements of the façade. As a consequence, the slender piers in between the windows are working as cantilevers and are accumulating damage at the base level. In addition, the 4^{th} floor of the reference model presented a rocking in plane failure that can be related also with an out-of-plane bending and collapse of the top part. This different behavior in the top level can be related with the lower compressive stress.

After the study of the reference model, a sensitivity analysis was made using the same tools as before: dynamic and static non linear analysis with the evaluation of the displacements (in plane and out-of-plane) and the strains. In Table 8 a summary of the results for the different models in terms of displacements and force capacity is presented. The biggest variation in terms of force capacity was detected when the number of floors is changed. For the model with 6 floors, the force capacity in the transversal direction decreased 62%. Even the failure mode changed with the increased of the number of floors. The ratio of the spandrels is also having a lot of influence; the slender piers are influencing a lot the behavior of the building, including the out and in plane behavior and the force capacity in both directions. The young's modulus of the walls is highly influencing the deformation of the building (around 40% differences) but also its capacity force (the difference can get until 27% in the transversal direction).

The effect of the floors and diaphragms is also evident in the results presented; the building without any floors presents a very high deformation and the vertical crack located at the top of the gable walls associated to the

out-of-plane failure. The model with 2x the thickness is showing a small increase on the performance but is still the best solution since it increased the in plane behavior and it is avoiding the development of the vertical crack on the gable walls associated with the out-of-plane behavior. It is important to underline the importance of a good connection between floors and masonry walls in order to secure the correct transmission of horizontal loads.

Furthermore, the RC slab is in the end proving not to be a good strengthening solution – the increase of the in plane stiffness (better for the redistribution of the forces) is not compensating the increase of the mass and consequently of the inertial forces. This extra weight and inertial forces need to be supported by the walls at the base allowing the development and concentration of damage on these parts. All the variations done are more evident in the transversal direction because it's the most fragile direction. Even the accumulation of damage points as well as the damage mechanisms evolved in each model with variation of the Young's Modulus is different, which means that for sure the presence of a more still or more deformable diaphragm in the structure is deeply influencing its behavior and seismic performance.

Table 8 – Summary of the sensitivity analysis results.

		Maximum top displacements				Maximum force capacity			
		Longitudinal Direction		Transversal Direction		Longitudinal Direction		Transversal Direction	
		Result (cm)	Variation (%)	Result (cm)	Variation (%)	Result (cm)	Variation (%)	Result (cm)	Variation (%)
Number of floors	Reference	1.94	-	5.58	-	0.23	-	0.10	-
	5 floors	3.63	0.87	18.88	2.39	0.12	-0.50	0.05	-0.50
	6 floors	18.48	8.53	33.79	5.06	0.10	-0.56	0.04	-0.62
Spandrels ratio	Short Spandrels	1.81	0.06	6.05	0.09	0.21	-0.11	0.11	0.19
	Reference	1.94	-	5.58	-	0.23	-	0.10	-
	Slender piers	2.24	0.15	6.39	0.15	0.18	-0.24	0.04	-0.55
E of the walls (GPa)	0.5 MPa	2.79	-0.44	7.50	0.35	0.30	0.29	0.07	-0.23
	Reference	1.94	-	5.58	-	0.23	-	0.10	-
	4 MPa	1.17	-0.40	3.75	-0.33	0.23	0.00	0.12	0.27
E of the floors (GPa)	Without floors	5.81	-2.00	13.04	1.34	0.15	-0.34	0.08	-0.21
	Reference	1.94	-	5.58	-	0.23	-	0.10	-
	2x thickness	1.59	-0.18	7.50	0.35	0.19	-0.17	0.10	0.01
	RC slab	4.33	1.23	4.74	-0.15	0.16	-0.32	0.07	-0.28

Although non linear incremental dynamic analysis is the most computationally intensive method available for evaluation of seismic response of structures, the results of the analysis performed for this study indicate that it is the more adequate method which can provide reliable results for the assessment of this type of buildings. In what concerns the use of pushover analysis to assess the behavior of these buildings, it seems that both the uniform and the modal load distribution it is not completely adequate for determine the seismic analysis of masonry building. Nevertheless, the pushover approach with uniform distribution of the loads is providing

acceptable results in the in plane response of the façades and in terms of force capacity.In the present case the structure is regular in plan and high, which is not common on ancient masonry structures, but still the mass is mostly distributed through the walls and not concentrated in the floors.

6.2 PROPOSAL OF FUTURE WORK

The *gaioleiro* building is a building typology already studied by several authors but its constructions problems and high properties dispersion makes this topic full of issues still to discuss. On the particular topic of seismic sensitivity of *gaioleiros* other geometries could have been tested; variation of the walls thickness in high, inclusion of the shaft in the numerical model, inclusion of the inclined roof and study of its influence in the compression stress state at the top and horizontal forces, variation of the dimensions in plan, the effect of adjacent constructions, and much more material properties. Furthermore, the dynamic identification on site could be also useful to calibrate all the models made around this kind of buildings.

The study of more possible strengthening hypothesis of the floors, like the use of light materials or modern materials like Fiber Reinforced polymers (FRP) or (SRG), etc. Also, the study of better solutions to improve the connections between the floors and walls would be important.

Furthermore, the conclusions should be used to prepare a set of recommendations on strengthening techniques associated to the parameters that most influence the response, aiming at reducing the seismic vulnerability and preventing the global and local collapse of this type of buildings.

REFERENCES

Andrade, H. (2011). *Caracterização de edifícios antigos. Edifícios Gaioleiros.* Portugal: Nova University.

Appleton, J. (2003). *Reabilitação de Edifícios Antigos: Patologias e Tecnologias de Intervenção.* Lisboa: Edições Orion.

Appleton, J. (2005). *Reabilitação de Edifícios Gaioleiros: Um quarteirão em Lisboa.* Lisboa: Orion.

Berto, L., Saetta, A., Scotta, R., & Vitaliani, R. (2004). *Shear behaviour of masonry panel: parametric FE analyses.*

Beyer, K., & Mangalayhu, S. (2013). *Review of strength models for masonry spandrels.* Springer Science and Business Media.

Branco, M. (2007). *Reforço Sísmico de Edifícios de Alvenaria. Aplicação a edifícios "Gaioleiros".* Portugal: Instituto Superior Técnico.

Brignola, A., & Podestà, S. (2008). In-plane stiffness of wooden floor. *New Zealand Society for Earthquake Eengineering Conference*, (p. Paper 49).

Candeias, P. (2008). *Avaliação da vulnerabilidade sísmica de edifícios de alvenaria.* Portugal: University of Minho.

Cardoso, R., Lopes, M., & Bento, R. (2003). Vulnerabilidade Sísmica de Edifícios Antigos de Alvenaria da Cidade de Lisboa. Lisboa: IST.

Chaimoon, K., & Attard, M. M. (2006). *Modeling of unreinforced masonry walls under shear and compression.* Elsevier.

Chen, S.-Y., Moon, F., & Yi, T. (2008). *A macro element for the nonlinear analysis of in-plane.* Elsevier.

Chopra, A. K. (1995). *Dynamics of Structures: Theory and Applications to Earthquake Engineering.* New Jersey: Prentice Hall.

D'Ayala, D., & Novelli, V. (2010). *Abacus of the most common seismic damage.* Perpetuate.

Deierlein, G., Reinhorn, A., & Willfor, M. (2010). *Nonlinear Structural Analysis For Seismic Design: A Guide for Practicing Engineers.* National Institute of Standard and Technology.

Fajfar, P. (2000). *A Nonlinear Analysis Method for Performance Based Seismic Design.*

FEMA 306. (1998). *Evaluation of earthquake damaged concrete and masonry wall buildings.* Washington D.C.: The Partnership for Response and Recovery, Federal Emergency Management Agency.

FEMA 440. (2005). *Improvement of nonlinear static seismic analysis procedures.* Washington D.C.: Department of Homeland Security, Federal Emergency Management Agency.

Galasco, A., Lagomarsino, S., & Penna, A. (2006). *ON THE USE OF PUSHOVER ANALYSIS FOR EXISTING MASONRY BUILDINGS.*

Gattesco, N., Clemente, I., Macorini, L., & Noè, S. (2008). Experimental investigation on the behavior of spandrels in ancient masonry buildings. *The 14th World Conference on Earthquake Engineering.* Beijing.

Gomes, R. (2011). *Sistema Estrutural de Edifícios Antigos de Lisboa - Os edifícios "Pombalinos" e os Edifícios "Gaioleiros".* IST.

Lopes, M. (2008). *Sismos e Edifícos.* Orion.

Lopes, M., Delgado, R., Fonseca, J., Oliveira, C., Azevedo, J., Bento, R., et al. (2008). *Sismos e Edifícios.* Orion.

Lourenço, P., Mendes, N., & Oliveira, D. (2011). Analysis of masonry structures without box behaviour. *International Journal of Architectural Heritage , 5*, 369-382.

Lourenço, P., Rots, J., & Blaauwendraad, J. (2011). Two approaches for the analytical masonry structures: micro and macro-modeling. *Heron* .

Magenes, G., & Calvi, G. M. (1997). In-plane seismic response of brick masonry walls. *Earthquake Engineering and Structural Dynamics , Vol. 26*, 1091-1112.

Marques, ,. R., & Lourenço, P. (2010). *Possibilities and comparison of structural component models for the seismic assessment of modern unreinforced masonry buildings.* Elsevier.

Mendes, N. (2012). *assessment of ancient masonry buildings: Shaking table tests and numerical analysis.* Portugal: Univeristy of Minho.

NP EN 1990. (2009). *Eurocode - Basis of structural design.* European Comittee for Standardization.

NP EN 1991-1-1. (2009). *Eurocode 1: Actions on surfaces.Part 1-1: General actions, Densities, self-weight, imposed loads for buildings.* European Committee for Standardization.

NP EN 1998-1-1. (2009). *Eurocode 8: Design of Structures for earthquake resistance. Part 1: General Rules, seismic actions and rules for buildings.* European Comitee for Standardization.

Ordem dos Engenheiros. (2013, Junho). *www.ordemengenheiros.pt*.

Parisi, F., & Augenti, N. (2013). *Earthquake damages to cultural heritage constructions and simplified assessment of artworks.* Italy: University of Naples Federico II.

Paula, R., & Cóias, V. (2006). Rehabilitation of Lisbon's old "seimic resistant" timber framed buildings using innovative techniques. *International workshop on "Earthquake Engineering on Timber Structures".* Coimbra.

Paulay, T., & Priestley, M. (1992). *Seismic design of reinforced concrete and masonry buildings.* John Wiley & Sons, Inc.

Perret, T., Partridge, V., & Purcell, K. (n.d.). *Bedford Borough Council Cultural Service*. Retrieved Maio 2013, from The Higgins Art Gallery & Museum: http://thehigginsbedfordcollections.blogspot.pt/

Ramos, L., & Lourenço, P. (2004). Advanced numerical analysis of historical centers: A case study in Lisbon. *EngineeringStructures , Vol. 26*.

Shariq, M., Abbas, H., Irtaza, H., & Qamaruddin, M. (2007). *Influence of openings on seismic performance of masonry building walls.* Elsevier.

Simões, A., & Bento, R. (2012). *Characterization and Classification of Lisbon Old Masonry Buildings.* ICIST.

TNO DIANA. (2011). *9.4.4 Diana user's manual.*

Yi, T. (2004). *Experimental investigation and numerical simulation of an unreinforced masonry structure with flexible diaphragms.* USA: Georgia Institute od Technology.

Zucchini, A., & Lourenço, P. (2004). *A coupled homogenisation–damage model for masonry cracking.* Elsevier.